DEVELOPMENT OF SEMI-EMPIRICAL MODELS TO MEASURE MASS FLOW RATE OF SOLIDS IN AN AIR SEEDER

A Thesis Submitted to

The College of Graduate Studies and Research

In Partial Fulfillment of the Requirements

For the Degree of Master of Science

In the Department of Mechanical Engineering

University of Saskatchewan

Saskatoon, Saskatchewan

By

MOHAMMAD SHABBIR HOSSAIN

PERMISSION TO USE

In presenting this thesis in partial fulfilment of the requirements for a Postgraduate degree from the University of Saskatchewan, I agree that the Libraries of this University may make it freely available for inspection. I further agree that permission for copying of this thesis in any manner, in whole or in part, for scholarly purposes may be granted by the professors who supervised my thesis work or, in their absence, by the Head of the Department or the Dean of the College in which my thesis work was done. It is understood that any copying or publication or use of this thesis or parts thereof for financial gain shall not be allowed without my written permission. It is also understood that due recognition shall be given to me and to the University of Saskatchewan in any scholarly use which may be made of any material in my thesis.

Requests for permission to copy or to make other use of material in this thesis in whole or in part should be addressed to:

Head of the Department of Mechanical Engineering
University of Saskatchewan
57 Campus Drive
Saskatoon, Saskatchewan
S7N 5A9

ABSTRACT

The air seeder, which is primarily used for seeding, plays a significant role in the large-scale agricultural industry. Air seeding technology is based on the principles of pneumatic conveying where seed or fertilizer are conveyed by air from a reservoir to the land through pipe. Although air seeding technology has seen many developments since its arrival in the 1950s, it still lacks in the area of mass flow measurement of conveyed solids. An effective method of on-line seed flow monitoring is important to reduce product wastage and also, to anticipate plugging in the lines. The goal of this research has therefore been to develop methods to measure mass flow rate in horizontal gas-solid flow in a way that can be implemented in an air seeder.

In order to do that, two novel methods have been described. Both of the methods develop relationships between the solids flow rate, the pressure drop in the pipeline and the average air velocity by conducting experiments with wheat in a laboratory prototype air seeder. Pressure drop and average air velocity are two quantities that can be measured without difficulty under all conditions that an air seeder operates. Hence, these two quantities were chosen as the independent variables and material mass flow rate was chosen as the dependent variable.

An earlier empirical model for mass flow measurement was developed prior to this research. But that model was only valid under its test condition and did not provide any insight on the flow mechanism. Hence, this investigation developed models based on existing relationships for gas-solid flow. These models provide better understanding of the mechanism of pressure drop and also, show superior potential for adaptability from test to real-time conditions.

The first model was developed by modifying a relationship described for horizontal gas-solid flow by Hinkle (1953), Cabrejos and Klinzing (1992) and a few other researchers. That relationship between the specific pressure drop and the mass loading ratio was valid for fully-developed flow and higher air velocities. It needed modification because generally air seeders have a straight horizontal section in the non-developed region of the flow. The modified model is the first of its genre that describes the relationship between the specific pressure drop and the mass loading ratio in the non-developed flow region for both higher and lower air velocities. Although it was developed to be implemented on an air seeder, it can be applied to any horizontal gas-solid flow.

The second model for mass flow measurement of solids used the so-called "dimensionless" state diagram for horizontal flow. The primary relationship between the mass

loading ratio and the Froude number described in the dimensionless state diagram remains unchanged for all products being pneumatically conveyed. Only a single parameter varies with the mass flow rate of solids. This varying parameter was correlated with specific pressure drop in this second model. Again, this model is one of the first models to use the dimensionless state diagram for solids mass flow measurement.

Both models had errors less than 20% in the predicted mass flow rate when tested. The first model had less than 10% error for 73% of the total estimates. The second model had less than 6% error for 60% of the total estimates. For the rest of the estimates, the error values varied between 10% and 15%. These results indicate that both of the models have promising potential to be implemented into an air seeder.

ACKNOWLEDGEMENT

I would like to express heartiest gratitude to my honorable supervisors, Dr. Scott Noble and Dr. David Sumner. I owe my *Master's* degree to Dr. Noble, who has always been there when I was in need of his guidance and support. He has extended his generous help on both academic and non-academic issues and believed in me in my tough times.

From the first contact through mail till the last word of my thesis, Dr. Sumner's precise, professional, easy to follow, yet very effective advice and instructions have guided me academically from the start to the finish. Both of my supervisors have the ability to bring the best out of their students and I am thankful to them for understanding me as an individual.

I would also like to thank Mr. Tyrone Keep for his endless help on the experimental setup and also, for sharing his profound knowledge of air seeders with me. Thanks to Mr. Lav Mittal as well for the discussions. It was from such discussions that I suddenly developed an idea on how to use the dimensionless state diagram.

In the end, I would like to thank Mr. Jim Henry, Mr. Joel Gervais and other related personnel from CNH Saskatoon, who have graciously provided the funding and equipment for this research. Last but not least, I would like to gratefully acknowledge the support of the Natural Science and Engineering Research Council's (NSERC) Collaborative Research and Development program.

TABLE OF CONTENTS

NOMENCLATURE

Greek Symbols

Symbol	Quantity	Units
α	Specific pressure drop	-
β	Velocity ratio related to particle fall velocity in a cloud	-
λ_L	Air resistance coefficient	-
λ_Z	Pressure drop factor due to solids	-
λ_Z^*	Impact and friction factor for solids	-
μ	Mass loading ratio	-
ρ	Density of air	kg/m^3

English Symbols

Symbol	Quantity	Units
c	Particle velocity	m/s
D	Diameter of pipe	m
Fr	Froude number	-
f_s	Friction factor for solids	-
f_g	Friction factor for air	-
g	Acceleration due to gravity	m/s^2
k	Slope of specific pressure drop vs. mass loading ratio	-
K	Experimental constant	-
ΔL	Length between the points of pressure drop	m
M_a	Mass flow rate of air	kg/s
M_s	Mass flow rate of solids	kg/s
$M_{s(act)}$	Actual mass flow rate of wheat	kg/s
$M_{s(est)}$	Estimated mass flow rate of wheat	kg/s
Δp	Total pressure drop	Pa
Δp_L	Pressure drop due to air only	Pa
Δp_Z	Pressure drop due to solids only	Pa
v	Average/Superficial air velocity	m/s

Chapter 1. Introduction

The air seeder, which is primarily used for seeding, plays a significant role in the large-scale agricultural industry. Air seeding technology is based on the principles of pneumatic conveying where seed or fertilizer are conveyed by air from a reservoir to the land through pipe. This technology originated in Germany in the 1950's and was later adopted in Canada and Australia during the 1960's (Memory and Atkins, 2005). A number of manufacturers make air seeders in different types and sizes. CNH, John Deere, Bourgault and Morris are a few of the leading manufacturers of air seeders.

While configurations may vary from manufacturer to manufacturer, the basic design is more or less the same for all air seeders. An air seeding cart generally consists of one or more hoppers with metering devices, a distribution system of flexible hoses, a centrifugal fan and air hoe drills. Air from the fan is supplied through the distribution system which conveys seed or fertilizer dropped from the hopper. The metering device ensures the proper seeding rate. The air hoe drills, which are soil engaging tools, deliver seed to the ground. Figure 1-1 shows an air seeder in operation (Case IH Agriculture, 2014).

Figure 1-1 A Case IH air seeder (A. Tractor, B. Air hoe Drill, C. Air seeding cart)

Proper seeding rates promote higher yields and less waste. For this reason, accurate knowledge of product flow rate while the machine is in operation is vital for the operator. At present, there is no "closed-loop" product flow monitoring in the air seeders. There are a few procedures that the operator follows prior to starting seeding in order to have a rough estimate of product flow. All these procedures are basically related to calibration of the metering device.

Metering systems can be broadly classified into two types based on their working principles. The first one is a variable displacement metering system, in which the flow rate is varied by changing the exposure length of the meter or opening a cut-off gate. This system is prone to inaccuracy while metering small seeds at low flow rates. The second type is a variable speed metering system, in which the flow rate is regulated by means of a variable-speed drive with either discrete speed settings or continuously variable speeds within a specific range (Atkins, 2004) . This variable-speed drive is typically known as the meter roller. Factors that could influence metering accuracy are material size and density, application rate, field slope, ground speed of the tractor and field bounce (Atkins, 2004). Hence, field calibration of the metering device has to be performed prior to seeding.

A traditional approach for calibration is filling up the tank and driving a specified distance to calculate the area covered. Then, a measurement of the quantity needed to refill the seeder gives the material flow rate. Another approach is to collect material in a special cup for a certain period of time. The material application rate can then be determined from a chart provided by the manufacturer. Calibration can also be performed by means of a sample collector. A collection device is mounted below the metering box or attached to the primary distribution line while the meter roller is turned a specified number of times. The product flow rate is then derived from the weight of the collected material (Atkins, 2004). Opening and closing the primary distribution manifold to access the metering device is a tiresome routine in the latter case.

All of these calibration procedures require time and effort, which eventually affects productivity. The time required for calibration could be used to plant more area. Unavailability of a closed-loop flow monitoring system means the operator can only assume that products are flowing at the pre-calibrated rate without actually knowing the instantaneous flow rate. This could cause excess or inadequate product distribution which is one of the reasons behind poor coverage and wastage.

Plugging is a common phenomenon associated with pneumatic conveying of solids which is caused when the velocity of air is not sufficient to carry the particles. The current product flow metering technologies are not dependent on air flow parameters such as air velocity or pressure. Hence, detection of imminent plugging becomes impossible for an operator. At present, a sensor can only indicate blockage when a pipeline has already plugged. Conventional practice to avoid plugging is to run the fan at higher a speed than is actually required to obtain a safe air velocity. This leads to unnecessary consumption of power (Binsirawanich, 2011).

Closed-loop flow monitoring is therefore essential to cut down on, or completely eliminate, metering calibration time. An instantaneous knowledge of product flow will also give the operator an upper hand when it comes to detection and prevention of plugging as he/she would be able to increase the air velocity when required. Implementation of such real time flow monitoring is bound to improve metering accuracy as well.

One of the few attempts to develop a model for closed-loop product flow monitoring was made by Binsirawanich (2011). Due to unavailability of literature on mass flow monitoring in air seeders, his approach was purely empirical. Binsirawanich's model proved to be valid under the test conditions. This model could only be implemented in an air seeder if these test conditions were fulfilled in real time. Being one of the first attempts of its kind, Binsirawanich's concentration was mainly focused on developing the experimental methods and setup. Hence, no attempt was made to develop the relationship on parameters that provides insight on flow mechanism.

A model that has rational explanations behind its construction, is more likely to remain valid in both test and real time conditions. When a model is able to capture the underlying trend, it can accurately forecast changes that could be expected under different conditions. Hence, this research concentrates solely on developing models that can explain the relationship that exists between its variables and associated parameters, so that a reliable non-intrusive mass flow sensor can be constructed based on these models. Two different approaches will be followed to develop models based on the relationship between the pressure drop, the mass flow rate of product and the average air velocity in the conveying line. These models will be developed based on established relationships that have been used for other industrial pneumatic conveying applications. In the next few sections, the objective, the scope, the methodology and the expected research contributions for this research will be stated.

1.1 Objective

The objective of this research is to develop semi-empirical models to measure mass flow rate of conveyed product in an air seeder.

1.2 Scope

Models for mass flow rate measurement will be developed by establishing the relationship between the line pressure drop, the mass flow rate of product and the average air velocity in the conveying line while conveying wheat in a prototype air seeder. The models will then be solved for the mass flow rate of solids. Models will be constructed in such a way that the basic form of the models can be used for mass flow rate measurement of other products by following the same procedure.

1.3 Methodology

Experiments were be conducted in a laboratory prototype air seeder with wheat (geometric mean diameter[1]: 4.14 mm, particle density: 1424 kg/m^3) inside a straight horizontal pipe. Pressure drop were measured at various locations along a straight horizontal pipe at different air velocities and different product flow rates. In order to develop model, the approach described by Cabrejos and Klinzing (1992) was followed with necessary modifications. Another model was developed based on the dimensionless state diagram. For both models, the line pressure drop, the average air velocity and the mass flow rate of wheat were the quantities that were correlated. All experiment were carried out in the operating range of an air seeder[2].

1.4 Expected Research Contribution

The first model will develop and explain the relationship between the pressure drop, the solids flow rate and the average air velocity in the non-developed section of the gas-solid flow (i.e. very near to the point of particle drop). A very few research studies in the field of pneumatic conveying have attempted to develop and explain such a relationship in the non-developed section of the flow.

The second model uses a form of the dimensionless state diagram in a unique way to measure the product flow rate in an air seeder. Although this form of the dimensionless state

[1] The Geometric mean diameter was calculated with the formula provided by Mohsenin (1986).
[2] The operating conditions for wheat in an air seeder was considered between the average air velocity of 15 m/s and 30 m/s (Reynolds number range 57000-114000), and the wheat mass flow rate of 0.0204 kg/s and 0.1025 kg/s.

diagram is not uncommon in pneumatic conveying, a few studies have described a method to use this diagram to develop a model to measure the mass flow rate of conveyed product.

1.5 Thesis Overview

Background for this research with sufficient literature review is discussed in detail in Chapter 2. Chapter 3 is dedicated to the experimental setup. The experimental procedures and results are discussed in Chapter 4. This chapter also builds up the foundation for model development. Two models are developed and tested based on the experimental results in Chapter 5. The thesis ends with conclusions, summary and recommendations in Chapter 6.

.

Chapter 2. Background and Literature Review

The intent of this chapter is to discuss the necessary background and related literature that lead to the objective of this research. The chapter starts with some basic discussion on pneumatic conveying and its adaptation in air seeders in Section 2.1. The few available mass flow sensing technologies and the reason behind the selection of pressure drop to measure product mass flow rate are discussed in Section 2.2. Section 2.3 contains relevant prior work where attempts have been made to correlate conveyed product flow rate to pressure drop. This chapter concludes with the unanswered problems that come out of the literature review. Attempts have been made to look at these problems in this research.

2.1 Pneumatic Conveying of Solids

Pneumatic conveying is the transportation of solid particles typically in granular or powdered form by means of air, or in some special cases, other gases. The transportation usually takes place through pipelines. In industrial applications, pneumatic conveying systems have several advantages such as low maintenance cost, use of a single pipeline for transportation of multiple products, and less dust generation in the surrounding environment. On the other hand, it has the disadvantage of high power consumption per conveyed unit mass. A wide range of product sizes and shapes can be transported by means of pneumatic conveying. Typically, products having diameters up to 15 mm are most suitable (Klinzing et al., 2010).

The essential elements of many pneumatic conveying systems are prime movers, the feeding/mixing zone, the conveying zone and the gas-solid separation zone. Prime movers can be fans, blowers, compressors or vacuum pumps depending on the type and amount of pressure needed in the system (positive or negative). The feeding zone contains rotary feeders that regulate material flow into the air stream. The conveying zone consists of piping and accessories to transport solids from the source to the destination. For some pneumatic conveying systems, gas-solid separation becomes important to keep system pressure loss and particle segregation unaffected. Cyclone separators, reverse jet filters, reverse flow filters, and cartridge filters are some common types of gas-solid separators (Klinzing et al., 2010).

Based on average particle concentration, pneumatic conveying can be classified into dilute phase and dense phase conveying. The term mass loading ratio or mass flow ratio (μ) is a convenient way to identify dilute or dense phase flow. The mass flow ratio is the ratio of mass flow

rate of solids to mass flow rate of air. According to Klinzing et al. (2010), gas solid flow that has a mass flow ratio greater than 15 is a dense flow. Otherwise, it can be considered as dilute flow. Most industrial operations are carried out in the dilute regime.

An air seeder generally moves on rough terrain. It also has to make sharp turns during its operation. Transport of products on a moving frame of this nature is made possible by conveying through flexible pipelines. Moving air is the proper medium to carry solids through flexible conduits. For this reason, air seeders use pneumatic conveying to transport seeds and fertilizers to the ground. Air flow can be regulated and distributed very conveniently through the pipelines. This makes it possible to have better seed placement and distribution. Another advantage of using pneumatic conveying for seeding is that a single source of air can be used to convey different products at a time. Air seeders differ to some extent from conventional pneumatic conveying systems. There is no gas-solid separation zone in air seeders. Also, in some air seeders, multiple conveying lines transport different products in simultaneous operation.

2.2 Available Technologies for Mass Flow Sensing of Solids

Non-intrusive conveyed product mass-flow sensors for air seeders, were studied and reviewed by Noble (2008) in his report to CNH Canada Ltd. These candidate technologies, which also meet the constraints to be implemented on an air seeder, are electrostatic, ultrasound and optical sensing. The reviews in the report are summarized below.

Electrostatic sensors are based on the change in the electric field between the flow medium and an alternating electric field. The concept of using induced charge in the conveyed material to measure mass flow rate started in the late 1960s. For example, King (1973) developed a non-intrusive method that measured induced voltage to determine product flow rate. Electrostatic flow measurement is dependent on parameters such as particle type, size, velocity, mass flow, moisture content of air and density, etc. This method can only be used successfully in cases where mass flow rate is the dominant variable (Zhang, 2012). All of the parameters mentioned above are subject to change in an air seeder. Hence, this method is not suitable for air seeders. Moreover, devices used to detect changes in electric field perform better in the dense flow condition (Sun et al., 2008).

Velocimetry with ultrasound is well recognized in the industry with many commercially available devices. There are two methods of using ultrasound for measuring fluid flow: Doppler method and transient time method. The Doppler method requires reflectors of ultrasonic waves in

the fluid and is only used in a few special applications. The transient time method requires a sender and a receiver that are placed across the pipeline at an angle. This method has many industrial applications (Hofmann, 2000). Ultrasonic flow meters are reliable in measuring fluid flow only. However measurement of the flow rate of solids in a gas-solid flow is the main challenge for an air seeder. Hence, ultrasonic sensors are not suitable for this application.

Optical methods can also be used for flow measurements which detect interruption of light beams. This method is relatively inexpensive and has a fast response. But application of this technique is limited by dust generated from the conveyed material and complex installation (Noble, 2008). At present, an intrusive optical flow detection sensor is available for air seeders. This sensor can only detect the presence of flow but cannot measure the quantity of solids.

Evans et al. (2004) used flow-induced pipe vibration to measure air-water flow in a laboratory environment. But isolation and measurement of vibration induced by product flow in an air seeder in operating conditions, where there are many additional sources of vibration, is a subject requiring further in-depth study before proceeding further.

On the other hand, pressure drop along pipelines has always been an important parameter of interest in pneumatic conveying. It is a variable that is strongly dependent on the mass flow rates of solids. Previous studies have been made to measure product flow rate based on pressure drop, which will be discussed in Section 2.3. Pressure sensing elements are rugged enough to tolerate the difficult field conditions that an air seeder faces. They are inexpensive and easy to mount. For this reason, this research will also concentrate on product flow rate measurement in an air seeder based on pressure drop in the primary run of an air seeder.

2.3 Pressure Drop in Gas-Solid Flow

Pressure drop in gas-solid flow is a function of various factors such as, gas velocity, particle shape and density, forces acting on particles, particle-particle interactions, and particle wall interactions. Hence, calculation of pressure drop through a generalized model has not been possible so far. However, irrespective of the types of solids being conveyed, the trend of pressure drop is similar against air velocity in horizontal conveying. The state diagram (Zenz and Othmer, 1960) represents the relationship between pressure drop and air velocity in pneumatic conveying. Although this research is not directly focused on identifying the flow regime by plotting the state diagram, a form of the dimensionless state diagram will be used to develop one of the models to measure mass flow rate.

2.3.1 The State Diagram

Introduced by Zenz and Othmer (1960), the state diagram is a convenient way to describe gas-solid flow. It is a plot of pressure gradient versus superficial air velocity at any point in a pipeline. Figure 2-1 shows the typical nature of a state diagram adapted from Klinzing et al. (2010). The line AB represents the case when only air is flowing through the pipeline. With increasing air velocity, the pressure drop also increases due to the rise in frictional losses. When solid particles are introduced into the air, the line follows the path CDEF for a particular solids flow rate. At higher velocities, particles are fully suspended and the pressure drop is caused by drag on the particles and particle-wall interactions. As air velocity is reduced, the particle velocity also reduces, resulting in less frictional losses. Hence, pressure drop gradually decreases from point C to D. At point D, the air velocity is just enough to keep the particles suspended in the air. This velocity is known as the saltation velocity. When the velocity is reduced below the saltation velocity, particles are no longer completely suspended in air and move forward by means of fluidized bed behavior causing an increase in pressure drop due to higher solids loading ratio.

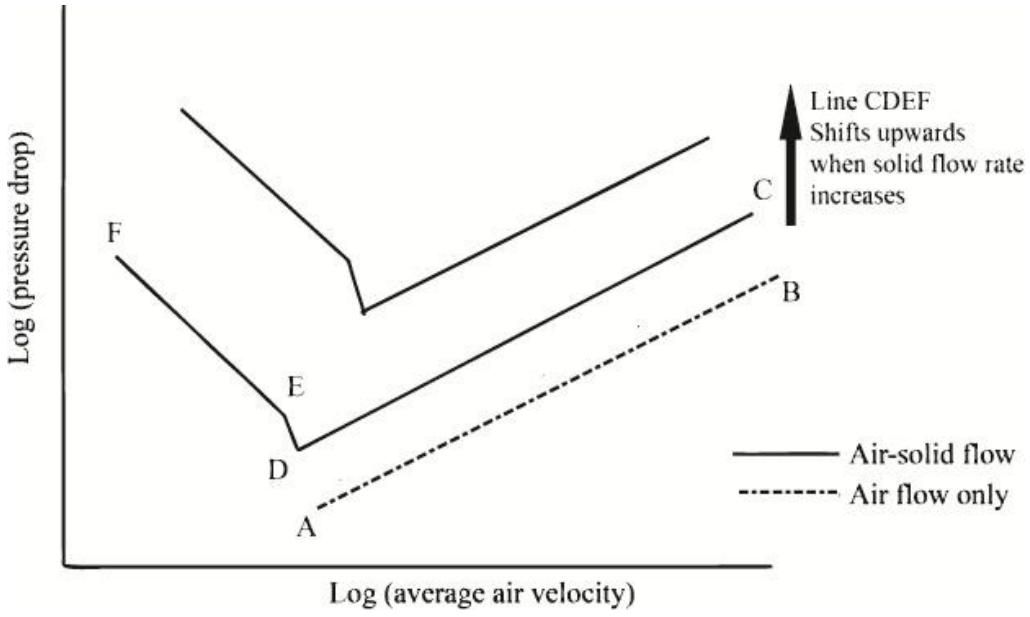

Figure 2-1 State Diagram for gas-solid flow (Klinzing et al., 2010)

With gradual increase of solid mass flow rate for the same velocity range, the line CDEF shifts upwards, but the nature of the graph remains the same.

Another form of the state diagram, known as the dimensionless state diagram, can be obtained by plotting mass loading ratio (μ) vs. Froude number (Fr) in log-log format. The Froude number is a dimensionless number and can be calculated by Equation 2-1,

$$Fr = \frac{v}{\sqrt{gD}} \ , \qquad 2\text{-}1$$

where v is the air velocity [m/s],

g is the acceleration due to gravity [m/s^2], and

D is the pipe diameter [m].

Figure 2-2 shows the basic shape of the dimensionless state diagram.

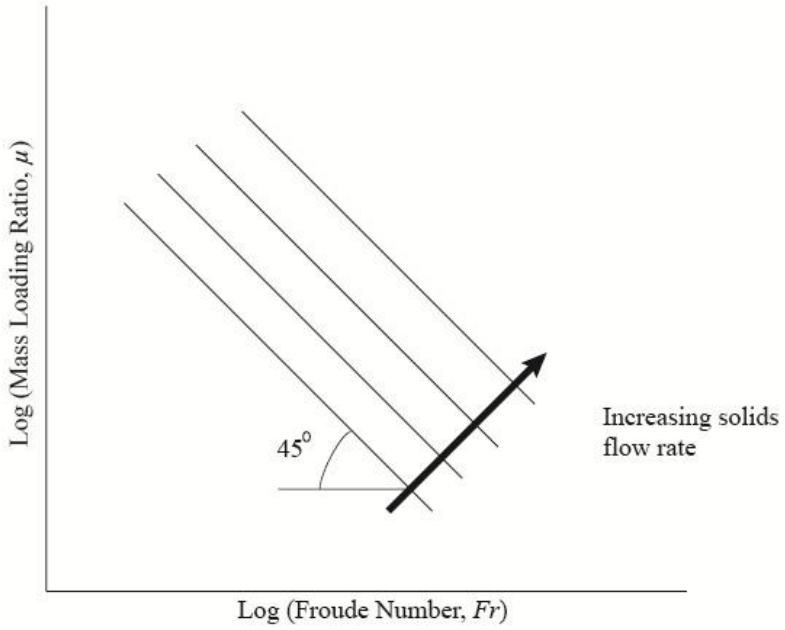

Figure 2-2 The dimensionless state diagram (Klinzing et al., 2010)

Regardless of the solids being conveyed, a series of parallel lines is obtained when the dimensionless state diagram is plotted. The spacing between the lines is proportional to the mass flow rate of solids. Usually, the dimensionless state diagram is used to check the reliability of experimental data (Klinzing et al., 2010).

2.3.2 Measuring Solids Mass Flow Rate using Pressure Drop

When it comes to the use of pressure drop in conveying lines for a non-intrusive and online method to measure product flow rate, the work of Cabrejos and Klinzing (1992) is the most relevant to this research. However, it was Binsirawanich (2011) who made one of the first attempts to correlate pressure drop with product flow rate for an air seeder.

Based on the relationship proposed by Gasterstadt (1924), Cabrejos and Klinzing (1992) described an approach to determine solids flow rate for horizontal conveying. They were motivated to adopt this approach as Farbar (1949), Hinkle (1953) and Rizk (1973) obtained satisfactory agreement between their experiments and Gasterstadt's findings. According to this relationship, for higher gas velocities and a fully-developed flow, the specific pressure drop has a linear relationship with solids loading ratio. Here, fully-developed flow is the region where particles are assumed to have attained a constant average velocity and specific pressure drop (α) is the ratio of the pressure drop per unit length of solid-air mixture to pressure drop per unit length of air only.

The relationship is shown in Equation 2-2,

$$\alpha = 1 + k\mu \qquad 2\text{-}2$$

where α is the specific pressure drop [dimensionless],

μ is the mass loading ratio [dimensionless], and

k is the slope of the straight line.

All the previous studies showed that, for gas velocities 50% above the saltation velocity, the value of k is independent of gas velocity. Cabrejos and Klinzing (1992) carried out their experiments with 450-µm spherical glass beads conveyed by air inside 50-mm and 41-mm I.D. straight horizontal pipes. Both the test sections were 14.5 m long. Pressure drop was measured 1 m apart in the fully-developed region of the test sections. For both the test sections, their specific pressure drop vs. solids loading ratio plot agreed with equation 2-1 when the air velocity was sufficiently above saltation. That is, the relationship is linear, and the value of k is constant for a particular diameter of pipe within the tested velocity range as shown in Figure 2-3.

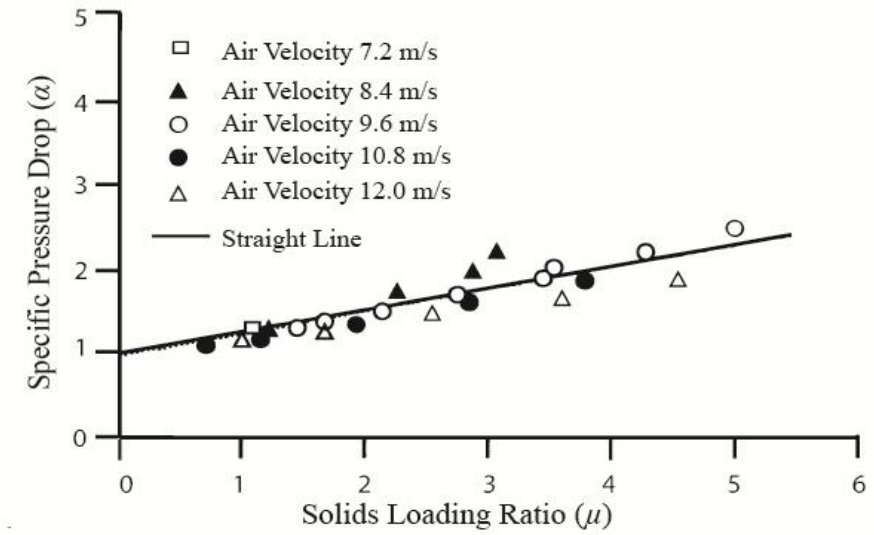

Figure 2-3 Specific pressure drop for horizontal conveyance of glass beads in a pipe of I.D. = 50 mm (adapted from Cabrejos and Klinzing, 1992)

By determining the value of slope, *k* from the graph and with the help of Equation 2-2, Cabrejos and Klinzing (1992) were able to measure solids flow rate in their experiment with good accuracy, but, the conditions for accurate measurement in their method are:

1) The flow has to be fully developed. That is, measurement of pressure drop must be done at a significant distance from the point of particle drop, where the particles have attained a constant velocity.
2) Air velocity should be typically 50% above saltation velocity.

Binsirawanich (2011) made one of the first attempts to use pressure drop to measure product flow rate for an air seeder. His approach to correlate pressure drop to product flow rate was based on an empirical relationship developed via experiments conducted on a laboratory prototype air seeder. He conducted tests on canola, wheat, chickpea and granular fertilizer while measuring pressure drop between two points in an inclined test section. The idea behind an inclined test section was to elevate the pressure drop. The test section is shown and marked in Figure 2-4.

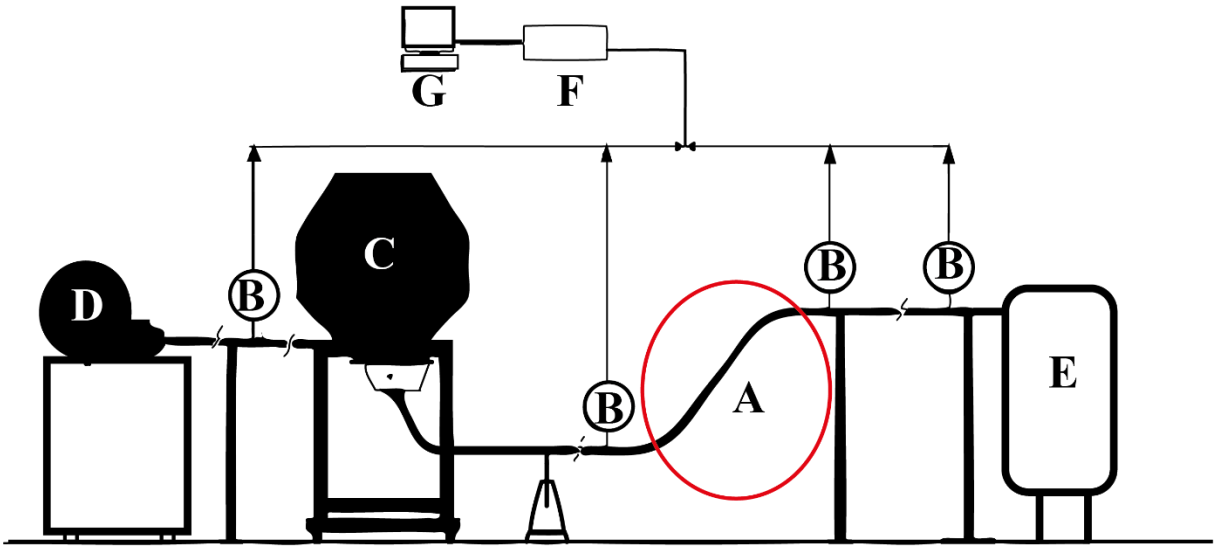

Figure 2-4 Experimental setup of Binsirawanich (2011) with inclined test section which consisted of two 45-degree bends each with a 0.45-m radius. (A. Test section B. Pressure sensors C. Seed tank D. Fan E. Collection tank F. DAQ Module G. Computer)

Binsirawanich (2011) developed his model through regression analysis on collected experimental data. The model is shown in Equation 2-3 (Binsirawanich et al., 2013),

$$M_s = M_a \left[\left(a_1 e^{a_2 \cdot v} \right) \Delta p - ln\left(b_1 v^3 + b_2 v^2 + b_3 v + b_4 \right) \right] \qquad 2\text{-}3$$

where M_s is material mass flow rate [kg/s],

M_a is air mass flow rate [kg/s],

Δp is the pressure drop [kPa],

v is the average air velocity [m/s], and

a_1, a_2, b_1, b_2, b_3 and b_4 are coefficients that have different values for each product.

The developed model was very accurate when applied to individual data sets for all four products. The overall percent errors of the material mass flow rate estimates based on their medians varied between 3% and 5%. But when data from all four materials were combined, the model was not as accurate as it was in case of individually tested materials.

An interesting observation was made by Noble (2013) when Binsirawanich's (2011) experimental data were rearranged and plotted according to the approach described by Cabrejos

and Klinzing (1992). Although Binsirawanich conducted experiments with an inclined test section, the plot of specific pressure drop vs. solids loading ratio showed a trend quite similar to that of Cabrejos and Klinzing (1992). The plot is shown in Figure 2-5.

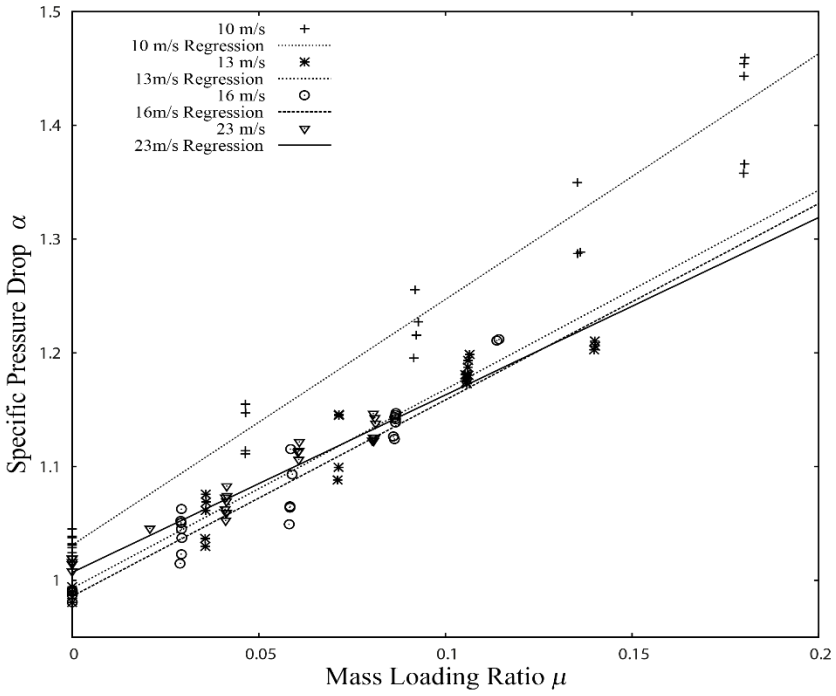

Figure 2-5 Specific pressure drop vs. mass flow ratio from Binsirawanich's data plotted by Noble (2013)

To determine the proper approach for model development in this research, initial experiments were performed with wheat pneumatically conveyed in a straight horizontal primary run (pipe I.D. of 57.3 mm and length 14 m) of a prototype air seeder (a detailed description of the experimental setup is given in Chapter 3). After plotting the specific pressure drop vs. mass loading ratio graph, strong agreement was observed with Equation 2-2. For higher velocities, a straight line with fairly constant slope (k) was obtained in the fully-developed region of the pipe. For lower velocities, the value of slope varied. Figure 2-6 shows a plot of specific pressure drop vs. mass loading ratio from a preliminary experiment with wheat.

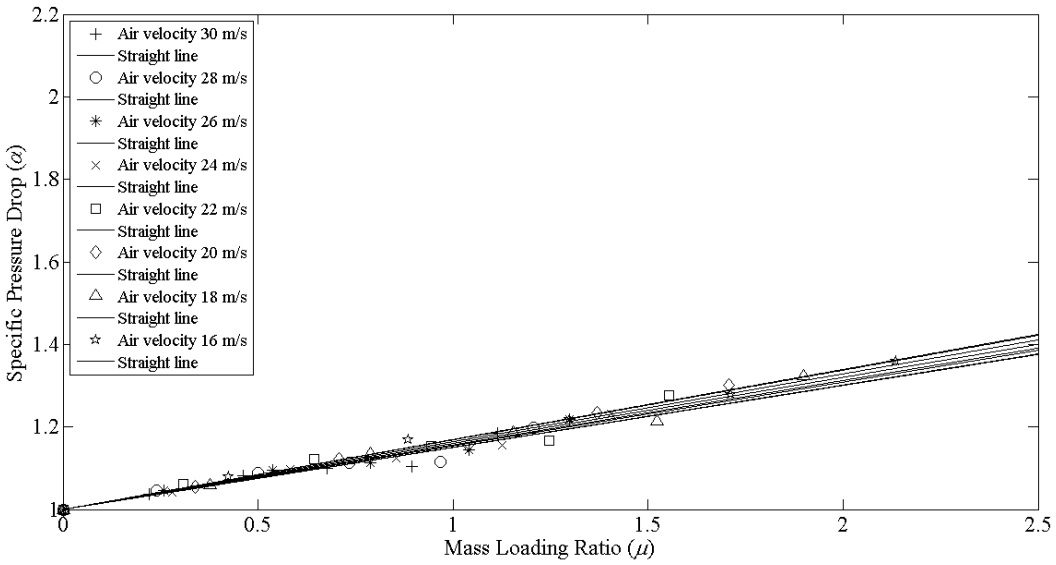

Figure 2-6 Specific pressure drop vs. mass loading ratio from initial experiments with wheat (pressure drop measured between 7.3 m and 8.2 m from product inlet)

Figure 2-7 is a plot of the value of slope (k) against air velocities in the developed zone of the test section from initial experiments with wheat. This also indicates that above a certain velocity, the value of the slope is constant throughout.

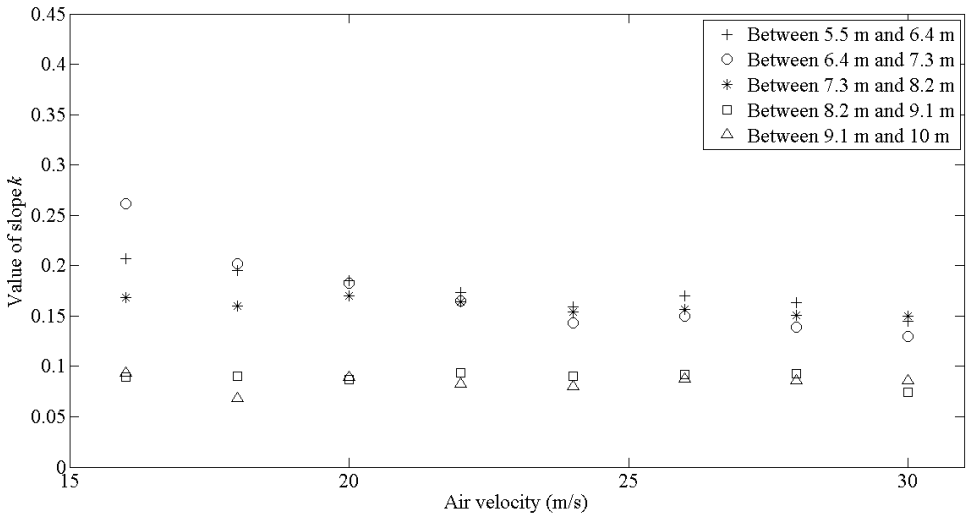

Figure 2-7 Slope (k) of equation 2-1 vs. average air velocity from initial experiments with wheat

2.4 Conclusion

The mass flow measurement method described by Cabrejos and Klinzing (1992) was meant for gas velocities well above the saltation velocity (typically 50% above). An air seeder may operate at a lower velocity range to reduce conveying power and minimize seed damage. Hence, for equation 2-2 to be applicable for an air seeder, the relationship between the variable values of *k* to lower air velocities must be studied. Not only Cabrejos and Klinzing (1992), but a number of researchers also verified that the linear relationship between pressure drop and mass loading ratio holds true for fully-developed flow (Vogt and White, 1948; Kraus, 1980; Woodcock and Mason, 1987). This fact is evident in the preliminary studies of this research also. To ensure that the flow is fully developed, pressure difference is measured far away from the location of solids release so that it can be assumed that the particle velocity is constant. But so far no air seeder has a straight horizontal primary run of such length as to attain a fully-developed flow. The first 1 m or so from the metering box is the only available straight horizontal section in an air seeder at present. For this reason, pressure drop vs. mass loading ratio relationship at various air velocities must be studied in a non-developed flow section. This means that although the method described by Cabrejos and Klinzing (1992) holds true for horizontal flow of wheat, certain modification should be made to their described relationship to develop a model that can estimate mass flow rate in the non-developed section of a pipe.

Another possible method to develop a model to measure solids flow rate is by utilizing the features of the dimensionless state diagram (Figure 2-2). But the dimensionless state diagram cannot be directly used to solve for mass flow rate of solids. Because the spacing between the lines is a function of the mass flow rate of solids (Figure 2-2). On the other hand, mass loading ratio is plotted against the Froude number (*Fr*). If an attempt is made to develop a relationship between these three parameters, the mass flow rate of solids will be eliminated from the equation. Hence, indirect method to solve the mass loading ratio vs. Froude number relationship must be developed to construct a model based on the dimensionless state diagram.

Chapter 3. Experimental Set-up

Experiments were conducted in a laboratory prototype air seeder configured to carry out multiple research projects simultaneously. This chapter will discuss only that portion of the setup which is relevant to this research. Binsirawanich (2011) described most components of the setup in an elaborate manner. Hence, those components will be described briefly along with the additional components and the modified venturi-based air velocity measurement. Table 3-1 lists the equipment for the setup.

Table 3-1 List of equipment for the experimental set-up to develop models for mass flow measurement

No	Equipment Name	Comment
1.	Fan with VFD (Variable Frequency Drive)	Prototype Seeder
2.	Seed Tank and Metering System	
3.	57.3-mm ID Acrylic Pipe (14.5-m length)	Test Section
4.	2 m × 1 m × 1 m Wooden Box for collecting seeds	
5.	2 × 0-40 in H_2O Pressure Sensors (Dwyer Instruments; Model 616-5)	Air Flow and Velocity Measurement
6.	Venturi Flow Meter	
7.	2 × 0-20 in H_2O Pressure Sensors (Dwyer Instruments; Model 616-4)	Pressure Measurement
8.	10 × 0-1 in H_2O Pressure Sensors (Dwyer Instruments; Model 648B-04)	
9.	8 × 0-2.5 in H_2O Pressure Sensors (Dwyer Instruments; Model 648B-05)	
10.	LabVIEW 2012 and computers	Data Acquisition and Fan Control
11.	NI 9203 Input module (8 channel, 16 bit, ±20 mA, analog)	
12.	NI USB-6009 (8 single ended analog input, 2 analog output, 12 digital I/O, 32 bit, USB interface)	
13.	HTM 25X0LF – Temperature and Relative Humidity Module	
14.	MPXHZ6116A Barometric Pressure Sensor	

Figure 3-1 shows a schematic of the experimental set-up. The numbers correspond to the list in Table 3-1. For convenience, the groups of pressure sensors in 8 and 9 are represented by a single block.

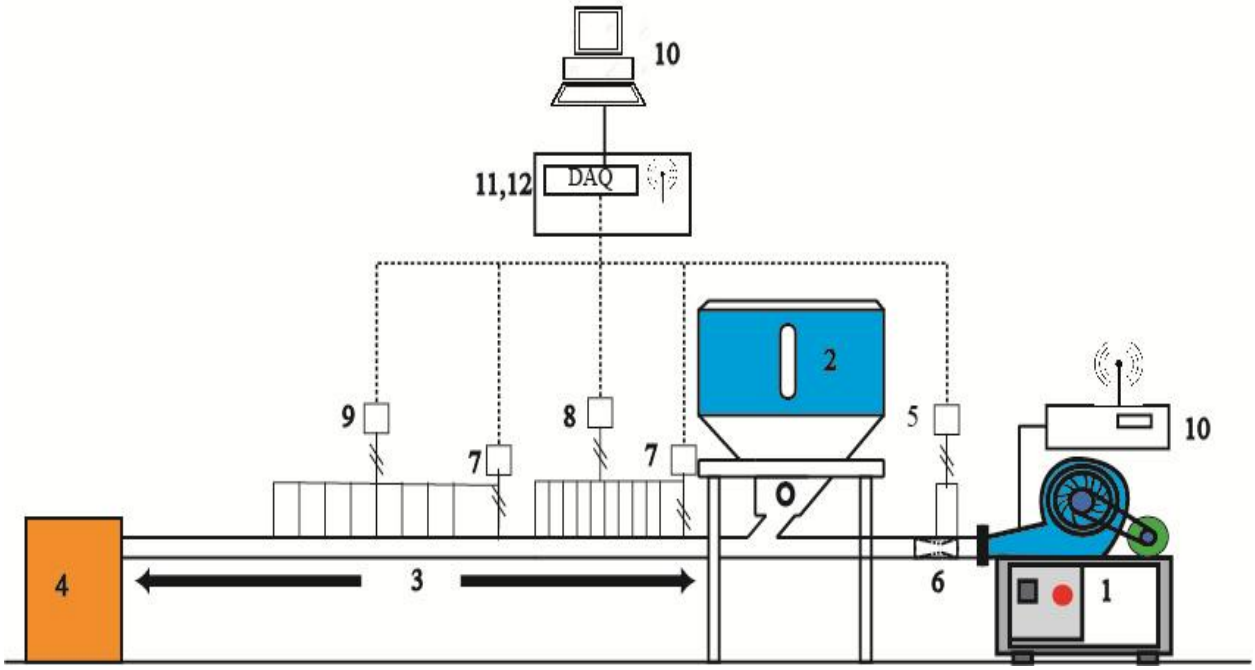

Figure 3-1 Experimental set-up for developing model to estimate mass flow rate of wheat (1. Fan with VFD; 2. Seed Tank and Metering system; 3. Acrylic pipe (test section); 4. Seed collection box; 5. 0-40 inch H_2O pressure sensors; 6. Venturi Flow meter; 7. 0-20 in H_2O Pressure Sensors; 8. 0-1 in H_2O Pressure Sensors; 9. 0-2.5 in H_2O Pressure Sensors; 10. Computer; 11. NI 9203 Input module; 12. NI USB-6009)

Air generated by the fan (1) flowed through a 57.5-mm-ID steel pipe to the air cart simulator (2). The steel pipe had a venturi (6) installed inside it for air velocity measurement. The air cart simulator (2) consisted of seed tank, and a meter roller which was connected to a stepper motor. With the rotation of the meter roller, seeds from tank were dispensed through a flexible tube to the test section (3). Seeds were conveyed by air through the test section to the wooden collection box (4). DAQ (Data Acquisition) modules (11, 12) received signals from the sensors (5, 7, 8, 9, 11,14) and the measured quantities were recorded by one of the computers (10). Another computer was dedicated for fan control which established wireless communication with the data acquisition computer. User inputs for controlling the fan or the speed of the stepper motor were also transmitted through the DAQ modules. A computer program (Noble and Keep, 2013) written in LabVIEW

2012 was used for data collection and fan control. The program also had a user interface for input and monitoring. Some key components of the set-up are described briefly in the following sections.

3.1 Fan with Motor and Variable Frequency Drive

The fan was driven by an electric motor, the speed of which could be regulated with a variable frequency drive. The 3.7 kW, 60 Hz, 230 VAC, 3-phase electric motor was connected to the fan via a belt drive. Figure 3-2 shows the fan, motor and control box mounted on a cart.

Figure 3-2 : Components of the fan unit (A. The Fan; B. The Motor; C. The Control Box that contains the Variable Frequency Drive)

The variable frequency drive (Automation Direct, Model: GS2-25P0) regulated fan speed proportional to a 4 mA to 20 mA input signal (Binsirawanich, 2011). The fan system had the option to be operated in both auto and manual mode with an emergency stop switch within the reach of the operator.

3.2 Venturi Flow Meter for Air Velocity and Air Mass Flow Rate Measurement

Using the continuity and Bernoulli's equation, the venturi flow meter measures air velocity and flow rate by measuring pressure difference between the entrance and the throat of a reduced

cross-section. The venturi flow meter used in the experimental set-up was rapid prototyped according to ISO standards (ISO 5167-4, 2003). Figure 3-3 shows a cross-sectional view of the venturi (Keep 2014).

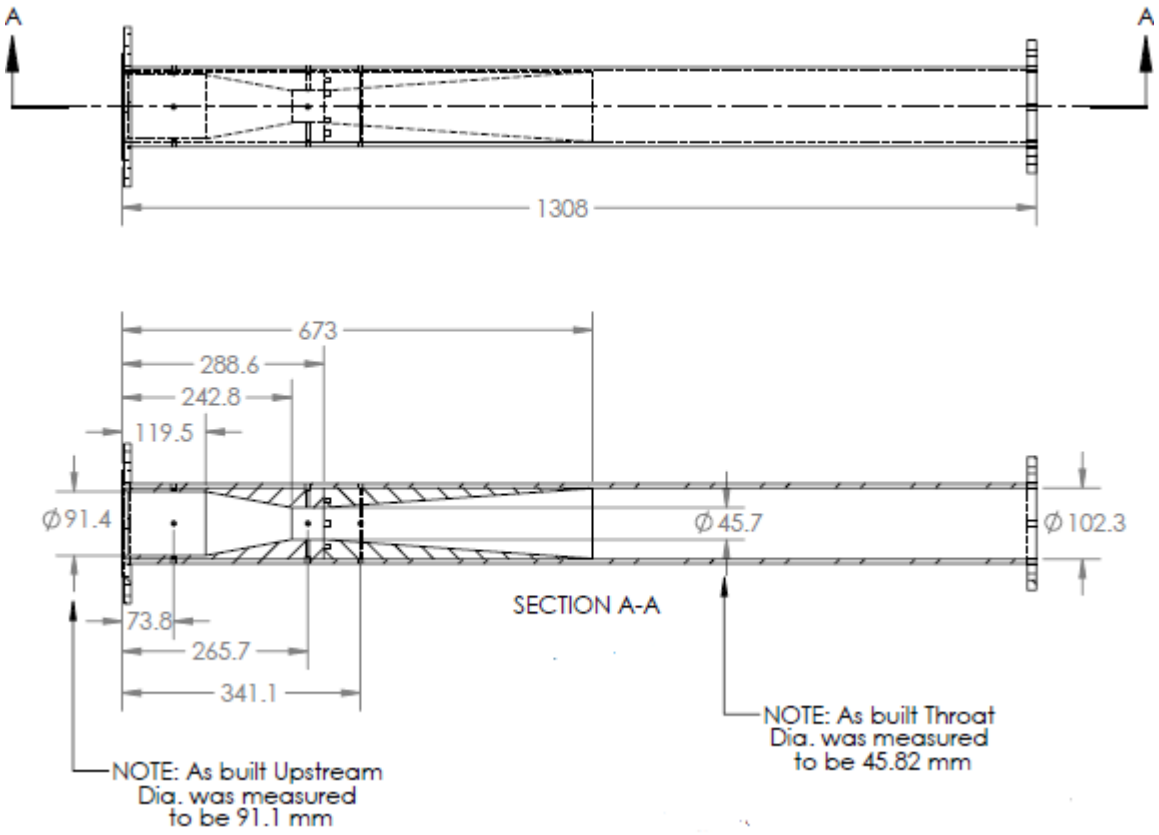

Figure 3-3 : Sectional view of the venturi flow meter (Keep, 2014). Direction of flow is from left to right. All dimensions in mm

The venturi was calibrated against velocity readings obtained from a Pitot tube traverse method on a 0.1107-m-ID pipe with 48 points (4 angular positions, 12 radial points in each position). Two pressure sensors (0-40 inch H_2O) were installed to measure the pressure difference between the entrance and the throat of the venturi. According to ISO 5167-4: 2003, the equation for air flow rate calculation also requires the air density and viscosity. The atmospheric pressure sensor, relative humidity and temperature sensors were installed for calculating the air density and viscosity at working conditions.

3.3 The Seed Tank and Meter Roller

The seed tank acts as storage for seed or fertilizer in an air seeder. Wheat from the seed tank was introduced into the air stream by gravitational assistance and by rotation of the meter roller. The meter roller ensured grains were introduced into the air stream at the required rate. The "Fine" type meter roller was coupled with a stepper motor. For dispensing wheat at a particular rate, the stepper motor was operated at a certain speed. A calibration between the stepper motor speed and the mass flow rate of wheat was performed beforehand by manually collecting and weighing wheat at a particular speed for a certain amount of time. Figure 3-4 shows the seed tank and metering system.

Figure 3-4: The Seed Tank and Metering system (A. Tank; B. Stepper Motor; C. Metering Box)

The fine meter roller resided inside the metering box, which is indicated by the red arrow in Figure 3-4. The speed of the stepper motor was set and maintained through the LabVIEW program written for data acquisition (Noble and Keep, 2013).

3.4 The Test Section

The test section for the experiments was a straight 14.5-m-long horizontal acrylic pipe (I.D 57.3 mm). Several supports were placed under the pipe to maintain its level. Figure 3-5 shows the test section.

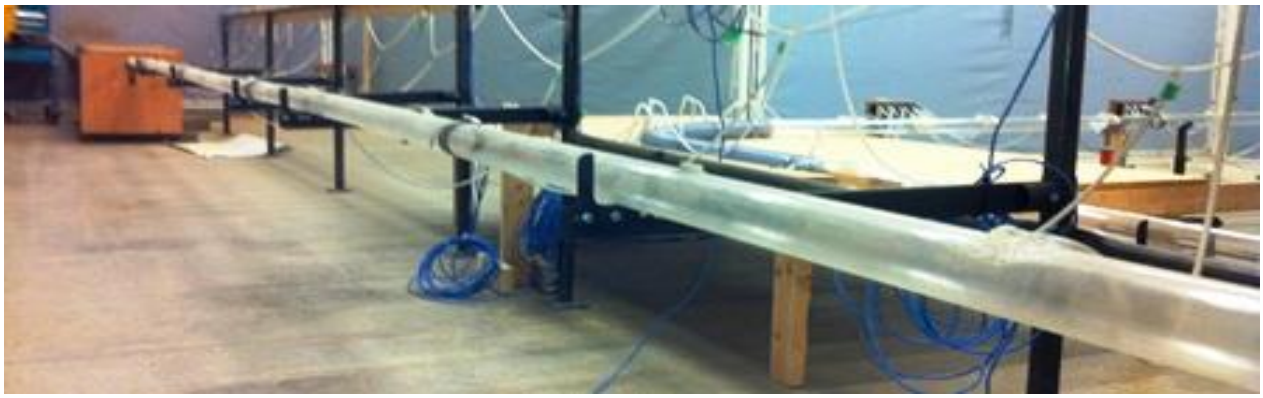

Figure 3-5: The straight horizontal test section used for model development

In total, 20 pressure taps were installed on the test section. These taps were connected to the pressure sensors through 7.5-mm flexible rubber tube. The first 11 pressure taps were installed in between the first 0.3 m and 2.3 m of the pipe at 20 cm apart. The second set of 9 pressure taps was installed at 90 cm apart in between the 2.3 m and 10 m points of the pipe. The reason for such spacing of the pressure taps is to observe the nature of pressure drop in the developed and non-developed section of the flow.

3.5 The Pressure Sensors

The first pressure sensor of the set of 11 sensors that was mounted in between 0.3 m and 2.3 m of the test section had an operating range 0-20 inch of H_2O (Dwyer Model 616-4, accuracy ±0.25% F.S. (Full Scale)). It measured the static gauge pressure at 0.3 m. The next 10 sensors had an operating range of 0-1 inch of H_2O (Dwyer Model 648B-04, accuracy ±0.8% F.S.) each. These sensors measured the differential pressure across intervals of 20 cm starting from 0.3 m to 2.3 m of the pipe. The range of the differential pressure sensors was selected based on the assumption that pressure difference would be low at intervals of only 20 cm. Figure 3-6 shows the pressure sensors that were used to measure the static and differential pressures at different locations of the test section.

Figure 3-6: Pressure sensors that were used to measure static and differential pressures in the test section (A. 0-20 inch H_2O; B. 0-1 inch H_2O; C. 0-2.5 inch H_2O)

Similarly, the first pressure sensors of the set of nine sensors that was mounted in between 2.3 m and 10 m of the test section had an operating range of 0-20 inch H_2O (Dwyer Model 616-4, accuracy ±0.25% F.S.). As it measured the static pressure at a distance 2.3 m from the metering box, the next 8 sensors in this set had an operating range of 0-2.5 inch H_2O (Dwyer Model 648B-05, accuracy ±0.8% F.S.). These sensors measured differential pressure at intervals of 90 cm. All the sensors had a 4 – 20 mA output signal in. The sensors were calibrated by adjusting their span and zero in between their working ranges.

Chapter 4. Data Collection and Experimental Results

The experimental results for development of a model to measure solids mass flow rate for an air seeder are discussed in this chapter. The data collection procedure and reasons for collecting data in two sets from two different regions of the test section are discussed in Section 4.1. The results and outcomes of the first sets of experiments are described in Section 4.2. Section 4.3 describes the second set of experiments. Section 4.4 looks at the physical interpretation of the results from both sets which leads to model development in the next chapter (Chapter 5).

4.1 Data Collection Procedure

Cabrejos and Klinzing's (1992) approach for solids mass flow measurement presents a novel way to correlate the variables (pressure drop, solids flow rate and air velocity) for fully accelerated solid particles. If such a relationship also exists for horizontal conveying of wheat, it could be used as the required model for solids mass flow measurement. But the shapes of wheat grains are more elliptical in nature and their sizes are also much larger than the glass beads used by Cabrejos and Klinzing. Hence, the first sets of data were collected to see if the linear relationship between specific pressure drop and mass loading ratio, as mentioned by Cabrejos and Klinzing, exists. The second sets of data were collected to observe possible changes in the relationship when the particles are not fully accelerated.

4.1.1 Data Set 1

Data Set 1 (Appendix A.1) was collected in between 2.5 m and 10 m of the straight horizontal test section. Nine sensors (0-1 inch H_2O) were used to measure pressure drop across this length. All the sensors were placed 90 cm apart across the length as described in Chapter 3. For each set of differential pressures measured by a sensor at a particular location, specific pressure drop (α) vs. mass loading ratio (μ) was plotted for different air velocities. Pressure drops were measured across different locations to see if the value of the slope of the straight line obtained from the plot approached a constant value when the flow is fully developed and particles are fully accelerated, as indicated by Cabrejos and Klinzing (1992). Five mass loading ratios were considered by setting the metering roller speed to 10, 20, 30, 40 and 50 RPM. A calibration curve (Keep, 2013) was used to convert the stepper motor speeds to kg/s. Air velocity was decreased from 30 m/s to 13 m/s with a decrement of 1 m/s. For each air velocity, data were recorded for 60 seconds. A minimum of three test runs was performed for each set of data points and then the values from these tests were averaged to plot specific pressure drop vs. mass loading ratio. The minimum and

maximum range of roller speed and air velocity were chosen based on practical operating conditions for an air seeder operating with wheat.

4.1.2 Data Set 2

Due to design constraints, the primary run of an air seeder cannot usually be straight and horizontal up to the point where the particles are fully accelerated. A straight run can only be found within the first meter or two from the metering box in an air seeder. However, the wheat kernels may or may not be fully accelerated within such a short distance. To observe the nature of the relationship that exists between specific pressure drop and mass loading ratio when pressure drop is measured in a section close to the solids inlet, Data Set 2 (Appendix A.2) was collected. Pressure drop was measured between 0.3 m and 2.3 m from the metering box for Data Set 2. Eleven pressure sensors placed 20 cm apart from each other were used to measure pressure drop within these two meters. These sensors were placed to observe whether there was any non-linearity in the streamwise pressure drop and also, to look for trends in the specific pressure drop vs. mass loading plot. The air velocity and the mass flow were varied in a similar manner as Data Set 1.

4.2 Results from Data Set 1

The two major findings of Cabrejos and Klinzing's (1992) experiments were:

1. There is a linear relationship between specific pressure drop and mass loading ratio when the particles are fully accelerated, and
2. A constant value of the slope exists in that linear relationship when the air velocity is at least 50% higher than the saltation velocity.

Data Set 1 was collected to see if these findings hold true in the case of wheat. The location in the pipe where the flow becomes fully developed and wheat kernels attain full acceleration was not known for these experiments. Hence, pressure drop was measured at different points within the downstream part of the test section. The general assumption was that the further the wheat grains travel after being dispensed from the metering box, the better the possibility of obtaining a fully-developed flow. This implies that if the relationship described by Cabrejos and Klinzing holds true for wheat, pressure drop measured from the sensors placed at the farthest end of the test section will yield the best agreement. Figure 4-1 is the plot of specific pressure drop vs. mass loading ratio when pressure drop is measured in between 2.5 m and 3.4 m of the test section.

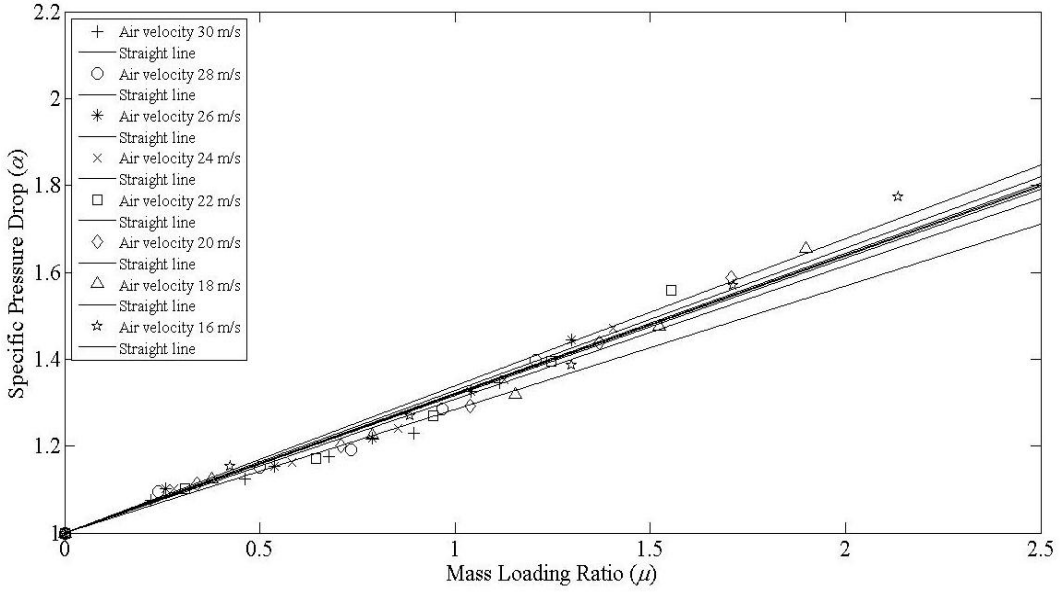

Figure 4-1: Specific pressure drop vs. mass loading ratio for horizontal conveying of wheat (pressure drop measured between 2.5 m and 3.4 m).

Within the tested range of velocity and mass loading ratio, the relationship was found to be linear. The values of the slopes were from 0.28 to 0.32 for velocities from 30 m/s to 20 m/s and increased gradually with the reduction of velocity.

Moving farther downstream in the flow, Figure 4-2 shows specific pressure drop vs. mass loading ratio where the pressure drop was measured between 4.6 m and 5.5 m of the test section.

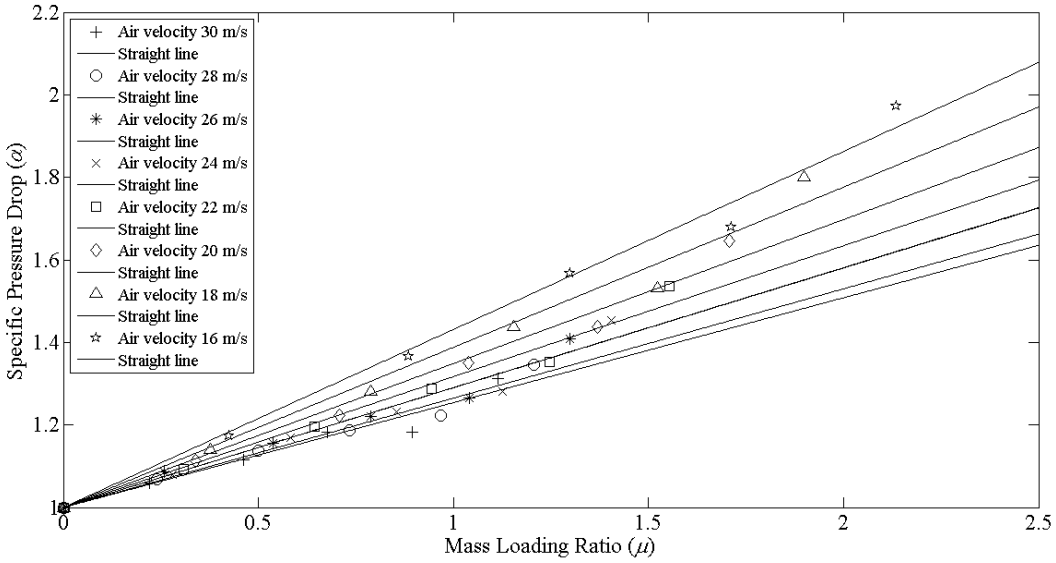

Figure 4-2: Specific pressure drop vs. mass loading ratio for horizontal conveying of wheat (pressure drop measured between 4.6 m and 5.5 m).

A linear relationship is observed once again. In this case, the values of the slopes for higher velocities (above 20 m/s) remain in the range of 0.25 to 0.31, and the trend of increasing values for decreasing velocities remains the same.

Figure 4-3 shows the specific pressure drop vs. mass loading ratio relationship from measurement of pressure drop between 7.3 m and 8.2 m of the test section. Straight lines with slope values ranging from 0.15 to 0.16 for a velocity range of 30 m/s to 20 m/s are observed. From this plot it becomes evident that the values of slopes approach a constant value at higher velocities as particles travel farther along the test section.

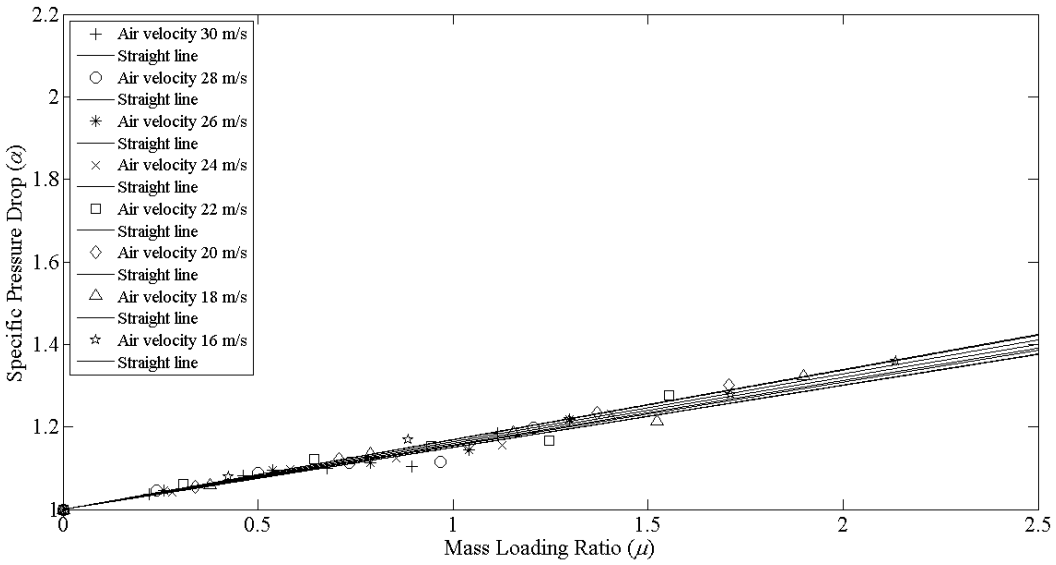

Figure 4-3: Specific pressure drop vs. mass loading ratio for horizontal conveying of wheat (pressure drop measured between 7.3 m and 8.2 m).

Measurement of pressure drop from the last pair of sensors (placed between 9.1 m and 10.0 m) shows even better agreement with Cabrejos and Klinzing's (1992) findings. The specific pressure drop vs. mass loading ratio plot shown in Figure 4-4 shows an almost constant value of slope of 0.09 for velocities ranging between 30 m/s and 20 m/s. For lower velocities, the values of slope increase gradually following the trend shown in the other plots. As the interval of differential pressure measurement shifts downstream along the pipe, it can be observed that the overall values of the slope decrease. Lower values of slope indicate lesser rate of change in pressure drop for different mass loadings. The reason for this is that the particles approach full acceleration and suspension as they travel along the test section. This minimizes pressure drop due to particle acceleration and friction.

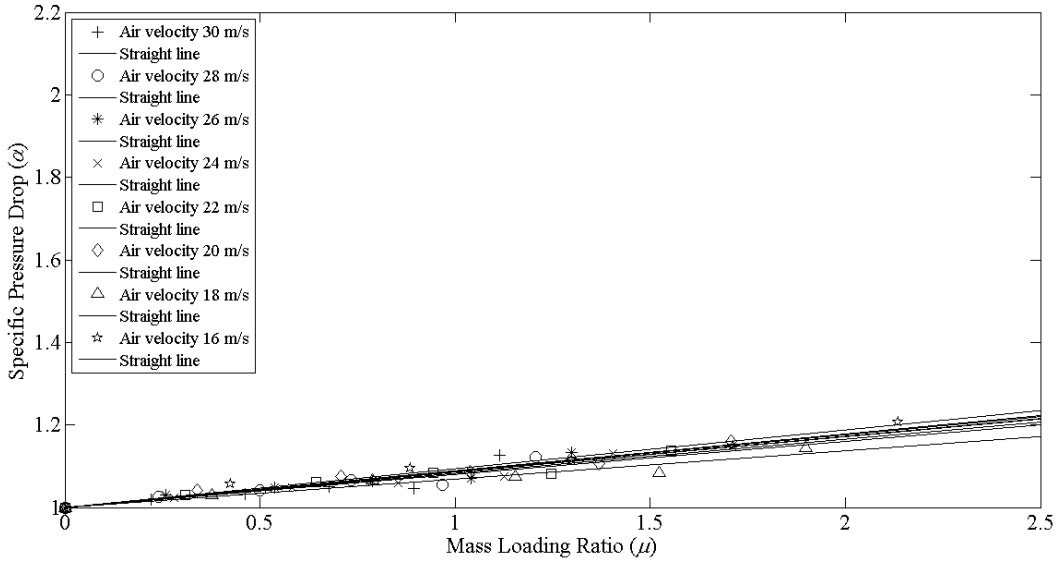

Figure 4-4 Specific pressure drop vs. mass loading ratio for horizontal conveying of wheat (pressure drop measured between 9.1 m and 10 m).

The values of the slopes (k) for different air velocities for the cases mentioned above are given in Table 4-1.

Table 4-1: Values of the slopes at different air velocities

Air Velocity (m/s)	Value of Slope (k) (2.5 m -3.4 m)	Value of Slope (k) (4.6 m -5.5 m)	Value of Slope (k) (7.3 m -8.2 m)	Value of Slope (k) (9.1 m -10.0 m)
30	0.28	0.25	0.15	0.09
28	0.31	0.26	0.15	0.09
26	0.32	0.29	0.16	0.09
24	0.32	0.29	0.15	0.08
22	0.33	0.32	0.16	0.08
20	0.32	0.35	0.17	0.09
18	0.32	0.39	0.16	0.07
16	0.34	0.43	0.17	0.09
14	0.39	0.42	0.16	0.11

Figure 4-5 shows the values of the slopes (k) for pressure sensors placed in between 4.6 m to 10 m of the test section.

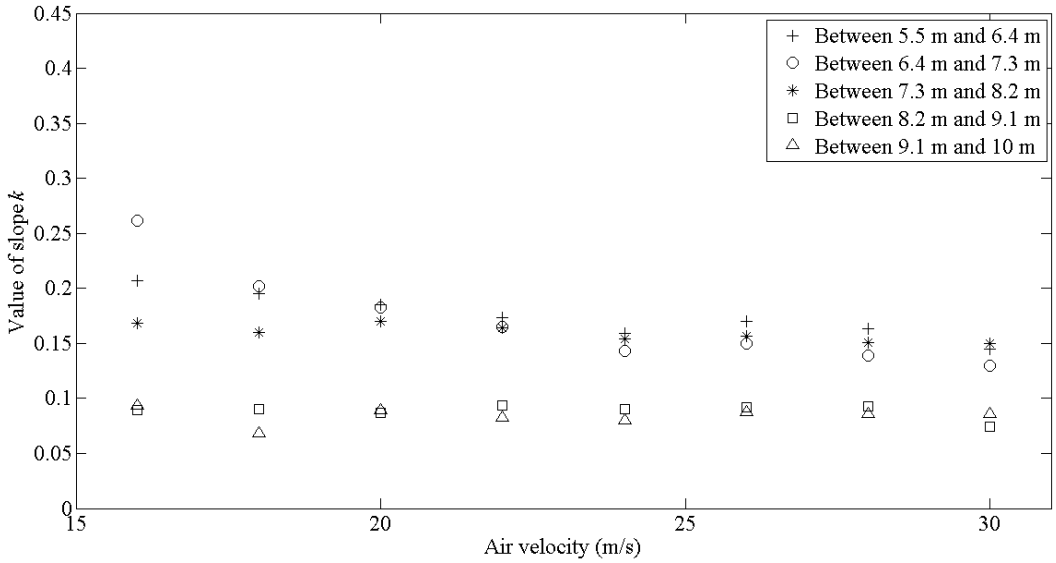

Figure 4-5: Values of the slope (k) from specific pressure drop vs. mass loading ratio plots for different air velocities (pressure drop measured at 5 locations in the test section).

This plot summarizes Data Set 1. It can be seen that within the velocity range of 20 m/s to 30 m/s, the value of the slope remains more or less constant. For locations where pressure drop was measured closer to the metering box, the values of the slopes fluctuate around a constant value. As pressure measurement moves towards the more developed section of the pipe, the values of slope almost become constant within the velocity range. Hence, it can be said that for horizontal conveying of wheat, the findings of Cabrejos and Klinzing (1992) are applicable. If the primary run of an air seeder was straight and horizontal long enough for the wheat particles to be fully accelerated, a mass flow sensor could be constructed based on these findings from Data Set 1. But in reality, the length of a straight horizontal run from the metering box of an air seeder is much shorter (usually 1 m or so). This leads to the collection and analysis of Data Set 2.

4.3 Results from Data Set 2

It was expected that the observations from Data Set 2 would not agree with the linear relationship between specific pressure drop and mass loading ratio, as pressure drop was measured in locations very close to the metering box (between 0.3 m to 2.3 m). The analysis of Data Set 2 started with a plot of streamwise pressure drop at different mass flow rates and air velocities. This was done to see if any non-linear trend existed in streamwise pressure drop. Figures 4-6 (a) and 4-6 (b) show pressure drop between 0.3 m and 2.3 m for maximum (30 m/s) and minimum (13 m/s) air velocities at three different mass flow rates of wheat. The graphs are plotted separately for better resolution as the pressure drop is very low.

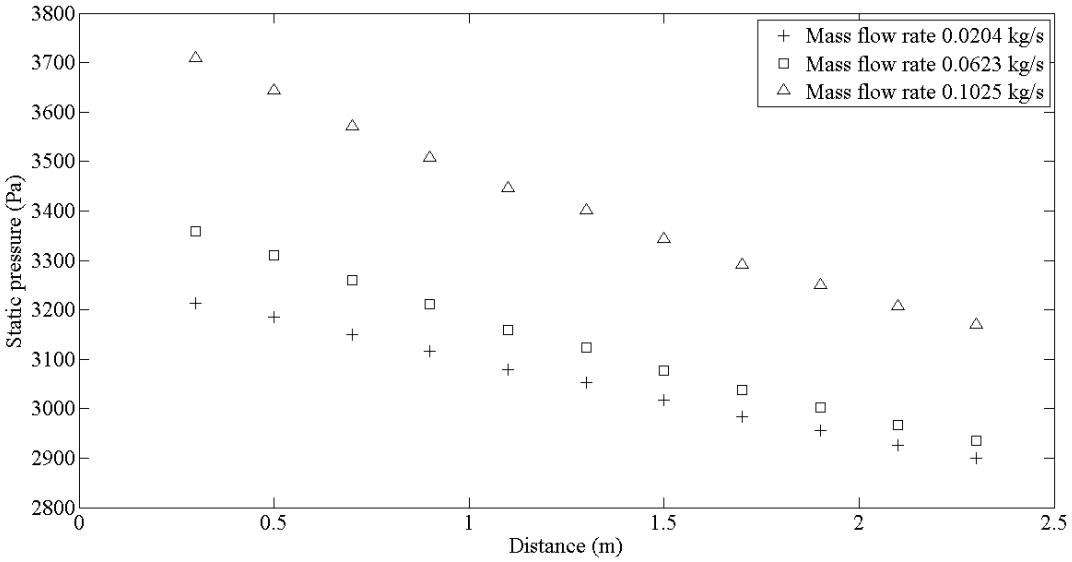

4-6 (a)

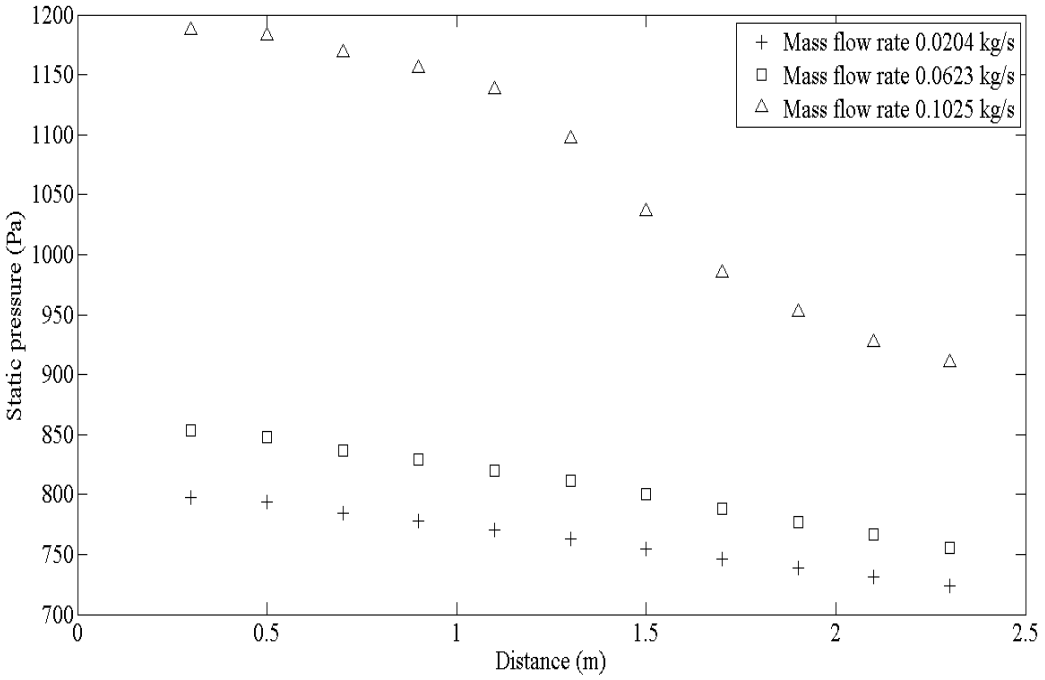

4-6(b)

Figure 4-6: Streamwise pressure drop in between 0.3 m and 2.3 m of the test section: (a) Air velocity of 30 m/s at a wheat mass flow rate of 0.0204 kg/s, 0.0623 kg/s and 0.1025 kg/s; (b) Air velocity of 13 m/s at a wheat mass flow rate of 0.0204 kg/s, 0.0623 kg/s and 0.1025 kg/s;

At 30 m/s (Figure 4-6 (a)), the plots have a linear trend, although non-linearity can be observed at the mass flow rate of 0.1025 kg/s. That means, even at the highest velocity of the tested range, higher mass flow rates of wheat introduce non-linearities. At 13 m/s (Figures 4-6 (b)), for low and medium mass flow rates, the pressure drop trends show a non-linear pattern which becomes prominent when wheat flow rate is the maximum (0.01025 kg/s). Based on these observations, an assumption can be made that the specific pressure drop and mass loading ratio relationship for Data Set 2 will be linear at higher velocities and lower mass loadings, but non-linear at lower velocities and higher mass loadings.

Figures 4-7 (a) and 4-7 (b) show specific pressure drop vs. mass loading ratio when the pressure drop was measured between 1.5 m and 2.1 m. Separate plots were made to facilitate better observation of the trends.

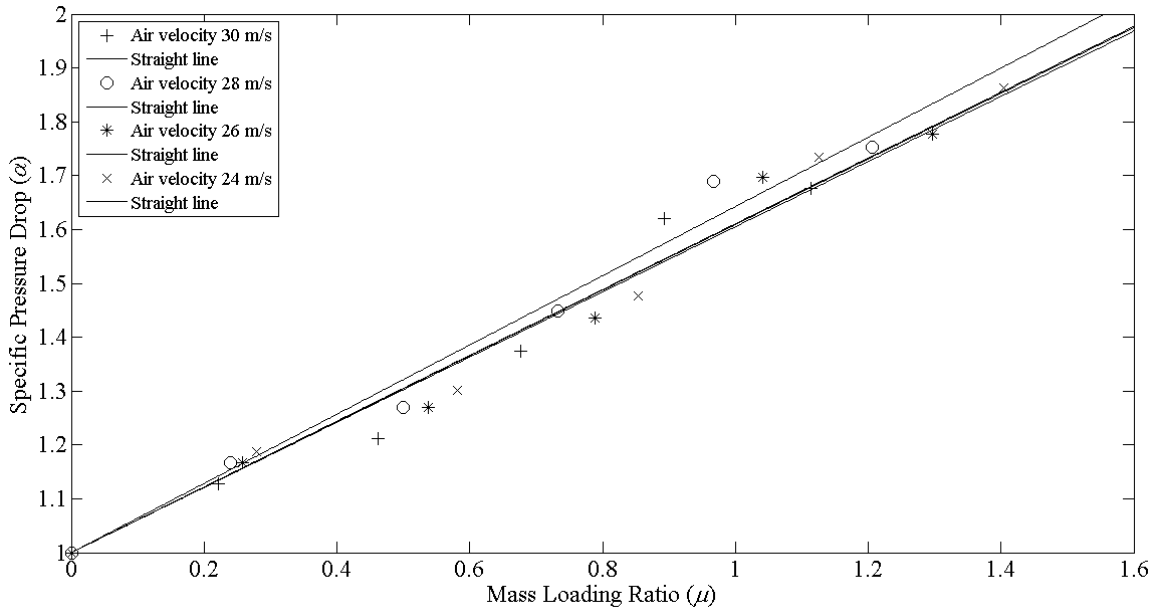

4-7 (a)

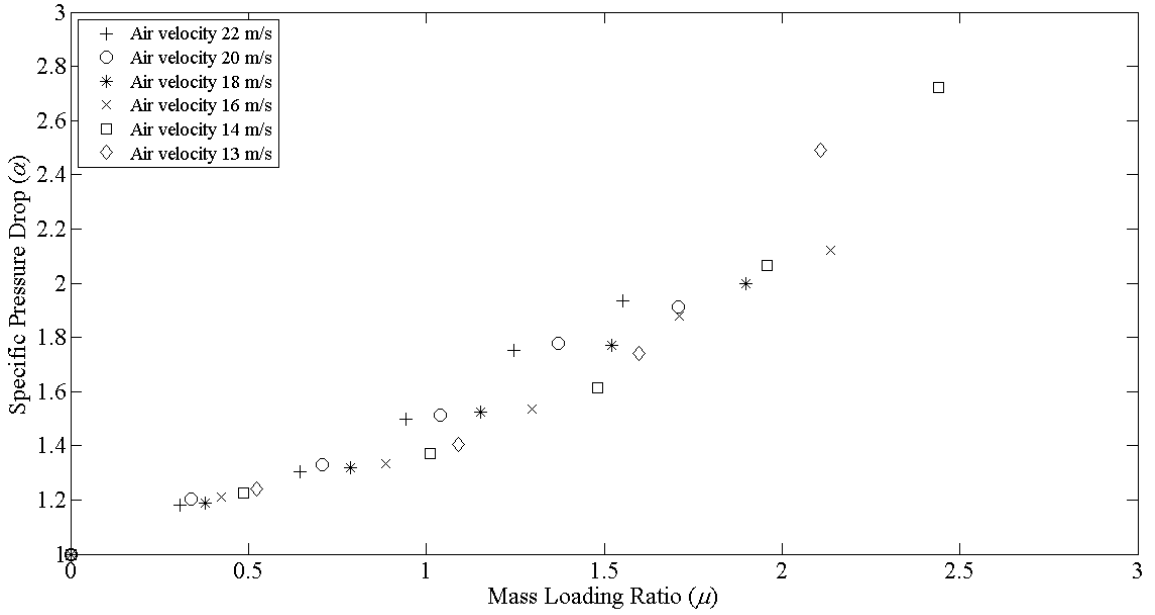

4-7 (b)

Figure 4-7: Specific pressure drop vs. mass loading ratio for (a) air velocities 30 m/s to 24 m/s; (b) air velocities 22 m/s to 13 m/s; (pressure drop measured between 1.5 m and 2.1 m)

From Figure 4-7 (a), it can be seen that for higher velocities, a single straight line could describe the relationship between specific pressure drop and mass loading ratio. For lower velocities (Figure 4-7 (b)), visible non-linearity starts below 16 m/s. A change in slope can be observed before and after the mass loading range of 1.0 - 1.5 for these lower velocities (Figure 4-7 (b)).

Figures 4-8 (a) and 4-8 (b) show specific pressure drop vs. mass loading ratio plots where pressure drop was measured between 0.9 m to 1.5 m from the metering box. Description of these plots can be given in a similar manner as Figures 4-7 (a) and 4-7 (b).

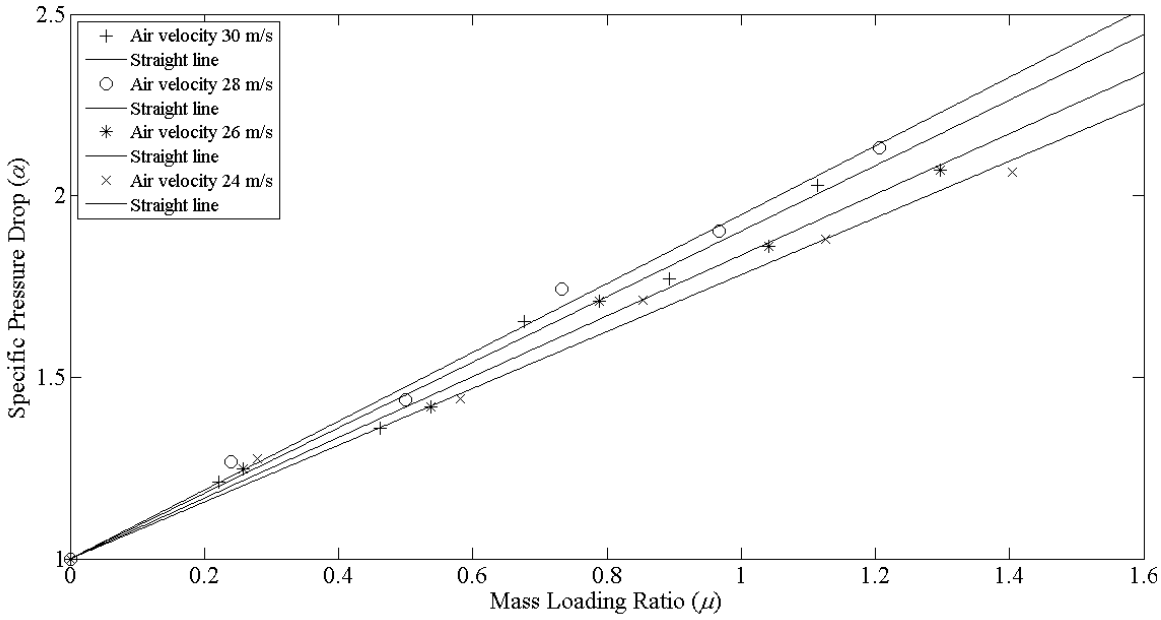

4-8 (a)

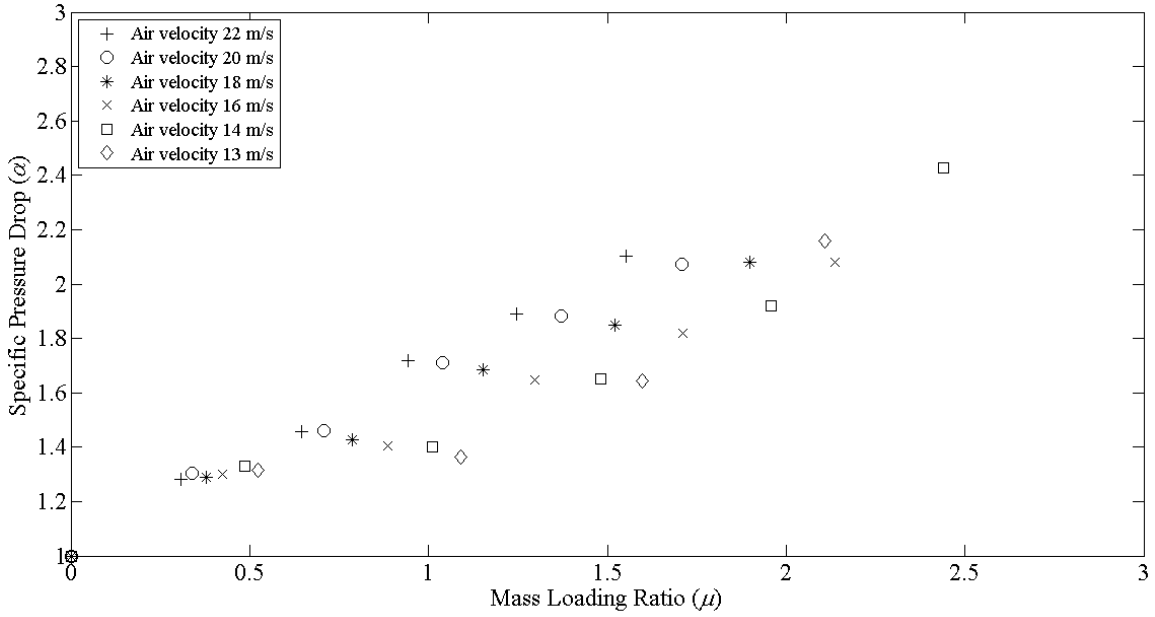

4-8 (b)

Figure 4-8 :Specific pressure drop vs. mass loading ratio for (a) air velocities 30 m/s to 24 m/s; (b) air velocities 22 m/s to 13 m/s; (pressure drop measured between 0.9 m and 1.5 m)

Pressure drop was measured between 0.3 m and 0.9 m from the metering box in the plots of Figures 4-9 (a) and 4-9 (b). These plots reveal dominant non-linearity at and below an air velocity of 20 m/s.

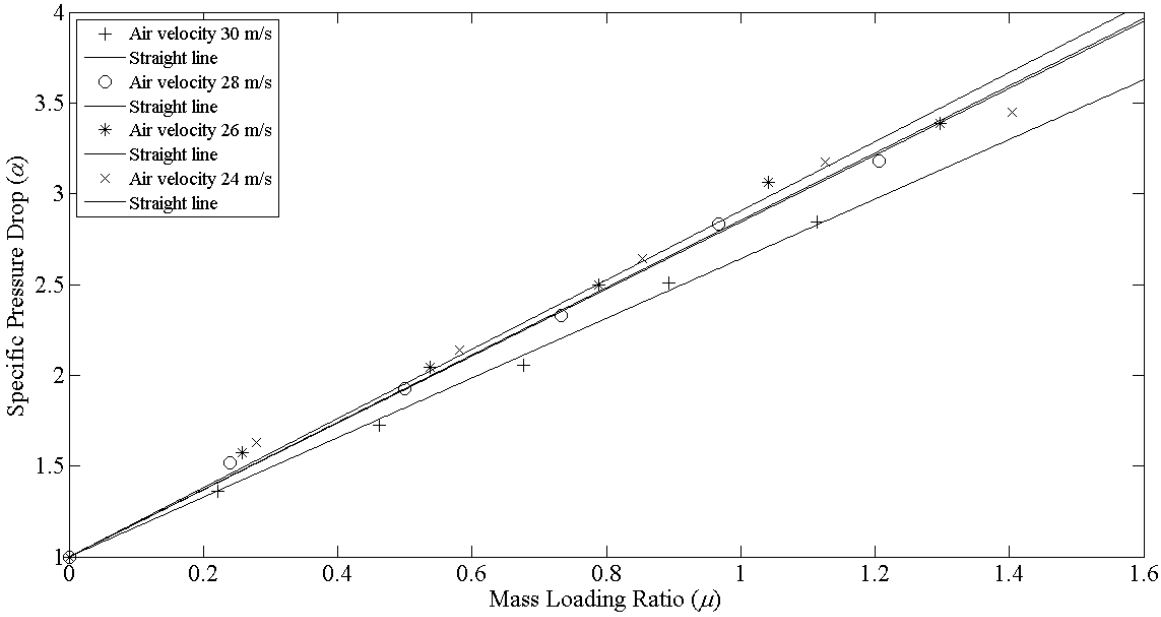

4-9 (a)

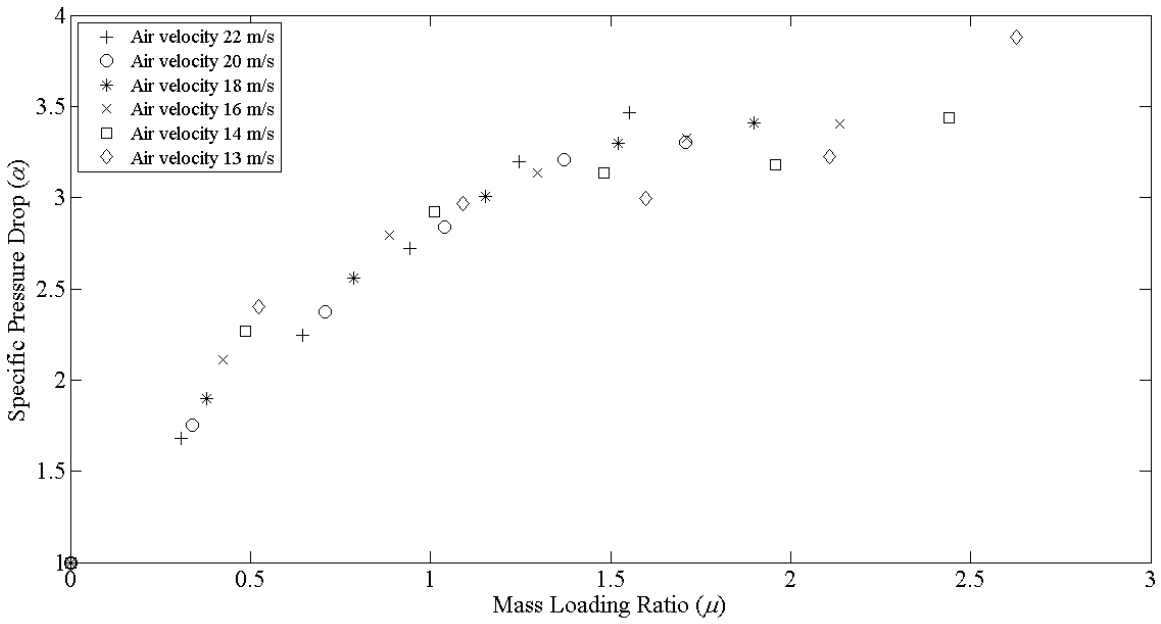

4-9 (b)

Figure 4-9 :Specific pressure drop vs. mass loading ratio for (a) air velocities 30 m/s to 24 m/s; (b) air velocities 22 m/s to 13 m/s; (pressure drop measured between 0.3 m and 0.9 m)

For all the cases described above, 20 m/s seems to be the transitional velocity below which the trend of the specific pressure drop vs. mass loading ratio plot becomes non-linear.

4.4 Physical Interpretation of the Results

In his work, Hinkle (1953) studied a common method for the prediction of pressure drop in horizontal pneumatic conveying. He obtained the specific pressure drop to mass loading ratio relationship of the form

$$\alpha = 1 + \left(\frac{f_s}{f_g}\right)\left(\frac{c}{v}\right)\mu\,, \qquad 4\text{-}1$$

where f_s is the friction factor for solids [dimensionless],

f_g is the friction factor for air [dimensionless],

c is the particle velocity [m/s], and

v is the superficial air velocity [m/s].

Cabrejos and Klinzing (1992) also described the value of the slope (k) as the product of the ratios of friction factors and velocities for solids and gases.

On the other hand, Klinzing et al. (2010) provided expressions for pressure drop due to gas and solids for horizontal conveying in their textbook. According to them, the pressure drop due to air only is given by

$$\Delta p_L = \lambda_L \frac{\rho}{2} v^2 \frac{\Delta L}{D}, \qquad 4\text{-}2$$

where Δp_L is the pressure drop due to air only [Pa],

λ_L[3] is the air resistance coefficient [dimensionless],

ρ is the air density [kg/m^3],

v is the superficial air velocity [m/s],

ΔL is the length for the pressure drop measurement [m], and

D is the pipe diameter [m].

The pressure drop due to solids is given by

$$\Delta p_Z = \mu \lambda_Z \frac{\rho}{2} v^2 \frac{\Delta L}{D}, \qquad 4\text{-}3$$

where, Δp_z is the pressure drop due to solids only [Pa],

λ_z is the pressure drop factor due to solids [dimensionless], and

μ is the mass loading ratio [dimensionless].

If Δp is the pressure drop of the gas-solid flow, then

$$\Delta p = \Delta p_L + \Delta p_Z . \qquad 4\text{-}4$$

Since, specific pressure drop, is given by,

$$\alpha = \frac{\frac{\Delta p}{\Delta L}}{\frac{\Delta p_L}{\Delta L}}, \qquad 4\text{-}5$$

then by combining and rearranging Equation 4-2, 4-3, 4-4 and 4-5 it can be written as

[3] λ_L is also known as the Darcy friction factor in many literature on fluid mechanics.

$$\alpha = 1 + \left(\frac{\lambda_Z}{\lambda_L} \right) \mu . \qquad 4\text{-}6$$

This means the value of the slope *(k)* is the ratio of pressure drop factors for solids to air resistance coefficients. The difference between the friction factor for solids in Equation 4-1 and the pressure drop factor for solids in Equation 4-6 is that the pressure drop factor considers pressure loss due to gravitational forces as well as frictional forces. There are many empirical models for the calculation of pressure drop factors for solids developed by a number of researchers. For dilute flow, Weber (1973) proposed a model for the pressure drop factor (λ_z) which, if simplified by neglecting the gravitational effects in horizontal flow, takes the form

$$\lambda_Z = \lambda_Z^* \frac{c}{v}, \qquad 4\text{-}7$$

where λ_Z^* is the impact and friction factor for solids [dimensionless],

c is the particle velocity [m/s], and

v is the superficial air velocity [m/s].

The air resistance coefficient (λ_L) of Equation 4-6 is actually four times the value of friction factor for air in Equation 4-1 (Klinzing et al., 2010). Combining Equations 4-6 and 4-7, the expression for specific pressure drop can be written as

$$\alpha = 1 + \left(\frac{\lambda_Z^*}{\lambda_L} \right) \left(\frac{c}{v} \right) \mu . \qquad 4\text{-}8$$

By comparing Equation 4-1 and 4-8, it can be said without doubt that the slope (k) is a function of air and solids friction factor, as well as their respective velocities.

The plots of specific pressure drop vs. mass loading ratio (Figure 4-1 to 4-4 and Figure 4-7 to 4-9) indicate that the ratio of the product of friction factor and velocity of solids to air held a constant value for higher air velocities at the farther end of the pipe. When particles are fully suspended at higher velocities, there is less interaction between the particles. Hence, the frictional resistance of particles remained constant irrespective of the air velocities. As the pressure drop measurement gradually came closer to the point of particle release, this ratio varied with all air velocities, but still maintaining a linear relationship after the first 1.5 m of the pipe. Data taken from

experiments conducted by Rizk (1976), Klinzing et al. (2010) showed that the velocity ratio of solids to air (*c/v*) remains constant against average air velocity. This means the change in the ratio of friction factors is the only contributor to the change in the slope. The observed non-linearity for lower velocities when the pressure drop measurement approached within 1.5 m of the pipe (Figures 4-8 and 4-9), could only mean that the linear relationship between specific pressure drop and mass loading ratio does not hold true in this section. So, the linear model should be modified by including a non-linear term of mass loading ratio.

Chapter 5. Model Development

Chapter 4 concluded with the findings that the specific pressure drop (α) vs. mass loading ratio (μ) closer to the metering box does not follow the trend described by Cabrejos and Klinzing (1992). Although the relationship is linear for higher velocities, the slope is not constant. And when the air velocity decreases, the specific pressure drop vs. mass loading ratio plot shows a non-linear trend. This chapter looks at this source of non-linearity and then develops the model for solids mass flow rate estimation based on that. Section 5.1 looks at the source of the non-linearity and then develops the general model. Section 5.2 discusses an alternative approach based on Froude number to develop a model for mass flow measurement. All the models are tested for accuracy in Section 5.3. This chapter concludes with overall discussion on the models in Section 5.4.

5.1 Source of Non-linearity and Model Development

In Chapter 4, Weber's (1973) model for calculating the pressure drop factor for solids (λ_z) was presented in a simplified form by neglecting the effect of gravity in Equation 4-7. That assumption could be made when the particles have travelled far enough to be considered fully suspended. But when the pressure drop measurement comes within the first meter or so, neglecting gravitational effect may not be a valid assumption, especially, for lower superficial air velocities. Weber's complete representation of pressure drop factor for solids (λ_Z) is shown in Equation 5-1,

$$\lambda_Z = \lambda_Z^* \frac{c}{v} + \frac{2\beta}{\frac{c}{v} Fr^2}, \qquad 5\text{-}1$$

where λ_Z^* is the impact and friction factor for solids [dimensionless],

c is the particle velocity [m/s],

v is the superficial air velocity [m/s],

β is the velocity ratio related to particle fall velocity in a cloud [dimensionless],

and

Fr is the Froude number [dimensionless].

The Froude number (Fr) in Equation 5-1 is the ratio of inertial force and gravitational force, whereas β is the ratio of particle fall velocity due to gravity and superficial air velocity. With the

representation of pressure drop according to Equation 5-1, the expression for specific pressure drop shown in Equation 4-6 takes the form

$$\alpha = 1 + \left(\frac{\lambda_Z^* \frac{c}{v} + \frac{2\beta}{\frac{c}{v} Fr^2}}{\lambda_L} \right) \mu \, . \qquad 5\text{-}2$$

In separate experiments, Siegel (1970) and Rizk (1973) determined the relationship between mass loading ratio (μ) and Froude number (Fr) at the pressure minimum condition. They conducted experiments with Polystyrol (diameter 1 mm – 2.5 mm) inside carbon steel pipe. The developed relationship was valid for pipe diameters of 50 mm – 400 mm. It is given by

$$\mu = KFr^4 , \qquad 5\text{-}3$$

where K is an experimental constant [dimensionless].

Assuming Equation 5-3 valid for this research as well, putting $Fr^2 = \sqrt{\frac{\mu}{K}}$ in equation 5-2 gives the expression for specific pressure drop as

$$\alpha = 1 + \left(\frac{\lambda_Z^*}{\lambda_L} \right) \left(\frac{c}{v} \right) \mu + \frac{2\beta\sqrt{K}}{\left(\frac{c}{v} \right) \lambda_L} \sqrt{\mu} \, . \qquad 5\text{-}4$$

Letting $A = \left(\frac{\lambda_Z^*}{\lambda_L} \right) \left(\frac{c}{v} \right)$, 5-5

and $B = \frac{2\beta\sqrt{K}}{\left(\frac{c}{v} \right) \lambda_L}$, 5-6

equation 5-4 then takes the form

$$\alpha = 1 + A\mu + B\sqrt{\mu} \, . \qquad 5\text{-}7$$

Equation 5-7 has both linear and non-linear components. If the value of *B* is smaller compared to the value of *A*, the specific pressure drop vs. mass loading ratio should be linear. If gravitational effects become significant at lower velocities, the plot will become non-linear because the value of *B* in that case will not be negligible. The experimental plots obtained when pressure drop was measured between 0.3 m and 0.9 m of the test section, were also linear for higher velocities and nonlinear for lower velocities (Figure 4-9). To see whether Equation 5-7 can represent both the linear and nonlinear trends observed in the experiments, it was optimized to determine the values of unknown parameters *A* and *B* at each air velocity being considered.

Optimization was carried out by using the MATLAB function "fminsearch", which uses the Nelder-Mead simplex algorithm (Lagarias et al., 1998). This algorithm is best suited for non-linear optimization. Data Set 2 was used for optimization. Table 5-1 lists the value of parameters A and B for different air velocities. The codes for performing the optimization are given in in Appendix B.

Table 5-1: Values of parameters *A* and *B* at different air velocities

Air Velocity (m/s)	Value of *A*	Value of *B*
30	1.7818	-0.1287
28	1.6573	0.1784
26	1.6494	0.2547
24	1.387	0.4825
22	1.0593	0.7139
20	0.5058	1.1983
18	0.2056	1.5464
16	-0.2585	2.0845
14	-0.4723	2.2856
13	-0.1951	1.965

It can be seen from the table that the value of *A* dominates at higher velocities. As the air velocity decreases, the value of *B* starts to dominate. All of these optimizations had an R-Square value greater than 0.99. Equations 5-5 and 5-6 suggest that parameters *A* and *B* are ratios of positive

dimensionless numbers and velocity magnitudes. Hence they cannot have negative values. For this reason optimized values of *A* and *B* were adjusted with the curve fitting tool of MATLAB. The Trust Region algorithm (Yuan, 1999) was used with the constraint that the values of *A* and *B* must be greater than zero. These adjusted values of *A* and *B* (with 95% confidence interval) are presented in Table 5-2 along with the R-Square values.

Table 5-2: Adjusted values of Parameter *A* and *B* at different air velocities

Air Velocity (m/s)	Value of *A*	Value of *B*	R-Square
30	1.65	0.05	0.9923
29	1.65	0.15	0.9977
28	1.65	0.20	0.9977
27	1.65	0.25	0.9850
26	1.65	0.30	0.9953
25	1.48	0.40	0.9966
24	1.39	0.48	0.9962
23	1.25	0.53	0.9951
22	1.06	0.71	0.9969
21	0.95	0.79	0.9919
20	0.75	0.93	0.9842
19	0.65	1.03	0.9857
18	0.48	1.23	0.9840
17	0.23	1.37	0.9804
16	0.15	1.61	0.9747
15	0.001	1.72	0.9703

The value of parameter *A* remains constant at higher velocities and gradually decreases with air velocity. This indicates that even when pressure drop is measured closer to the meter box, the majority of the particles are fully accelerated at higher velocities. For this reason the value of *A* remains constant in agreement with the findings of Cabrejos and Klinzing (1992). But due to the presence of parameter *B* (i.e. due to some particles not attaining full acceleration), the overall value of the slope was different at higher velocities (Chapter 4). Below 15 m/s the value of *A* becomes

negative. Therefore, the model presented in Equation 5-7 is valid for air velocities from 15 m/s – 30 m/s. Figure 5-1 (a) to 5-1(e) compares the experimental specific pressure drop vs. mass loading ratio data to curves obtained from Equation 5-7 with adjusted optimized parameters.

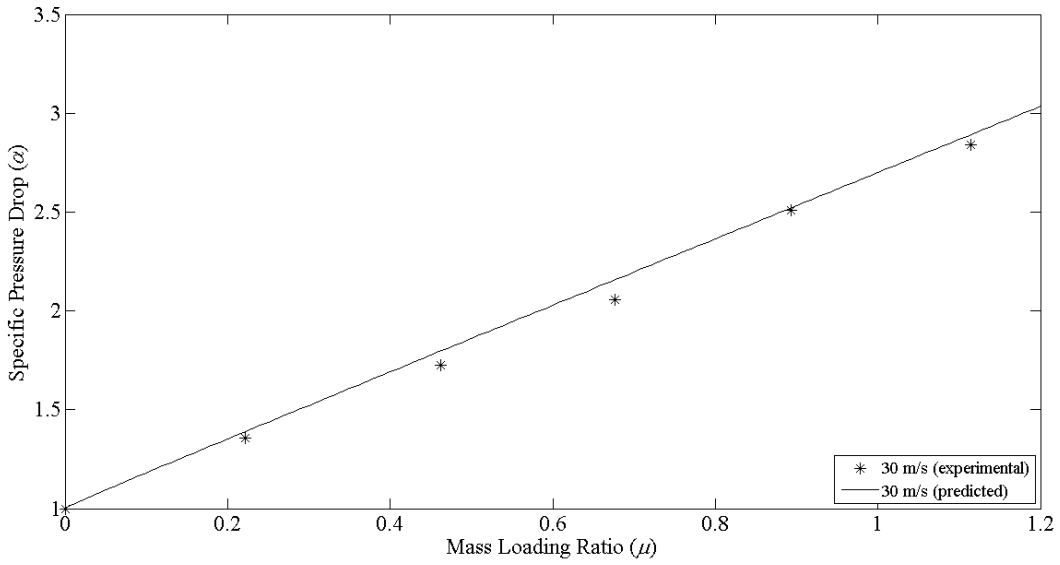

5-1 (a)

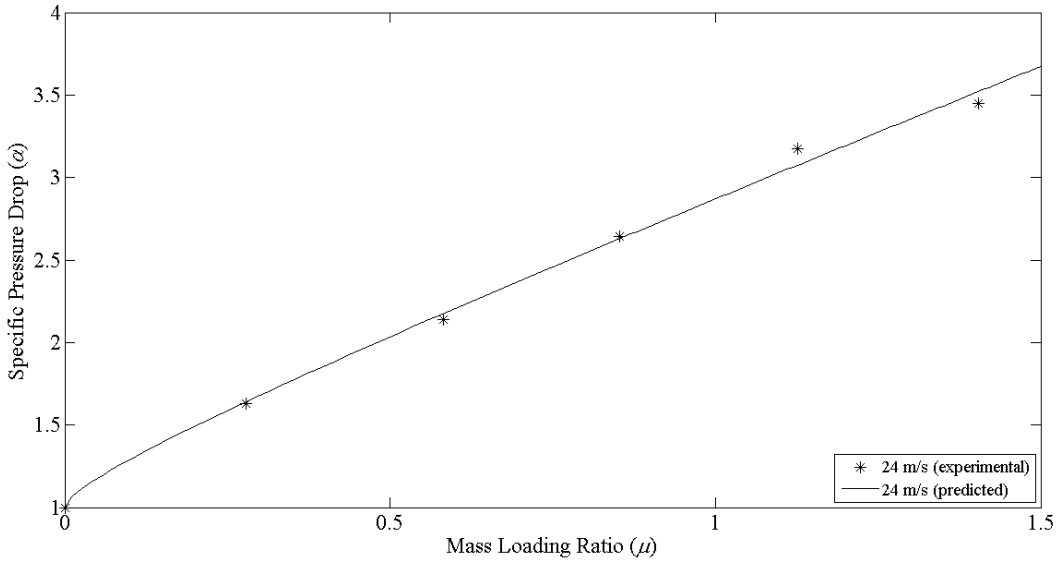

5-1(b)

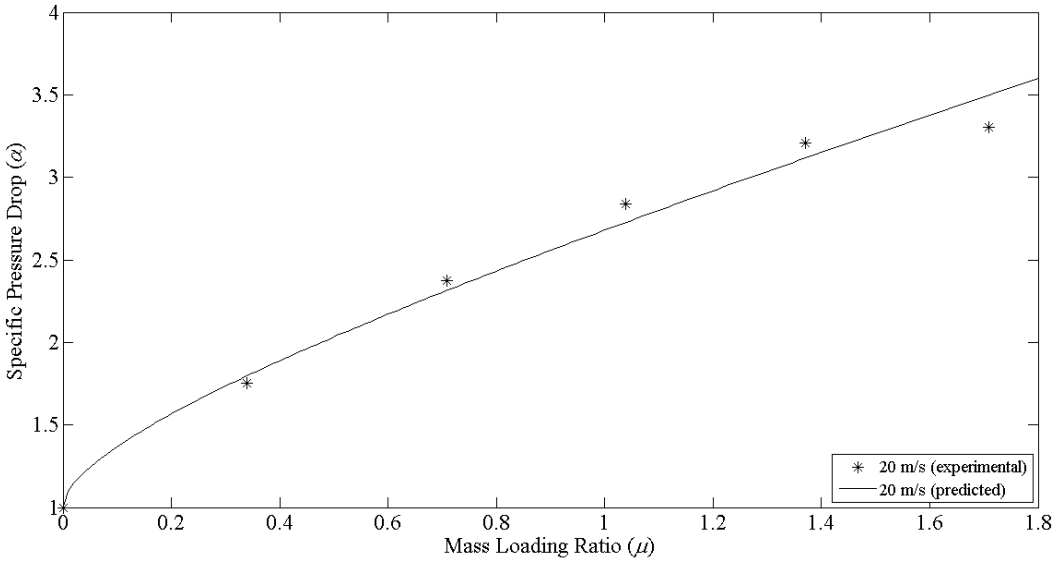
Specific Pressure Drop (α)
Mass Loading Ratio (μ)
20 m/s (experimental)
20 m/s (predicted)

5-1(c)

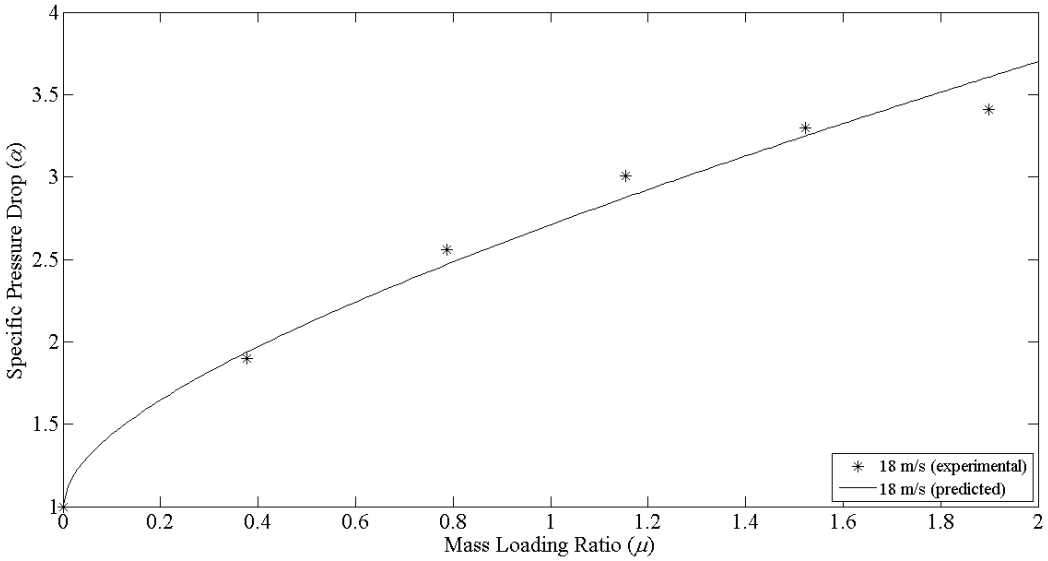
Specific Pressure Drop (α)
Mass Loading Ratio (μ)
18 m/s (experimental)
18 m/s (predicted)

5-1(d)

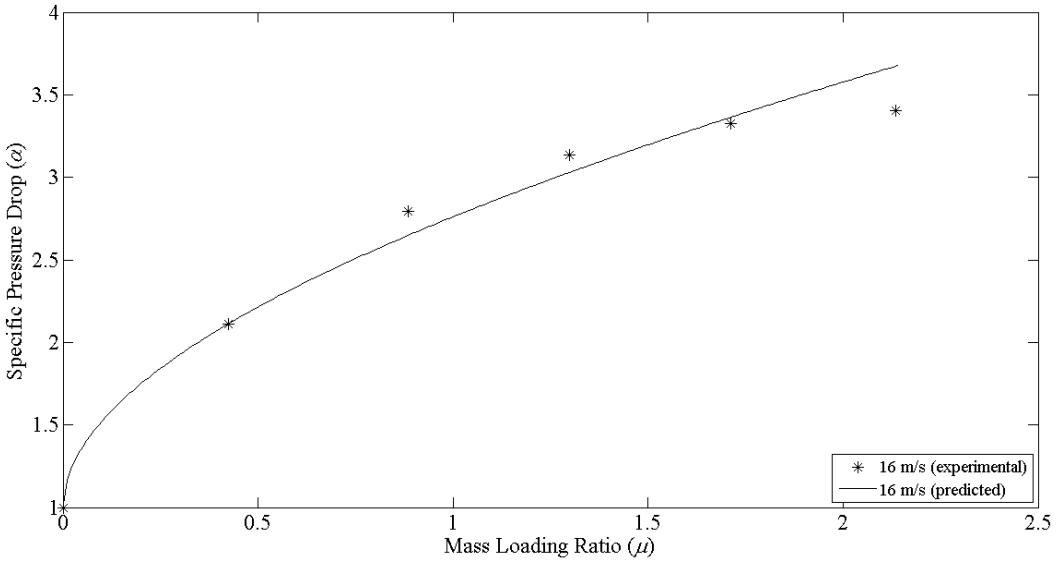

5-1 (e)

Figure 5-1: Comparison between experimental and predicted plot of specific pressure drop vs. mass loading ratio at air velocity (pressure drop measured between 0.3 m and 0.9 m) : (a) 30 m/s (b) 24 m/s (c) 20 m/s (d) 18 m/s (e) 16 m/s.

All the comparisons shown in Figure 5-1 suggest that the model constructed in Equation 5-7 is capable of predicting both the linearity at higher velocities, and the nonlinearity at lower velocities due to the additional term, "$B\sqrt{\mu}$". At this point, if relationships can be established between parameters *A* and *B* and air velocity, Equation 5-7 will become a function of pressure drop, mass flow ratio and air velocity. As pressure drop, air velocity and air mass flow rate can be measured, it will be possible to calculate product mass flow rate with the help of Equation 5-7. To establish the relationship between parameters *A* and *B* to air velocity, their values were plotted against air velocity, which is shown in Figure 5-2 and 5-3.

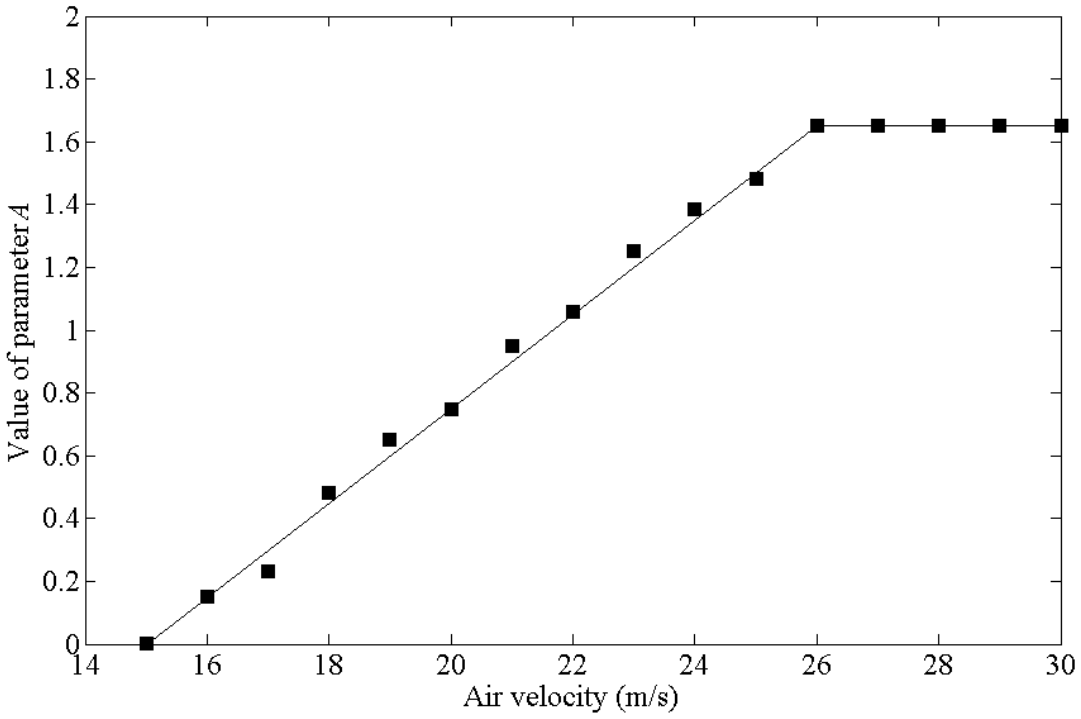

Figure 5-2: Values of parameter *A* at different air velocities.

The curve fitting tool of MATLAB was used to fit the plots in a model. The relationship between parameter *A* and air velocity was found to be

$$A = a_1 v + a_2 \text{ (between 15 m/s to 26 m/s),} \quad 5\text{-}8$$

where $a_1 = 0.152$, 5-9

$a_2 = -2.279$, 5-10

and, $A = 1.65$ (Between 26 m/s to 30 m/s) . 5-11

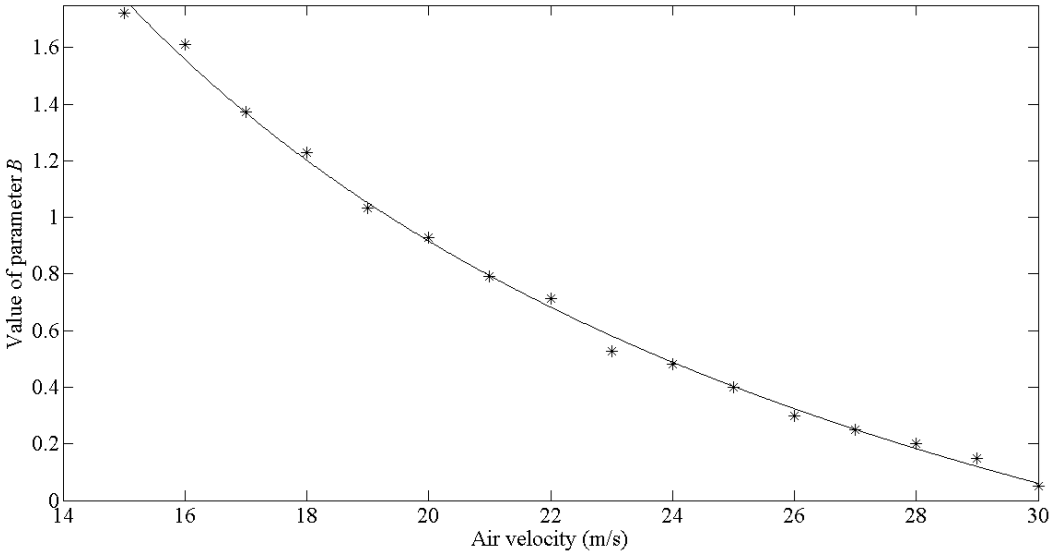

Figure 5-3: Values of parameter *B* at different air velocities.

On the other hand, the relationship between parameter *B* and air velocity is given by

$$B = b_1 + \frac{b_2}{v} \ , \qquad 5\text{-}12$$

where, b_1 = -1.651, and 5-13

b_2 = 51.35. 5-14

The goodness of fit statistics for Figure 5-2 and 5-3 are presented in Table 5-3.

Table 5-3 Goodness of fit statistics for parameters *A* and *B* vs. air velocity plot (95% confidence interval)

	A vs. Air Velocity	*B* vs. Air Velocity
SSE (Sum of Squares due to Error)	0.01314	0.01257
R-Square	0.996	0.9971
Adjusted R-square	0.9956	0.9968
RMSE (Root Mean Squared Error)	0.03625	0.02997

With the established relationship between parameters *A* and *B* and air velocity, it is now possible to calculate mass flow ratio by solving Equation 5-7. Equation 5-7 can be written as

$$AX^2 + BX + C = 0, \tag{5-15}$$

where $X^2 = \mu$, and 5-16

$$C = 1 - \alpha. \tag{5-17}$$

The acceptable root of Equation 5-15 is

$$X = \frac{-B + \sqrt{B^2 - 4AC}}{2A}. \tag{5-18}$$

Since *C* is always negative, parameter *A* must always be positive to avoid non-real solutions. This just establishes the assumption made earlier that *A* must always have a positive value. By putting the values of *A*, *B* and *C* from Equations 5-8, 5-12 and 5-17 into Equation 5-18, the value of *X* can be calculated. Then, with the help of Equation 5-16, the mass loading ratio can be determined. The mass flow rate of solids can finally be calculated with

$$M_s = \mu M_a, \tag{5-19}$$

where M_s is the mass flow rate of solids [kg/s], and

M_a is the mass flow rate of air [kg/s].

5.2 Model Development: An Alternative Approach

The model presented in Equation 5-7 was based on the assumption that the relationship between Froude number and mass loading ratio (Equation 5-3) described by Siegel (1970) and Rizk (1973) is valid for wheat as well. Observing Figures 5-1 (a) to 5-1 (f), this assumption appears to be reasonable. That relationship was obtained at the minimum pressure condition by plotting mass loading ratio vs. Froude number, also known as the dimensionless state diagram (Klinzing et al., 2010). As previously mentioned, the dimensionless state diagram is generally used to check the reliability of experimental data. Two unique properties of the dimensionless state diagram of mass loading ratio vs. Froude number make it very suitable for developing a model to calculate mass flow rate.

These properties, as mentioned by Klinzing et al. (2010), are:

1) For every mass flow rate of solid, the log-log plot of mass loading ratio vs. Froude number will be a straight line;
2) All of these straight lines will be parallel to each other.

The log-log plot of mass loading ratio vs. Froude number from the present experimental data is shown in Figure 5-4.

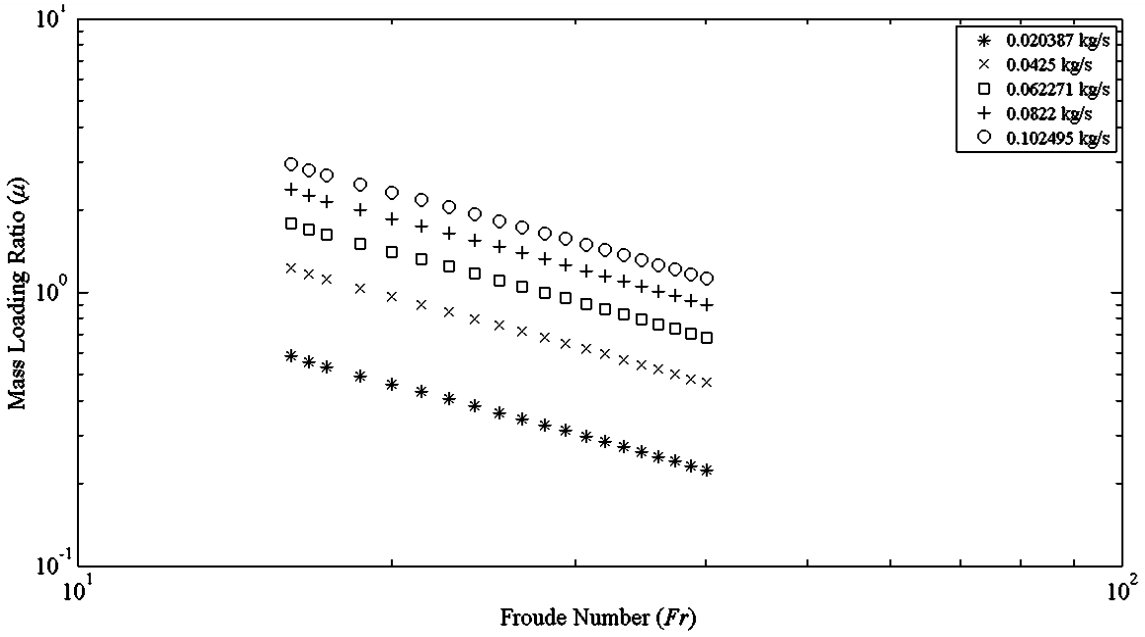

Figure 5-4: Mass loading ratio vs. Froude number at different solids flow rate (Material: Wheat; Pipe diameter: 0.0573 m).

The relationship shown in Figure 5-4 can be expressed by,

$$\log \mu = -1.0419 \log Fr + K_1 \ . \qquad 5\text{-}20$$

The parameter K_1 has a constant value for each product mass flow rate and its value increases with the increment of mass flow rate as the straight line shifts upwards. Since the value of K_1 is only dependent on solids mass flow rate, the temptation would be to develop a relationship between K_1 and solids mass flow rate. In that case, Equation 5-20 will have the same value of solids mass flow rate on both sides and it will be eliminated from the Equation. Probably for this reason, the mass loading ratio vs. Froude number relationship has not been used in any previous investigations to

calculate solids flow rate. But, if an indirect relationship is established between K_1 and solids mass flow rate, Equation 5-20 can be solved for the mass flow rate of solids. That is, not developing a direct relationship between K_1 and solids mass flow rate, but between K_1 and other quantities that are also dependent on solids mass flow rate. Pressure drop is one such quantity.

From Figure 5-4, it is evident that for the same Froude number, there exists infinite mass loading ratios. On the other hand, the same mass loading ratio can occur at different Froude numbers. It is therefore necessary to locate the intercept (i.e. the value of K_1) of Equation 5-20. At the same air velocity, the pressure drop is different for different solids mass flow rates. Since the pipe diameter and gravitational acceleration are constant, it can be said that pressure drop is different for different solids mass flow rates at the same Froude number. Hence developing a relationship between K_1 and pressure drop will make Equation 5-20 solvable for the mass loading ratio. The question still remains at which air velocity this relationship should be developed? The unique feature of Figure 5-4 has the answer to this question. Since the value of K_1 does not change with air velocity once its value is determined, the relationship could be developed at any air velocity within the operating range. The system just needs to be operated at that air velocity before the actual run starts to determine the value of K_1. Once K_1 is determined, Equation 5-20 can be used to determine the mass loading ratio at any air velocity. Every time the mass flow rate of solids is changed, the system first needs to run at that particular air velocity or velocities where calibration equations between K_1 and pressure drop are available.

To explain this concept, a plot of K_1 vs. specific pressure drop at an air velocity of 20 m/s is shown in Figure 5-5. Specific pressure drop was used to make it a dimensionless plot. Pressure drop was measured between 0.3 m and 0.9 m of the test section. K_1 values were obtained for five different mass flow rates of wheat including the maximum and minimum possible mass flow rate for wheat in an air seeder. At this point it must be mentioned that for every conveyed product, the relationship between K_1 and specific pressure drop must be developed by considering the highest and lowest possible mass flow rate of that product and points in-between.

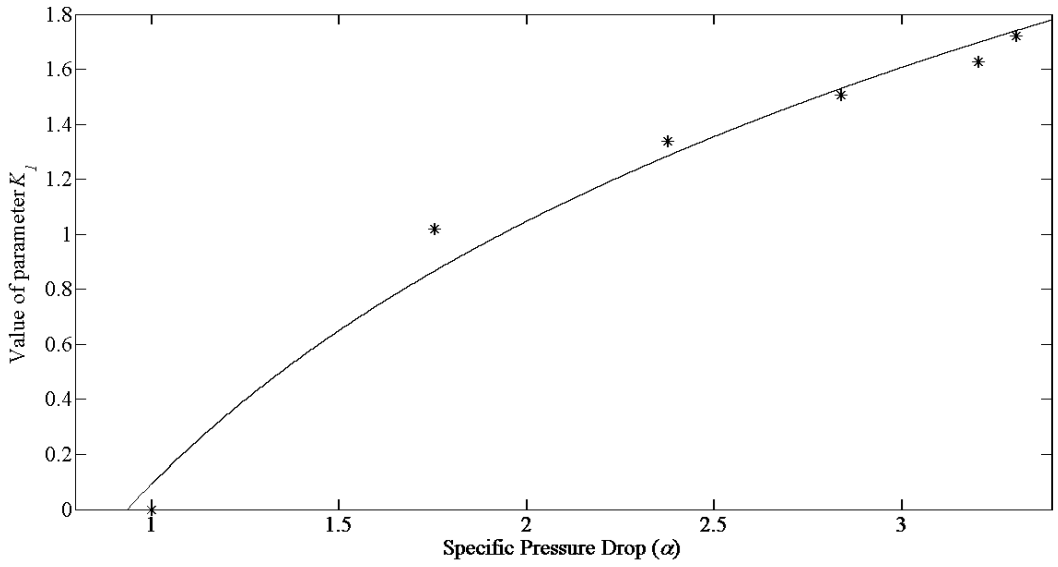

Figure 5-5: Relationship between K_1 and Specific Pressure drop at air velocity 20 m/s (Product: Wheat).

The relationship between K_1 and specific pressure drop with an R-square value of 0.9918 and at air velocity 20 m/s was found to be

$$K_1 = 2.429 \log \alpha + 0.4228. \qquad 5\text{-}21$$

If the system has Equation 5-21 for determination of K_1, once the operator selects wheat as the product and starts dispensing at a particular rate, the system will first set air velocity to 20 m/s and determine K_1. The operator can then operate at any velocity with that product flow rate. Every time the flow rate is changed, the operator will experience a bit of waiting time for the system to reach 20 m/s and determine K_1. The mass flow ratio can be calculated with Equation 5-20 and the product flow rate with equation 5-19. Attempts have been made to construct a continuous relationship between K_1, specific pressure drop and air velocity to eliminate the need for the system to reach a calibration velocity every time mass flow rate is changed, but it was not possible to obtain a reliable continuous relationship.

5.3 Testing of Models

Separate Data Sets were used for testing the models. The models described in Sections 5.1, and 5.2 will be termed as Model 1 and Model 2 respectively for convenience in discussion.

For Model 1, around 73% of the estimates had an error less than 10%. Only 2.5% of the estimates exceeded an error of 20% with highest error not exceeding 23%. These errors were evaluated considering an operating air velocity range of 15 m/s to 20 m/s. Figure 5-6 shows a comparison between actual and estimated mass flow rate by Model 1.

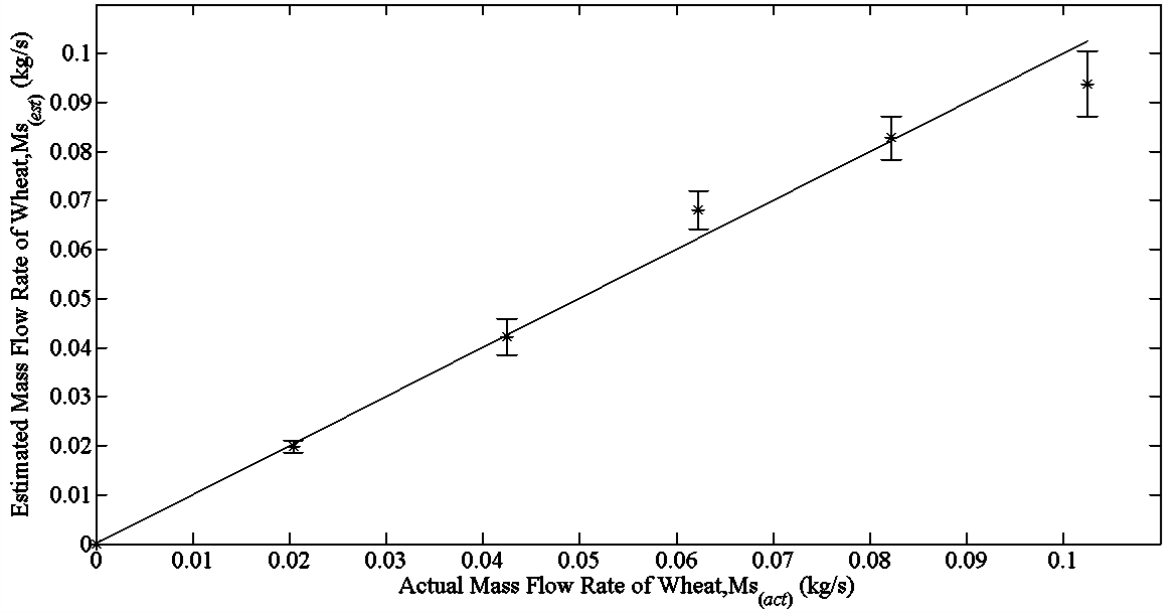

Figure 5-6: Comparison between estimated and actual mass flow rate of wheat by Model 1.

While testing Model 1, most of the errors occurred during the estimation of the higher mass flow rates. These errors actually occurred at the lower air velocities. An air seeder is most unlikely to be operated at the lower air velocities when the mass flow rate of solids is high. If these estimations of the higher mass flow rates at the lower air velocities are omitted, the accuracy of Model 1 will improve even more. Figure 5-7 shows the percent error at different mass flow rates of wheat.

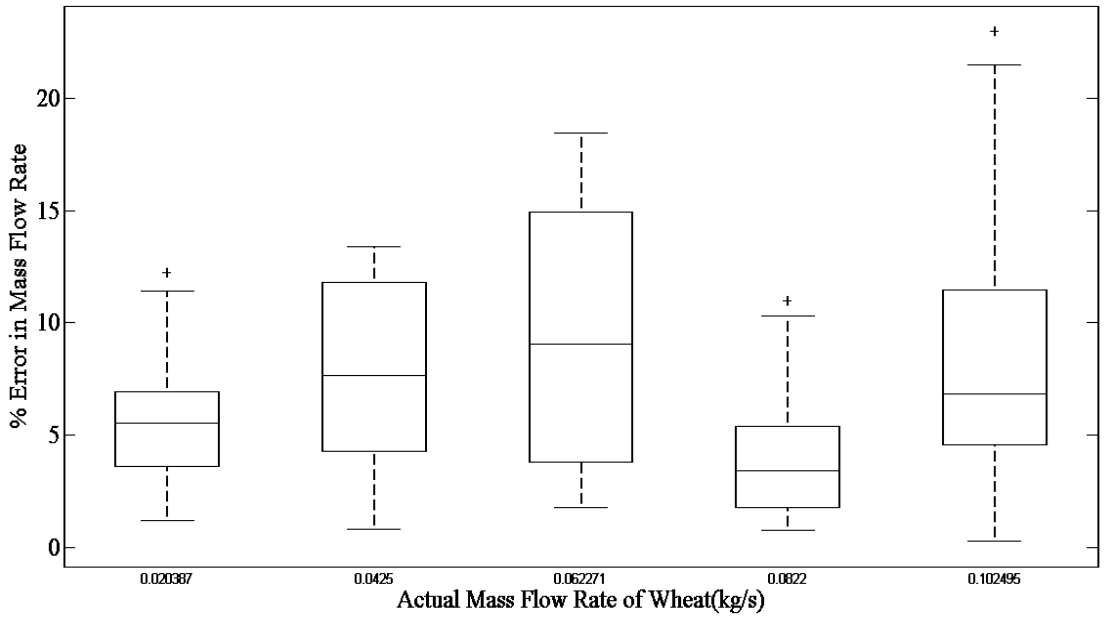

Figure 5-7: Percent error while estimating different mass flow rate of wheat with Model 1.

Model 1 is solely dependent on specific pressure drop, which was measured within the first meter of particle entrance. Hence, at low air velocity and high mass flow rate of wheat the pressure drop values were not consistent which caused the most error.

For Model 2, around 59% of the estimates had an error of less than 6%. The rest had an error value in between 10% to 15%. This model was evaluated within the air velocity range of 14 m/s to 30 m/s. Figure 5-8 shows a comparison between actual and estimated mass flow rates by Model 2.

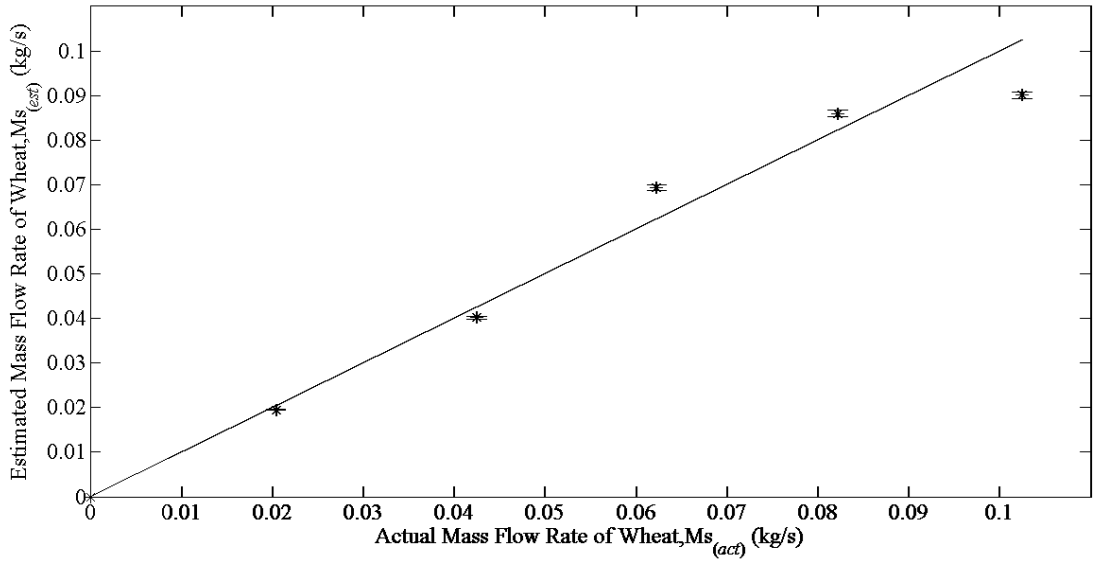

Figure 5-8: Comparison between estimated and actual mass flow rate of wheat by Model 2.

Figure 5-9 shows percent error at different mass flow rates of wheat while using Model 2 for estimation.

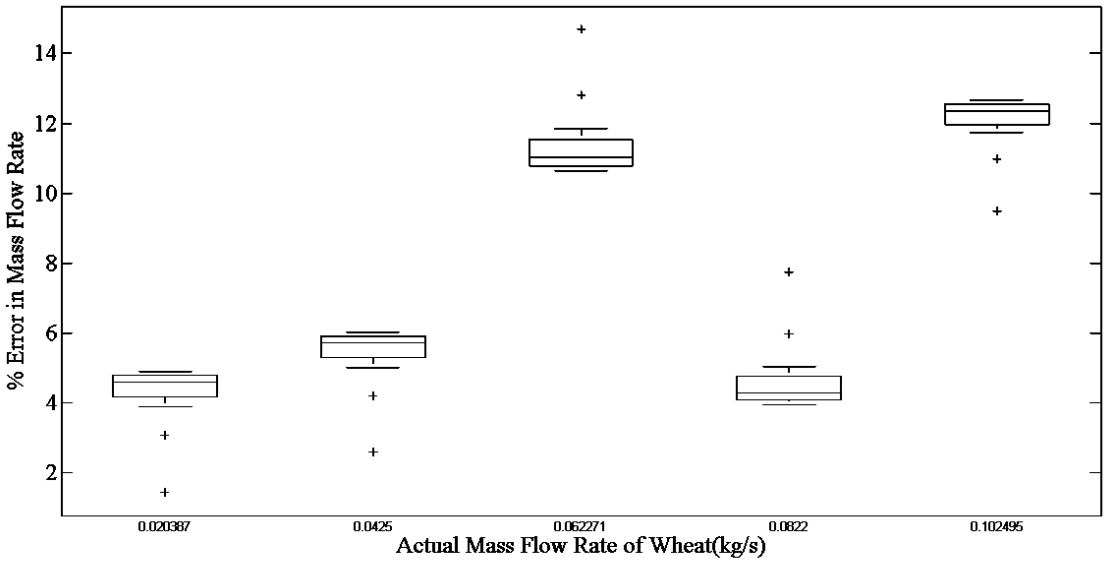

Figure 5-9: Percent error while estimating different mass flow rate of wheat with Model 2.

In Model 2, a relationship was developed between parameter K_1 and specific pressure drop at different mass flow rate of solids. The promising aspect of Model 2 is that none of the estimated error value exceeded 15%. This gives a clear indication that a calibration between K_1 and specific

pressure drop with more data points (i.e. testing at more mass flow rate of wheat in between the maximum and the minimum) will reduce the error in estimation significantly.

5.4 Conclusion

Model 1 provides valuable insight into the development of the flow. It answers the question not answered by Cabrejos and Klinzing (1992) and many other researchers, namely, what happens to the specific pressure drop vs. mass loading ratio relationship when particles are not fully accelerated. It is the first model that can be applied to measure solids mass flow rate in air seeders and similar other applications where, due to design constraints, pressure drop must be measured in the non-developed section. Model 1 was constructed from mathematical manipulation of different established correlations based on experiments conducted with a variety of products of different sizes and shapes. It was then validated with experimental data collected from horizontal conveying of wheat. Hence, it is almost certain that the basic form of the model shown in Equation 5-7 will not change substantially for other agricultural products. On the other hand, the pressure drop measurement in Model 1 is highly location and orientation dependent. For example, the equations developed for parameter estimation (Equations 5-8, 5-11, 5-12) are only valid when the pressure drop is measured in between 0.3m and 0.9 m from the point of particle drop in a straight horizontal section. Model 1 requires solution of a quadratic equation. The solution is then squared to obtain the mass loading ratio. This may lead to error in cases where mass loading ratio is less than unity if enough significant digits are not included in the solution of the quadratic equation.

Model 2 is much simpler and less prone to error from a solutions point of view. It has only one unknown parameter and its basic form (Equation 5-20) is fixed for any conveyed product. It has the advantage of being a location and orientation independent pressure drop measurement. That is, pressure drop can be measured at any location and orientation of the conveying line to correlate it with the unknown parameter $K_{1.}$ However, this model does not have a continuous solution. Each time the mass flow rate of product is changed, there is an associated waiting time for the system to reach the velocity at which the parameter is known. Also, Model 2 does not provide information on flow development.

Chapter 6. Conclusions and Recommendations

Air seeders have established their value in the large-scale agricultural industry for many years now. Still, there is no available technology that can effectively monitor product flow rate. An operator has to spend a significant amount of time to calibrate the roller speed against product flow rate to have an estimation of how much product is being delivered. This method is open-loop. There is no way to verify that products are actually flowing at the required rate.

Hence, the objective of this research was to develop models that could estimate mass flow rate of product based on flow parameters in an air seeder. Pressure drop and average air velocity were the chosen flow parameters based on which the models were developed. Experiments were conducted with wheat in a laboratory prototype air seeder. Pressure drop was measured at various locations in a straight horizontal test section.

Due to design constraints, air seeders usually have only a meter or so of straight horizontal section. For this reason the first model (Model 1) was developed by measuring pressure drop between 0.3 m and 0.9 m (distance measured from the metering box) of the horizontal test section. This model was developed by modifying the relationship between specific pressure drop and mass loading ratio described by Cabrejos and Klinzing (1992). For this model, 73% of the estimates had an error of less than 10%. For the rest of the estimates, the error did not exceed 20%.

The second model (Model 2) was developed from the relationship between mass loading ratio and Froude number (*Fr*) obtained by plotting the dimensionless state diagram for wheat. The unknown parameter of this model was correlated with specific pressure drop. This model had less than 6% error for 60% of the estimates. The rest of the estimates had an error of 10% to 15%.

Although developed for an air seeder, both of the models should be valid for horizontal dilute phase pneumatic conveying in general, because these models were developed by using established correlations for horizontal conveying.

The outcomes of this research are

1. No other research has described the relationship between specific pressure drop and mass loading ratio in the non-developed section of the flow. Model l provides the first explanation on this subject.

2. Model 2 used the dimensionless state diagram to develop a model for mass flow rate estimation. This is the first attempt of this kind.

6.1 Implementation Procedures

This section describes the implementation procedures of Model 1 and Model 2 in an air seeder. Although the models were developed using wheat as product, the methods to extend the models to other products are also mentioned.

6.1.1 Step By Step Procedure for Implementation of Model 1 in an Air Seeder (Product is wheat and the pressure drop is measured in between 0.3 m and 0.9 m)

Step 1: The system records the pressure drop over the entire range of air velocity once the operator starts machine.

Step 2: The operator dispenses product at desired roller speed and air velocity and the system records pressure drop.

Step 3: The system calculates specific pressure drop at the operating velocity (by dividing the pressure drop due to the mixture by the pressure drop due to air only).

Step 4: The system calculates the value of parameters *A* and *B* with the help of Equations 5-8, 5-11 and 5-12.

Step 5: The system estimates the mass flow rate of wheat by using Equations 5-16, 5-17, 5-18 and 5-19.

In a similar manner, the mass flow rate of any product can be estimated. The basic form of the model will remain same as Equation 5-7, which is given by

$$\alpha = 1 + A\mu + B\sqrt{\mu} \qquad 5\text{-}7$$

A relationship must be developed between parameters *A* and *B* and average air velocity separately for each product.

6.1.2 Step By Step Procedure for Implementation of Model 2 in an Air Seeder (Any product)

Step 1: The system records the pressure drop over the entire range air velocity once the operator starts machine.

Step 2: The operator starts dispensing product at the desired roller speed.

Step 3: The system automatically reaches the velocity where the value of K_1 is correlated to specific pressure drop. (For example 20 m/s to use Equation 5-21).

Step 4: The system calculates specific pressure drop at that velocity to determine K_1.

Step 5: The system hands over control to the operator who operates at any velocity at that roller speed. The system calculates the mass flow rate of product by solving Equation 5-20.

If the operator changes the roller speed, the system needs to repeat Steps 3, 4 and 5.

6.2 Future Work

1. For Model 1, the relationship between parameters *A* and *B* and air velocity should be developed for other agricultural products used in an air seeder.
2. For Model 2, the relationship between parameter K_1 and specific pressure drop should be developed for other agricultural products used in an air seeder.

REFERENCES

Atkins, R. P. (2004). *Accurate Metering of Seed and Fertilizer*. Retrieved April 30, 2014, from website of Alberta Government's Ministry of Agriculture and Rural development website: http://www1.agric.gov.ab.ca/$department/deptdocs.nsf/all/eng8023

Binsirawanich, P. (2011). *Mass Flow Sensor Development for an Air Seeding Cart.* Master's Thesis, University of Saskatchewan.

Binsirawanich, P., Noble, S. D., & Henry, J. (2013). U. S. Patent No. 8869718. Washington, DC: U.S. Patent and Trademark Office.

Cabrejos, F. J., & Klinzing, G. E. (1992). Solids Mass Flow Rate Measurements in Pneumatic Conveying. Proceedings of the ASME Winter Annual Meeting, November 8-13, 1992, Anaheim, CA.

Evans, R. P., Blotter, J. D., & Stephens, A. G. (2004). Flow Rate Measurements Using Flow-Induced Pipe Vibration. *ASME Journal of Fluids Engineering*, 126(2), pp. 280-285.

Farbar, L. (1949). Flow Characteristics of Solids-Gas Mixtures in a Horizontal and Vertical Circular Conduit. *Industrial & Engineering Chemistry*, 41(6), pp. 1184-1191.

Gasterstadt, J. (1924). Die Experimentelle Untersuchung des Pneumatischen Fordervorganges. *V.D.I. Zeitschrift*, 68(24), pp. 617-624.

Hinkle, B. L. (1953). *Acceleration of Particles and Pressure Drops Encountered in Horizontal Pneumatic Conveying.* Ph.D. Thesis, Georgia Institute of Technology.

Hofmann, F. (2000). *Fundamentals of Ultrasonic Flow Measurement for Industrial Applications*.

Retrieved 12 September, 2014, from http://www.investigacion.frc.utn.edu.ar/sensores/Caudal/HB_ULTRASONIC_e_144.pdf

Keep, T. (2013). Calibration of Mass Flow Rate of Wheat against Meter Roller Speed. Personal communication.

Keep, T. (2014). Sectional View of the Venturi Flow Meter. Personal communication.

King, P. W. (1973). Mass Flow Measurement of Conveyed Solids by Monitoring of Intrinsic Electrostatic Noise Levels. Proceedings of the 2nd International Conference on the Pneumatic Transport of Solids in Pipes (PNEUMOTRANSPORT 2), September 5-7, 1973, University of Surrey, Guildford, England.

Klinzing, G. E., Rizk, F., Marcus, R., & Leung, L. S. (2010). *Pneumatic Conveying of Solids: A Theoretical and Practical Approach* (3rd Edition). New York: Springer Dordrecht Heidelberg.

Kraus, M. N. (1980). *Pneumatic Conveying Systems for Bulk Materials* (2nd Edition). New York: McGraw-Hill Chemical Engineering.

Lagarias, J., Reeds, J., Wright, M., & Wright, P. (1998). Convergence Properties of the Nelder-Mead Simplex Method in Low Dimensions. *SIAM Journal on Optimization*, 9(1), pp. 112-147.

Memory, R., & Atkins, R. (2005). *Air Seeding- The North American Situation*. Retrieved May 15, 2013, from website of Alberta Government's Ministry of Agriculture and Rural development website: http://www1.agric.gov.ab.ca/$department/deptdocs.nsf/all/eng9937

Mohsenin, N. N. (1986). *Physical Properties of Plant and Animal Materials* (Second ed.). New York: Gordon and Breach Publishers.

Noble, S. D. (2008). Review of Candidate Technologies for Mass Flow Measurement. Report submitted to CNH Canada Ltd., Saskatoon, SK.

Noble, S. D. (2013). Plot of Specific Pressure Drop vs. Mass Loading Ratio from Binsirawanich's Experimental data. Personal communication.

Noble, S. D., & Keep, T. (2013). Data Acquisition and Fan Control Program for Measurement of Air Velocity, Pressure Drop and Solids Flow Rate. Personal communication.

Rizk, F. (1973). *Pneumatic Transport of Plastic Granules in Horizontal Ducts - The Simultaneous Effects of Gravity, Pipe Material, and Solid Properties, Particularly in the Optimal Operating Range.* Ph.D. Thesis, University of Karlsruhe.

Siegel, W. (1970). *Experimentelle Untersuchungen zur pneumatischen Förderung körniger Stoffe in waagerechten Rohren und Überprüfung der Ähnlichkeitsgesetzte.* VDI Research Bulletin, 538.

International Organization for Standardization (2003). *ISO 5167-4: Measurement of Fluid Flow by Means of Pressure Differential Devices Inserted in Circular Cross-section Conduits Running Full - Part 4: Venturi Tubes.*

Sun, M., Liu, S., & Li, Z. (2008). Mass Flow Measurement of Pneumatically Conveyed Solids using Electrical Capacitance Tomography. *Measurement Science and Technology*, 19, pp. 1-6.

Vogt, E. G., & White, R. R. (1948). Friction in the Flow of Suspensions. Granular Solids in Gases through Pipe. *Industrial & Engineering Chemistry*, 40(9), pp. 1731-1738.

Weber, M. (1974). *Strömungfördertechnik*. Germany: Krauskopf-Verlag.

Woodcock, C. R., & Mason, J. S. (1988). *Bulk Solids Handling: An Introduction to the Practice and Technology*. New York: Springer.

Yuan, Y.-X. (1999). A Review of Trust Region Algorithms for Optimization. Proceedings of the 4th International Congress on Industrial & Applied Mathematics (ICIAM 99), July 5-9, 1999, Edinburgh, Scotland.

Zenz, F. A., & Othmer, D. F. (1960). *Fluidization and Fluid-Particle Systems*. New York: Reinhold Publishing Corporation.

Zhang, J. (2012). Air-Solids Flow Measurement Using Electrostatic Techniques, *Electrostatics*, InTech. Retrieved September 29, 2014, from http://www.intechopen.com/books/electrostatics/air-solids-flow-measurement-using-electrostatic-techniques. doi: 10.5772/35937

APPENDIX A: SUMMARY OF COLLECTED DATA

A.1 Summary of Data Set 1

Table A-1: Values of specific pressure drop and mass loading ratio at different air velocities (pressure drop measured between 2.5 m and 3.4 m)

Average air Velocity (m/s)	Air mass flow rate (kg/s)	Wheat mass flow rate (kg/s)	Mass loading ratio (μ)	Pressure drop Air Only (inch H2O)	Pressure drop of mixture (inch H2O)	Specific pressure drop (α)
30	0.0920	0.0000	0.0000	0.5804	0.5804	1.0000
	0.0920	0.0204	0.2216	0.5804	0.6242	1.0754
	0.0920	0.0425	0.4620	0.5804	0.6529	1.1248
	0.0920	0.0623	0.6769	0.5804	0.6831	1.1768
	0.0920	0.0822	0.8935	0.5804	0.7131	1.2285
	0.0920	0.1025	1.1141	0.5804	0.7818	1.3469
28	0.0850	0.0000	0.0000	0.5024	0.5024	1.0000
	0.0850	0.0204	0.2398	0.5024	0.5497	1.0942
	0.0850	0.0425	0.5000	0.5024	0.5784	1.1512
	0.0850	0.0623	0.7326	0.5024	0.5988	1.1919
	0.0850	0.0822	0.9671	0.5024	0.6463	1.2864
	0.0850	0.1025	1.2058	0.5024	0.7020	1.3974
26	0.0790	0.0000	0.0000	0.4368	0.4368	1.0000
	0.0790	0.0204	0.2581	0.4368	0.4812	1.1018
	0.0790	0.0425	0.5380	0.4368	0.5041	1.1542
	0.0790	0.0623	0.7882	0.4368	0.5321	1.2184
	0.0790	0.0822	1.0405	0.4368	0.5791	1.3259
	0.0790	0.1025	1.2974	0.4368	0.6312	1.4452
24	0.0730	0.0000	0.0000	0.3785	0.3785	1.0000
	0.0730	0.0204	0.2793	0.3785	0.4168	1.1013
	0.0730	0.0425	0.5822	0.3785	0.4399	1.1622
	0.0730	0.0623	0.8530	0.3785	0.4698	1.2414
	0.0730	0.0822	1.1260	0.3785	0.5121	1.3532
	0.0730	0.1025	1.4040	0.3785	0.5565	1.4704
22	0.0660	0.0000	0.0000	0.3185	0.3185	1.0000
	0.0660	0.0204	0.3089	0.3185	0.3511	1.1021
	0.0660	0.0425	0.6439	0.3185	0.3733	1.1719
	0.0660	0.0623	0.9435	0.3185	0.4044	1.2695
	0.0660	0.0822	1.2455	0.3185	0.4446	1.3958
	0.0660	0.1025	1.5530	0.3185	0.4968	1.5595

Table A-1 (continues): Values of specific pressure drop and mass loading ratio at different air velocities (pressure drop measured between 2.5 m and 3.4 m)

Average air Velocity (m/s)	Air mass flow rate (kg/s)	Wheat mass flow rate (kg/s)	Mass loading ratio (μ)	Pressure drop Air Only (inch H2O)	Pressure drop of mixture (inch H2O)	Specific pressure drop (α)
20	0.0600	0.0000	0.0000	0.2693	0.2693	1.0000
	0.0600	0.0204	0.3398	0.2693	0.2998	1.1132
	0.0600	0.0425	0.7083	0.2693	0.3236	1.2014
	0.0600	0.0623	1.0379	0.2693	0.3481	1.2926
	0.0600	0.0822	1.3700	0.2693	0.3874	1.4384
	0.0600	0.1025	1.7083	0.2693	0.4275	1.5874
18	0.0540	0.0000	0.0000	0.2227	0.2227	1.0000
	0.0540	0.0204	0.3775	0.2227	0.2502	1.1234
	0.0540	0.0425	0.7870	0.2227	0.2726	1.2241
	0.0540	0.0623	1.1532	0.2227	0.2938	1.3193
	0.0540	0.0822	1.5222	0.2227	0.3284	1.4747
	0.0540	0.1025	1.8981	0.2227	0.3683	1.6537
16	0.0480	0.0000	0.0000	0.1784	0.1784	1.0000
	0.0480	0.0204	0.4247	0.1784	0.2058	1.1534
	0.0480	0.0425	0.8854	0.1784	0.2267	1.2706
	0.0480	0.0623	1.2973	0.1784	0.2475	1.3871
	0.0480	0.0822	1.7125	0.1784	0.2799	1.5689
	0.0480	0.1025	2.1353	0.1784	0.3166	1.7745
14	0.0420	0.0000	0.0000	0.1417	0.1417	1.0000
	0.0420	0.0204	0.4854	0.1417	0.1640	1.1574
	0.0420	0.0425	1.0119	0.1417	0.1812	1.2781
	0.0420	0.0623	1.4826	0.1417	0.2059	1.4529
	0.0420	0.0822	1.9571	0.1417	0.2524	1.7811
	0.0420	0.1025	2.4404	0.1417	0.2958	2.0873
13	0.0390	0.0000	0.0000	0.1221	0.1221	1.0000
	0.0390	0.0204	0.5227	0.1221	0.1457	1.1926
	0.0390	0.0425	1.0897	0.1221	0.1631	1.3354
	0.0390	0.0623	1.5967	0.1221	0.1931	1.5810
	0.0390	0.0822	2.1077	0.1221	0.3517	2.8791
	0.0390	0.1025	2.6281	0.1221	0.3376	2.7641

Table A-2: Values of specific pressure drop and mass loading ratio at different air velocities (pressure drop measured between 3.4 m and 4.6 m)

Average air Velocity (m/s)	Air mass flow rate (kg/s)	Wheat mass flow rate (kg/s)	Mass loading ratio (μ)	Pressure drop Air Only (inch H2O)	Pressure drop of mixture (inch H2O)	Specific pressure drop (α)
30	0.0920	0.0000	0.0000	1.3279	1.3279	1.0000
	0.0920	0.0204	0.2216	1.3279	1.3437	1.0119
	0.0920	0.0425	0.4620	1.3279	1.3020	0.9805
	0.0920	0.0623	0.6769	1.3279	1.4303	1.0771
	0.0920	0.0822	0.8935	1.3279	1.3358	1.0060
	0.0920	0.1025	1.1141	1.3279	1.5252	1.1486
28	0.0850	0.0000	0.0000	1.1425	1.1425	1.0000
	0.0850	0.0204	0.2398	1.1425	1.1762	1.0294
	0.0850	0.0425	0.5000	1.1425	1.1586	1.0141
	0.0850	0.0623	0.7326	1.1425	1.2517	1.0955
	0.0850	0.0822	0.9671	1.1425	1.1940	1.0450
	0.0850	0.1025	1.2058	1.1425	1.3566	1.1873
26	0.0790	0.0000	0.0000	0.9695	0.9695	1.0000
	0.0790	0.0204	0.2581	0.9695	1.0074	1.0391
	0.0790	0.0425	0.5380	0.9695	1.0017	1.0332
	0.0790	0.0623	0.7882	0.9695	1.0858	1.1200
	0.0790	0.0822	1.0405	0.9695	1.0518	1.0849
	0.0790	0.1025	1.2974	0.9695	1.1963	1.2339
24	0.0730	0.0000	0.0000	0.8388	0.8388	1.0000
	0.0730	0.0204	0.2793	0.8388	0.8665	1.0331
	0.0730	0.0425	0.5822	0.8388	0.8567	1.0214
	0.0730	0.0623	0.8530	0.8388	0.9339	1.1134
	0.0730	0.0822	1.1260	0.8388	0.9042	1.0780
	0.0730	0.1025	1.4040	0.8388	1.0417	1.2419
22	0.0660	0.0000	0.0000	0.6983	0.6983	1.0000
	0.0660	0.0204	0.3089	0.6983	0.7321	1.0484
	0.0660	0.0425	0.6439	0.6983	0.7315	1.0475
	0.0660	0.0623	0.9435	0.6983	0.8043	1.1517
	0.0660	0.0822	1.2455	0.6983	0.7839	1.1226
	0.0660	0.1025	1.5530	0.6983	0.9044	1.2951
20	0.0600	0.0000	0.0000	0.5768	0.5768	1.0000
	0.0600	0.0204	0.3398	0.5768	0.6145	1.0655
	0.0600	0.0425	0.7083	0.5768	0.6139	1.0644
	0.0600	0.0623	1.0379	0.5768	0.6867	1.1905
	0.0600	0.0822	1.3700	0.5768	0.6813	1.1812
	0.0600	0.1025	1.7083	0.5768	0.7859	1.3625

Table A-2 (continues): Values of specific pressure drop and mass loading ratio at different air velocities (pressure drop measured between 3.4 m and 4.6 m)

Average air Velocity (m/s)	Air mass flow rate (kg/s)	Wheat mass flow rate (kg/s)	Mass loading ratio (μ)	Pressure drop Air Only (inch H2O)	Pressure drop of mixture (inch H2O)	Specific pressure drop (α)
18	0.0540	0.0000	0.0000	0.4650	0.4650	1.0000
	0.0540	0.0204	0.3775	0.4650	0.5030	1.0819
	0.0540	0.0425	0.7870	0.4650	0.5099	1.0966
	0.0540	0.0623	1.1532	0.4650	0.5850	1.2581
	0.0540	0.0822	1.5222	0.4650	0.5790	1.2453
	0.0540	0.1025	1.8981	0.4650	0.6827	1.4682
16	0.0480	0.0000	0.0000	0.3676	0.3676	1.0000
	0.0480	0.0204	0.4247	0.3676	0.4082	1.1107
	0.0480	0.0425	0.8854	0.3676	0.4238	1.1530
	0.0480	0.0623	1.2973	0.3676	0.4923	1.3393
	0.0480	0.0822	1.7125	0.3676	0.4949	1.3463
	0.0480	0.1025	2.1353	0.3676	0.6036	1.6421
14	0.0420	0.0000	0.0000	0.2820	0.2820	1.0000
	0.0420	0.0204	0.4854	0.2820	0.3219	1.1418
	0.0420	0.0425	1.0119	0.2820	0.3469	1.2304
	0.0420	0.0623	1.4826	0.2820	0.4284	1.5192
	0.0420	0.0822	1.9571	0.2820	0.4564	1.6185
	0.0420	0.1025	2.4404	0.2820	0.5556	1.9705
13	0.0390	0.0000	0.0000	0.2410	0.2410	1.0000
	0.0390	0.0204	0.5227	0.2410	0.2859	1.1861
	0.0390	0.0425	1.0897	0.2410	0.3191	1.3241
	0.0390	0.0623	1.5967	0.2410	0.4115	1.7072
	0.0390	0.0822	2.1077	0.2410	0.5067	2.1022
	0.0390	0.1025	2.6281	0.2410	0.5283	2.1919

Table A-3: Values of specific pressure drop and mass loading ratio at different air velocities (pressure drop measured between 4.6 m and 5.5 m)

Average air Velocity (m/s)	Air mass flow rate (kg/s)	Wheat mass flow rate (kg/s)	Mass loading ratio (μ)	Pressure drop Air Only (inch H2O)	Pressure drop of mixture (inch H2O)	Specific pressure drop (α)
30	0.0920	0.0000	0.0000	0.5558	0.5558	1.0000
	0.0920	0.0204	0.2216	0.5558	0.5885	1.0589
	0.0920	0.0425	0.4620	0.5558	0.6196	1.1148
	0.0920	0.0623	0.6769	0.5558	0.6571	1.1822
	0.0920	0.0822	0.8935	0.5558	0.6572	1.1824
	0.0920	0.1025	1.1141	0.5558	0.7299	1.3132
28	0.0850	0.0000	0.0000	0.4875	0.4875	1.0000
	0.0850	0.0204	0.2398	0.4875	0.5207	1.0682
	0.0850	0.0425	0.5000	0.4875	0.5551	1.1388
	0.0850	0.0623	0.7326	0.4875	0.5789	1.1876
	0.0850	0.0822	0.9671	0.4875	0.5966	1.2238
	0.0850	0.1025	1.2058	0.4875	0.6561	1.3458
26	0.0790	0.0000	0.0000	0.4222	0.4222	1.0000
	0.0790	0.0204	0.2581	0.4222	0.4582	1.0854
	0.0790	0.0425	0.5380	0.4222	0.4877	1.1553
	0.0790	0.0623	0.7882	0.4222	0.5156	1.2212
	0.0790	0.0822	1.0405	0.4222	0.5344	1.2658
	0.0790	0.1025	1.2974	0.4222	0.5950	1.4094
24	0.0730	0.0000	0.0000	0.3687	0.3687	1.0000
	0.0730	0.0204	0.2793	0.3687	0.3981	1.0798
	0.0730	0.0425	0.5822	0.3687	0.4311	1.1693
	0.0730	0.0623	0.8530	0.3687	0.4542	1.2320
	0.0730	0.0822	1.1260	0.3687	0.4719	1.2801
	0.0730	0.1025	1.4040	0.3687	0.5361	1.4542
22	0.0660	0.0000	0.0000	0.3111	0.3111	1.0000
	0.0660	0.0204	0.3089	0.3111	0.3401	1.0933
	0.0660	0.0425	0.6439	0.3111	0.3723	1.1967
	0.0660	0.0623	0.9435	0.3111	0.4008	1.2885
	0.0660	0.0822	1.2455	0.3111	0.4209	1.3529
	0.0660	0.1025	1.5530	0.3111	0.4781	1.5368
20	0.0600	0.0000	0.0000	0.2630	0.2630	1.0000
	0.0600	0.0204	0.3398	0.2630	0.2931	1.1141
	0.0600	0.0425	0.7083	0.2630	0.3214	1.2218
	0.0600	0.0623	1.0379	0.2630	0.3553	1.3508
	0.0600	0.0822	1.3700	0.2630	0.3780	1.4371
	0.0600	0.1025	1.7083	0.2630	0.4332	1.6467

Table A-3 (continues): Values of specific pressure drop and mass loading ratio at different air velocities (pressure drop measured between 4.6 m and 5.5 m)

Average air Velocity (m/s)	Air mass flow rate (kg/s)	Wheat mass flow rate (kg/s)	Mass loading ratio (μ)	Pressure drop Air Only (inch H2O)	Pressure drop of mixture (inch H2O)	Specific pressure drop (α)
18	0.0540	0.0000	0.0000	0.2165	0.2165	1.0000
	0.0540	0.0204	0.3775	0.2165	0.2468	1.1398
	0.0540	0.0425	0.7870	0.2165	0.2775	1.2819
	0.0540	0.0623	1.1532	0.2165	0.3113	1.4377
	0.0540	0.0822	1.5222	0.2165	0.3318	1.5326
	0.0540	0.1025	1.8981	0.2165	0.3898	1.8005
16	0.0480	0.0000	0.0000	0.1750	0.1750	1.0000
	0.0480	0.0204	0.4247	0.1750	0.2055	1.1741
	0.0480	0.0425	0.8854	0.1750	0.2391	1.3661
	0.0480	0.0623	1.2973	0.1750	0.2745	1.5681
	0.0480	0.0822	1.7125	0.1750	0.2939	1.6792
	0.0480	0.1025	2.1353	0.1750	0.3452	1.9721
14	0.0420	0.0000	0.0000	0.1384	0.1384	1.0000
	0.0420	0.0204	0.4854	0.1384	0.1681	1.2150
	0.0420	0.0425	1.0119	0.1384	0.2010	1.4528
	0.0420	0.0623	1.4826	0.1384	0.2331	1.6849
	0.0420	0.0822	1.9571	0.1384	0.2420	1.7490
	0.0420	0.1025	2.4404	0.1384	0.2808	2.0296
13	0.0390	0.0000	0.0000	0.1193	0.1193	1.0000
	0.0390	0.0204	0.5227	0.1193	0.1506	1.2627
	0.0390	0.0425	1.0897	0.1193	0.1812	1.5191
	0.0390	0.0623	1.5967	0.1193	0.2075	1.7395
	0.0390	0.1025	2.6281	0.1193	0.2491	2.0888

Table A-4: Values of specific pressure drop and mass loading ratio at different air velocities (pressure drop measured between 5.5 m and 6.4 m)

Average air Velocity (m/s)	Air mass flow rate (kg/s)	Wheat mass flow rate (kg/s)	Mass loading ratio (μ)	Pressure drop Air Only (inch H2O)	Pressure drop of mixture (inch H2O)	Specific pressure drop (α)
30	0.0920	0.0000	0.0000	0.5702	0.5702	1.0000
	0.0920	0.0204	0.2216	0.5702	0.5935	1.0408
	0.0920	0.0425	0.4620	0.5702	0.6090	1.0681
	0.0920	0.0623	0.6769	0.5702	0.6275	1.1005
	0.0920	0.0822	0.8935	0.5702	0.6247	1.0956
	0.0920	0.1025	1.1141	0.5702	0.6754	1.1845
28	0.0850	0.0000	0.0000	0.4968	0.4968	1.0000
	0.0850	0.0204	0.2398	0.4968	0.5234	1.0536
	0.0850	0.0425	0.5000	0.4968	0.5358	1.0785
	0.0850	0.0623	0.7326	0.4968	0.5604	1.1281
	0.0850	0.0822	0.9671	0.4968	0.5602	1.1276
	0.0850	0.1025	1.2058	0.4968	0.6034	1.2145
26	0.0790	0.0000	0.0000	0.4330	0.4330	1.0000
	0.0790	0.0204	0.2581	0.4330	0.4551	1.0511
	0.0790	0.0425	0.5380	0.4330	0.4680	1.0809
	0.0790	0.0623	0.7882	0.4330	0.4885	1.1282
	0.0790	0.0822	1.0405	0.4330	0.4996	1.1539
	0.0790	0.1025	1.2974	0.4330	0.5394	1.2458
24	0.0730	0.0000	0.0000	0.3779	0.3779	1.0000
	0.0730	0.0204	0.2793	0.3779	0.3948	1.0449
	0.0730	0.0425	0.5822	0.3779	0.4069	1.0767
	0.0730	0.0623	0.8530	0.3779	0.4288	1.1347
	0.0730	0.0822	1.1260	0.3779	0.4394	1.1628
	0.0730	0.1025	1.4040	0.3779	0.4698	1.2432
22	0.0660	0.0000	0.0000	0.3190	0.3190	1.0000
	0.0660	0.0204	0.3089	0.3190	0.3386	1.0613
	0.0660	0.0425	0.6439	0.3190	0.3494	1.0952
	0.0660	0.0623	0.9435	0.3190	0.3705	1.1612
	0.0660	0.0822	1.2455	0.3190	0.3795	1.1897
	0.0660	0.1025	1.5530	0.3190	0.4133	1.2955
20	0.0600	0.0000	0.0000	0.2682	0.2682	1.0000
	0.0600	0.0204	0.3398	0.2682	0.2877	1.0727
	0.0600	0.0425	0.7083	0.2682	0.2990	1.1148
	0.0600	0.0623	1.0379	0.2682	0.3184	1.1871
	0.0600	0.0822	1.3700	0.2682	0.3303	1.2315
	0.0600	0.1025	1.7083	0.2682	0.3600	1.3422

Table A-4 (continues): Values of specific pressure drop and mass loading ratio at different air velocities (pressure drop measured between 5.5 m and 6.4 m)

Average air Velocity (m/s)	Air mass flow rate (kg/s)	Wheat mass flow rate (kg/s)	Mass loading ratio (μ)	Pressure drop Air Only (inch H2O)	Pressure drop of mixture (inch H2O)	Specific pressure drop (α)
18	0.0540	0.0000	0.0000	0.2217	0.2217	1.0000
	0.0540	0.0204	0.3775	0.2217	0.2379	1.0729
	0.0540	0.0425	0.7870	0.2217	0.2513	1.1334
	0.0540	0.0623	1.1532	0.2217	0.2741	1.2365
	0.0540	0.0822	1.5222	0.2217	0.2805	1.2651
	0.0540	0.1025	1.8981	0.2217	0.3101	1.3985
16	0.0480	0.0000	0.0000	0.1779	0.1779	1.0000
	0.0480	0.0204	0.4247	0.1779	0.1960	1.1018
	0.0480	0.0425	0.8854	0.1779	0.2115	1.1888
	0.0480	0.0623	1.2973	0.1779	0.2272	1.2770
	0.0480	0.0822	1.7125	0.1779	0.2403	1.3506
	0.0480	0.1025	2.1353	0.1779	0.2555	1.4360
14	0.0420	0.0000	0.0000	0.1402	0.1402	1.0000
	0.0420	0.0204	0.4854	0.1402	0.1565	1.1157
	0.0420	0.0425	1.0119	0.1402	0.1705	1.2160
	0.0420	0.0623	1.4826	0.1402	0.1856	1.3238
	0.0420	0.0822	1.9571	0.1402	0.2049	1.4612
	0.0420	0.1025	2.4404	0.1402	0.2188	1.5602
13	0.0390	0.0000	0.0000	0.1212	0.1212	1.0000
	0.0390	0.0204	0.5227	0.1212	0.1384	1.1422
	0.0390	0.0425	1.0897	0.1212	0.1553	1.2809
	0.0390	0.0623	1.5967	0.1212	0.1700	1.4030
	0.0390	0.1025	2.6281	0.1212	0.2092	1.7258

Table A-5: Values of specific pressure drop and mass loading ratio at different air velocities (pressure drop measured between 6.4 m and 7.3 m)

Average air Velocity (m/s)	Air mass flow rate (kg/s)	Wheat mass flow rate (kg/s)	Mass loading ratio (μ)	Pressure drop Air Only (inch H2O)	Pressure drop of mixture (inch H2O)	Specific pressure drop (α)
30	0.0920	0.0000	0.0000	0.5737	0.5737	1.0000
	0.0920	0.0204	0.2216	0.5737	0.5913	1.0308
	0.0920	0.0425	0.4620	0.5737	0.6040	1.0529
	0.0920	0.0623	0.6769	0.5737	0.6277	1.0942
	0.0920	0.0822	0.8935	0.5737	0.6173	1.0762
	0.0920	0.1025	1.1141	0.5737	0.6735	1.1741
28	0.0850	0.0000	0.0000	0.5041	0.5041	1.0000
	0.0850	0.0204	0.2398	0.5041	0.5221	1.0357
	0.0850	0.0425	0.5000	0.5041	0.5376	1.0664
	0.0850	0.0623	0.7326	0.5041	0.5535	1.0979
	0.0850	0.0822	0.9671	0.5041	0.5604	1.1117
	0.0850	0.1025	1.2058	0.5041	0.5998	1.1899
26	0.0790	0.0000	0.0000	0.4363	0.4363	1.0000
	0.0790	0.0204	0.2581	0.4363	0.4529	1.0381
	0.0790	0.0425	0.5380	0.4363	0.4724	1.0828
	0.0790	0.0623	0.7882	0.4363	0.4860	1.1138
	0.0790	0.0822	1.0405	0.4363	0.4907	1.1248
	0.0790	0.1025	1.2974	0.4363	0.5328	1.2211
24	0.0730	0.0000	0.0000	0.3794	0.3794	1.0000
	0.0730	0.0204	0.2793	0.3794	0.3927	1.0350
	0.0730	0.0425	0.5822	0.3794	0.4112	1.0836
	0.0730	0.0623	0.8530	0.3794	0.4245	1.1189
	0.0730	0.0822	1.1260	0.3794	0.4257	1.1220
	0.0730	0.1025	1.4040	0.3794	0.4689	1.2358
22	0.0660	0.0000	0.0000	0.3211	0.3211	1.0000
	0.0660	0.0204	0.3089	0.3211	0.3371	1.0496
	0.0660	0.0425	0.6439	0.3211	0.3537	1.1015
	0.0660	0.0623	0.9435	0.3211	0.3674	1.1440
	0.0660	0.0822	1.2455	0.3211	0.3782	1.1777
	0.0660	0.1025	1.5530	0.3211	0.4136	1.2880
20	0.0600	0.0000	0.0000	0.2699	0.2699	1.0000
	0.0600	0.0204	0.3398	0.2699	0.2860	1.0596
	0.0600	0.0425	0.7083	0.2699	0.3024	1.1204
	0.0600	0.0623	1.0379	0.2699	0.3168	1.1736
	0.0600	0.0822	1.3700	0.2699	0.3319	1.2295
	0.0600	0.1025	1.7083	0.2699	0.3620	1.3413

Table A-5 (continues): Values of specific pressure drop and mass loading ratio at different air velocities (pressure drop measured between 6.4 m and 7.3 m)

Average air Velocity (m/s)	Air mass flow rate (kg/s)	Wheat mass flow rate (kg/s)	Mass loading ratio (μ)	Pressure drop Air Only (inch H2O)	Pressure drop of mixture (inch H2O)	Specific pressure drop (α)
18	0.0540	0.0000	0.0000	0.2250	0.2250	1.0000
	0.0540	0.0204	0.3775	0.2250	0.2366	1.0516
	0.0540	0.0425	0.7870	0.2250	0.2584	1.1486
	0.0540	0.0623	1.1532	0.2250	0.2722	1.2098
	0.0540	0.0822	1.5222	0.2250	0.2950	1.3112
	0.0540	0.1025	1.8981	0.2250	0.3156	1.4029
16	0.0480	0.0000	0.0000	0.1808	0.1808	1.0000
	0.0480	0.0204	0.4247	0.1808	0.1949	1.0776
	0.0480	0.0425	0.8854	0.1808	0.2178	1.2046
	0.0480	0.0623	1.2973	0.1808	0.2339	1.2934
	0.0480	0.0822	1.7125	0.1808	0.2598	1.4365
	0.0480	0.1025	2.1353	0.1808	0.2920	1.6145
14	0.0420	0.0000	0.0000	0.1417	0.1417	1.0000
	0.0420	0.0204	0.4854	0.1417	0.1562	1.1025
	0.0420	0.0425	1.0119	0.1417	0.1821	1.2857
	0.0420	0.0623	1.4826	0.1417	0.2067	1.4595
	0.0420	0.0822	1.9571	0.1417	0.2424	1.7116
	0.0420	0.1025	2.4404	0.1417	0.2813	1.9859
13	0.0390	0.0000	0.0000	0.1228	0.1228	1.0000
	0.0390	0.0204	0.5227	0.1228	0.1388	1.1304
	0.0390	0.0425	1.0897	0.1228	0.1712	1.3942
	0.0390	0.0623	1.5967	0.1228	0.2035	1.6568
	0.0390	0.1025	2.6281	0.1228	0.2660	2.1660

Table A-6: Values of specific pressure drop and mass loading ratio at different air velocities (pressure drop measured between 7.3 m and 8.2 m)

Average air Velocity (m/s)	Air mass flow rate (kg/s)	Wheat mass flow rate (kg/s)	Mass loading ratio (μ)	Pressure drop Air Only (inch H2O)	Pressure drop of mixture (inch H2O)	Specific pressure drop (α)
30	0.0920	0.0000	0.0000	0.5789	0.5789	1.0000
	0.0920	0.0204	0.2216	0.5789	0.6003	1.0371
	0.0920	0.0425	0.4620	0.5789	0.6265	1.0823
	0.0920	0.0623	0.6769	0.5789	0.6368	1.1002
	0.0920	0.0822	0.8935	0.5789	0.6397	1.1052
	0.0920	0.1025	1.1141	0.5789	0.6862	1.1854
28	0.0850	0.0000	0.0000	0.5070	0.5070	1.0000
	0.0850	0.0204	0.2398	0.5070	0.5298	1.0449
	0.0850	0.0425	0.5000	0.5070	0.5516	1.0879
	0.0850	0.0623	0.7326	0.5070	0.5649	1.1141
	0.0850	0.0822	0.9671	0.5070	0.5650	1.1143
	0.0850	0.1025	1.2058	0.5070	0.6074	1.1979
26	0.0790	0.0000	0.0000	0.4420	0.4420	1.0000
	0.0790	0.0204	0.2581	0.4420	0.4626	1.0467
	0.0790	0.0425	0.5380	0.4420	0.4839	1.0948
	0.0790	0.0623	0.7882	0.4420	0.4918	1.1128
	0.0790	0.0822	1.0405	0.4420	0.5060	1.1449
	0.0790	0.1025	1.2974	0.4420	0.5381	1.2176
24	0.0730	0.0000	0.0000	0.3833	0.3833	1.0000
	0.0730	0.0204	0.2793	0.3833	0.3987	1.0403
	0.0730	0.0425	0.5822	0.3833	0.4203	1.0966
	0.0730	0.0623	0.8530	0.3833	0.4313	1.1253
	0.0730	0.0822	1.1260	0.3833	0.4429	1.1555
	0.0730	0.1025	1.4040	0.3833	0.4725	1.2327
22	0.0660	0.0000	0.0000	0.3231	0.3231	1.0000
	0.0660	0.0204	0.3089	0.3231	0.3427	1.0606
	0.0660	0.0425	0.6439	0.3231	0.3628	1.1226
	0.0660	0.0623	0.9435	0.3231	0.3729	1.1542
	0.0660	0.0822	1.2455	0.3231	0.3772	1.1673
	0.0660	0.1025	1.5530	0.3231	0.4125	1.2767
20	0.0600	0.0000	0.0000	0.2747	0.2747	1.0000
	0.0600	0.0204	0.3398	0.2747	0.2897	1.0548
	0.0600	0.0425	0.7083	0.2747	0.3081	1.1215
	0.0600	0.0623	1.0379	0.2747	0.3175	1.1560
	0.0600	0.0822	1.3700	0.2747	0.3391	1.2346
	0.0600	0.1025	1.7083	0.2747	0.3572	1.3004

Table A-6 (continues): Values of specific pressure drop and mass loading ratio at different air velocities (pressure drop measured between 7.3 m and 8.2 m)

Average air Velocity (m/s)	Air mass flow rate (kg/s)	Wheat mass flow rate (kg/s)	Mass loading ratio (μ)	Pressure drop Air Only (inch H2O)	Pressure drop of mixture (inch H2O)	Specific pressure drop (α)
18	0.0540	0.0000	0.0000	0.2274	0.2274	1.0000
	0.0540	0.0204	0.3775	0.2274	0.2410	1.0596
	0.0540	0.0425	0.7870	0.2274	0.2584	1.1359
	0.0540	0.0623	1.1532	0.2274	0.2698	1.1864
	0.0540	0.0822	1.5222	0.2274	0.2759	1.2130
	0.0540	0.1025	1.8981	0.2274	0.3010	1.3235
16	0.0480	0.0000	0.0000	0.1826	0.1826	1.0000
	0.0480	0.0204	0.4247	0.1826	0.1971	1.0791
	0.0480	0.0425	0.8854	0.1826	0.2136	1.1694
	0.0480	0.0623	1.2973	0.1826	0.2223	1.2174
	0.0480	0.0822	1.7125	0.1826	0.2334	1.2778
	0.0480	0.1025	2.1353	0.1826	0.2484	1.3603
14	0.0420	0.0000	0.0000	0.1441	0.1441	1.0000
	0.0420	0.0204	0.4854	0.1441	0.1556	1.0800
	0.0420	0.0425	1.0119	0.1441	0.1727	1.1985
	0.0420	0.0623	1.4826	0.1441	0.1822	1.2646
	0.0420	0.0822	1.9571	0.1441	0.1832	1.2716
	0.0420	0.1025	2.4404	0.1441	0.2004	1.3908
13	0.0390	0.0000	0.0000	0.1259	0.1259	1.0000
	0.0390	0.0204	0.5227	0.1259	0.1376	1.0934
	0.0390	0.0425	1.0897	0.1259	0.1543	1.2256
	0.0390	0.0623	1.5967	0.1259	0.1609	1.2783
	0.0390	0.1025	2.6281	0.1259	0.1761	1.3993

Table A-7: Values of specific pressure drop and mass loading ratio at different air velocities (pressure drop measured between 8.2 m and 9.1 m)

Average air Velocity (m/s)	Air mass flow rate (kg/s)	Wheat mass flow rate (kg/s)	Mass loading ratio (μ)	Pressure drop Air Only (inch H2O)	Pressure drop of mixture (inch H2O)	Specific pressure drop (α)
30	0.0920	0.0000	0.0000	0.6038	0.6038	1.0000
	0.0920	0.0204	0.2216	0.6038	0.6148	1.0182
	0.0920	0.0425	0.4620	0.6038	0.6211	1.0286
	0.0920	0.0623	0.6769	0.6038	0.6286	1.0410
	0.0920	0.0822	0.8935	0.6038	0.6219	1.0300
	0.0920	0.1025	1.1141	0.6038	0.6760	1.1195
28	0.0850	0.0000	0.0000	0.5267	0.5267	1.0000
	0.0850	0.0204	0.2398	0.5267	0.5396	1.0245
	0.0850	0.0425	0.5000	0.5267	0.5486	1.0415
	0.0850	0.0623	0.7326	0.5267	0.5621	1.0671
	0.0850	0.0822	0.9671	0.5267	0.5597	1.0625
	0.0850	0.1025	1.2058	0.5267	0.5987	1.1366
26	0.0790	0.0000	0.0000	0.4595	0.4595	1.0000
	0.0790	0.0204	0.2581	0.4595	0.4628	1.0071
	0.0790	0.0425	0.5380	0.4595	0.4793	1.0431
	0.0790	0.0623	0.7882	0.4595	0.4855	1.0566
	0.0790	0.0822	1.0405	0.4595	0.4927	1.0721
	0.0790	0.1025	1.2974	0.4595	0.5306	1.1548
24	0.0730	0.0000	0.0000	0.3967	0.3967	1.0000
	0.0730	0.0204	0.2793	0.3967	0.4046	1.0200
	0.0730	0.0425	0.5822	0.3967	0.4154	1.0472
	0.0730	0.0623	0.8530	0.3967	0.4232	1.0669
	0.0730	0.0822	1.1260	0.3967	0.4244	1.0699
	0.0730	0.1025	1.4040	0.3967	0.4611	1.1625
22	0.0660	0.0000	0.0000	0.3370	0.3370	1.0000
	0.0660	0.0204	0.3089	0.3370	0.3439	1.0204
	0.0660	0.0425	0.6439	0.3370	0.3533	1.0483
	0.0660	0.0623	0.9435	0.3370	0.3631	1.0776
	0.0660	0.0822	1.2455	0.3370	0.3713	1.1019
	0.0660	0.1025	1.5530	0.3370	0.3942	1.1699
20	0.0600	0.0000	0.0000	0.2831	0.2831	1.0000
	0.0600	0.0204	0.3398	0.2831	0.2927	1.0340
	0.0600	0.0425	0.7083	0.2831	0.2997	1.0589
	0.0600	0.0623	1.0379	0.2831	0.3076	1.0866
	0.0600	0.0822	1.3700	0.2831	0.3084	1.0895
	0.0600	0.1025	1.7083	0.2831	0.3321	1.1733

Table A-7 (continues): Values of specific pressure drop and mass loading ratio at different air velocities (pressure drop measured between 8.2 m and 9.1 m)

Average air Velocity (m/s)	Air mass flow rate (kg/s)	Wheat mass flow rate (kg/s)	Mass loading ratio (μ)	Pressure drop Air Only (inch H2O)	Pressure drop of mixture (inch H2O)	Specific pressure drop (α)
18	0.0540	0.0000	0.0000	0.2325	0.2325	1.0000
	0.0540	0.0204	0.3775	0.2325	0.2405	1.0344
	0.0540	0.0425	0.7870	0.2325	0.2488	1.0700
	0.0540	0.0623	1.1532	0.2325	0.2575	1.1075
	0.0540	0.0822	1.5222	0.2325	0.2604	1.1201
	0.0540	0.1025	1.8981	0.2325	0.2748	1.1822
16	0.0480	0.0000	0.0000	0.1869	0.1869	1.0000
	0.0480	0.0204	0.4247	0.1869	0.1960	1.0487
	0.0480	0.0425	0.8854	0.1869	0.2038	1.0908
	0.0480	0.0623	1.2973	0.1869	0.2101	1.1245
	0.0480	0.0822	1.7125	0.1869	0.2124	1.1365
	0.0480	0.1025	2.1353	0.1869	0.2224	1.1902
14	0.0420	0.0000	0.0000	0.1485	0.1485	1.0000
	0.0420	0.0204	0.4854	0.1485	0.1549	1.0430
	0.0420	0.0425	1.0119	0.1485	0.1608	1.0826
	0.0420	0.0623	1.4826	0.1485	0.1671	1.1252
	0.0420	0.0822	1.9571	0.1485	0.1630	1.0976
	0.0420	0.1025	2.4404	0.1485	0.1780	1.1983
13	0.0390	0.0000	0.0000	0.1277	0.1277	1.0000
	0.0390	0.0204	0.5227	0.1277	0.1377	1.0787
	0.0390	0.0425	1.0897	0.1277	0.1442	1.1297
	0.0390	0.0623	1.5967	0.1277	0.1484	1.1628
	0.0390	0.1025	2.6281	0.1277	0.1655	1.2963

Table A-8: Values of specific pressure drop and mass loading ratio at different air velocities (pressure drop measured between 9.1 m and 10 m)

Average air Velocity (m/s)	Air mass flow rate (kg/s)	Wheat mass flow rate (kg/s)	Mass loading ratio (μ)	Pressure drop Air Only (inch H2O)	Pressure drop of mixture (inch H2O)	Specific pressure drop (α)
30	0.0920	0.0000	0.0000	0.5281	0.5281	1.0000
	0.0920	0.0204	0.2216	0.5281	0.5387	1.0201
	0.0920	0.0425	0.4620	0.5281	0.5455	1.0331
	0.0920	0.0623	0.6769	0.5281	0.5550	1.0510
	0.0920	0.0822	0.8935	0.5281	0.5528	1.0469
	0.0920	0.1025	1.1141	0.5281	0.5953	1.1273
28	0.0850	0.0000	0.0000	0.4639	0.4639	1.0000
	0.0850	0.0204	0.2398	0.4639	0.4759	1.0258
	0.0850	0.0425	0.5000	0.4639	0.4835	1.0422
	0.0850	0.0623	0.7326	0.4639	0.4942	1.0653
	0.0850	0.0822	0.9671	0.4639	0.4897	1.0556
	0.0850	0.1025	1.2058	0.4639	0.5209	1.1229
26	0.0790	0.0000	0.0000	0.4039	0.4039	1.0000
	0.0790	0.0204	0.2581	0.4039	0.4160	1.0300
	0.0790	0.0425	0.5380	0.4039	0.4238	1.0492
	0.0790	0.0623	0.7882	0.4039	0.4293	1.0628
	0.0790	0.0822	1.0405	0.4039	0.4325	1.0707
	0.0790	0.1025	1.2974	0.4039	0.4576	1.1329
24	0.0730	0.0000	0.0000	0.3499	0.3499	1.0000
	0.0730	0.0204	0.2793	0.3499	0.3578	1.0225
	0.0730	0.0425	0.5822	0.3499	0.3665	1.0476
	0.0730	0.0623	0.8530	0.3499	0.3710	1.0603
	0.0730	0.0822	1.1260	0.3499	0.3757	1.0739
	0.0730	0.1025	1.4040	0.3499	0.3953	1.1299
22	0.0660	0.0000	0.0000	0.2949	0.2949	1.0000
	0.0660	0.0204	0.3089	0.2949	0.3041	1.0311
	0.0660	0.0425	0.6439	0.2949	0.3128	1.0606
	0.0660	0.0623	0.9435	0.2949	0.3195	1.0835
	0.0660	0.0822	1.2455	0.2949	0.3191	1.0820
	0.0660	0.1025	1.5530	0.2949	0.3356	1.1379
20	0.0600	0.0000	0.0000	0.2480	0.2480	1.0000
	0.0600	0.0204	0.3398	0.2480	0.2583	1.0416
	0.0600	0.0425	0.7083	0.2480	0.2666	1.0748
	0.0600	0.0623	1.0379	0.2480	0.2695	1.0864
	0.0600	0.0822	1.3700	0.2480	0.2746	1.1071
	0.0600	0.1025	1.7083	0.2480	0.2879	1.1606

Table A-8 (continues): Values of specific pressure drop and mass loading ratio at different air velocities (pressure drop measured between 9.1 m and 10 m)

Average air Velocity (m/s)	Air mass flow rate (kg/s)	Wheat mass flow rate (kg/s)	Mass loading ratio (μ)	Pressure drop Air Only (inch H2O)	Pressure drop of mixture (inch H2O)	Specific pressure drop (α)
18	0.0540	0.0000	0.0000	0.2084	0.2084	1.0000
	0.0540	0.0204	0.3775	0.2084	0.2149	1.0313
	0.0540	0.0425	0.7870	0.2084	0.2221	1.0660
	0.0540	0.0623	1.1532	0.2084	0.2240	1.0749
	0.0540	0.0822	1.5222	0.2084	0.2258	1.0834
	0.0540	0.1025	1.8981	0.2084	0.2384	1.1439
16	0.0480	0.0000	0.0000	0.1668	0.1668	1.0000
	0.0480	0.0204	0.4247	0.1668	0.1762	1.0564
	0.0480	0.0425	0.8854	0.1668	0.1825	1.0941
	0.0480	0.0623	1.2973	0.1668	0.1860	1.1151
	0.0480	0.0822	1.7125	0.1668	0.1915	1.1480
	0.0480	0.1025	2.1353	0.1668	0.2013	1.2070
14	0.0420	0.0000	0.0000	0.1323	0.1323	1.0000
	0.0420	0.0204	0.4854	0.1323	0.1399	1.0580
	0.0420	0.0425	1.0119	0.1323	0.1480	1.1192
	0.0420	0.0623	1.4826	0.1323	0.1524	1.1522
	0.0420	0.0822	1.9571	0.1323	0.1584	1.1977
	0.0420	0.1025	2.4404	0.1323	0.1723	1.3025
13	0.0390	0.0000	0.0000	0.1153	0.1153	1.0000
	0.0390	0.0204	0.5227	0.1153	0.1234	1.0701
	0.0390	0.0425	1.0897	0.1153	0.1319	1.1440
	0.0390	0.0623	1.5967	0.1153	0.1412	1.2248
	0.0390	0.1025	2.6281	0.1153	0.1680	1.4566

A.2 Summary of Data Set 2

Table A-9: Values of specific pressure drop and mass loading ratio at different air velocities (pressure drop measured between 0.3 m and 0.9 m)

Average air Velocity (m/s)	Air mass flow rate (kg/s)	Wheat mass flow rate (kg/s)	Mass loading ratio (μ)	Pressure drop Air Only (inch H2O)	Pressure drop of mixture (inch H2O)	Specific pressure drop (α)
30	0.0920	0.0000	0.0000	0.2852	0.2852	1.0000
	0.0920	0.0204	0.2216	0.2852	0.3875	1.3586
	0.0920	0.0425	0.4620	0.2852	0.4920	1.7252
	0.0920	0.0623	0.6769	0.2852	0.5866	2.0569
	0.0920	0.0822	0.8935	0.2852	0.7162	2.5111
	0.0920	0.1025	1.1141	0.2852	0.8106	2.8422
28	0.0850	0.0000	0.0000	0.2293	0.2293	1.0000
	0.0850	0.0204	0.2398	0.2293	0.3485	1.5195
	0.0850	0.0425	0.5000	0.2293	0.4416	1.9255
	0.0850	0.0623	0.7326	0.2293	0.5337	2.3268
	0.0850	0.0822	0.9671	0.2293	0.6496	2.8322
	0.0850	0.1025	1.2058	0.2293	0.7295	3.1806
26	0.0790	0.0000	0.0000	0.1900	0.1900	1.0000
	0.0790	0.0204	0.2581	0.1900	0.2989	1.5736
	0.0790	0.0425	0.5380	0.1900	0.3879	2.0417
	0.0790	0.0623	0.7882	0.1900	0.4743	2.4968
	0.0790	0.0822	1.0405	0.1900	0.5815	3.0608
	0.0790	0.1025	1.2974	0.1900	0.6440	3.3898
24	0.0730	0.0000	0.0000	0.1600	0.1600	1.0000
	0.0730	0.0204	0.2793	0.1600	0.2610	1.6309
	0.0730	0.0425	0.5822	0.1600	0.3422	2.1384
	0.0730	0.0623	0.8530	0.1600	0.4225	2.6401
	0.0730	0.0822	1.1260	0.1600	0.5080	3.1743
	0.0730	0.1025	1.4040	0.1600	0.5520	3.4492
22	0.0660	0.0000	0.0000	0.1332	0.1332	1.0000
	0.0660	0.0204	0.3089	0.1332	0.2240	1.6819
	0.0660	0.0425	0.6439	0.1332	0.2991	2.2460
	0.0660	0.0623	0.9435	0.1332	0.3626	2.7230
	0.0660	0.0822	1.2455	0.1332	0.4253	3.1941
	0.0660	0.1025	1.5530	0.1332	0.4615	3.4660

Table A-9 (continues): Values of specific pressure drop and mass loading ratio at different air velocities (pressure drop measured between 0.3 m and 0.9 m)

Average air Velocity (m/s)	Air mass flow rate (kg/s)	Wheat mass flow rate (kg/s)	Mass loading ratio (μ)	Pressure drop Air Only (inch H2O)	Pressure drop of mixture (inch H2O)	Specific pressure drop (α)
20	0.0600	0.0000	0.0000	0.1077	0.1077	1.0000
	0.0600	0.0204	0.3398	0.1077	0.1889	1.7545
	0.0600	0.0425	0.7083	0.1077	0.2559	2.3767
	0.0600	0.0623	1.0379	0.1077	0.3058	2.8395
	0.0600	0.0822	1.3700	0.1077	0.3451	3.2053
	0.0600	0.1025	1.7083	0.1077	0.3558	3.3043
18	0.0540	0.0000	0.0000	0.0815	0.0815	1.0000
	0.0540	0.0204	0.3775	0.0815	0.1546	1.8974
	0.0540	0.0425	0.7870	0.0815	0.2087	2.5609
	0.0540	0.0623	1.1532	0.0815	0.2450	3.0068
	0.0540	0.0822	1.5222	0.0815	0.2688	3.2984
	0.0540	0.1025	1.8981	0.0815	0.2776	3.4071
16	0.0480	0.0000	0.0000	0.0583	0.0583	1.0000
	0.0480	0.0204	0.4247	0.0583	0.1231	2.1102
	0.0480	0.0425	0.8854	0.0583	0.1630	2.7936
	0.0480	0.0623	1.2973	0.0583	0.1829	3.1353
	0.0480	0.0822	1.7125	0.0583	0.1939	3.3240
	0.0480	0.1025	2.1353	0.0583	0.1987	3.4065
14	0.0420	0.0000	0.0000	0.0410	0.0410	1.0000
	0.0420	0.0204	0.4854	0.0410	0.0930	2.2685
	0.0420	0.0425	1.0119	0.0410	0.1198	2.9208
	0.0420	0.0623	1.4826	0.0410	0.1287	3.1377
	0.0420	0.0822	1.9571	0.0410	0.1304	3.1786
	0.0420	0.1025	2.4404	0.0410	0.1410	3.4380
13	0.0390	0.0000	0.0000	0.0330	0.0330	1.0000
	0.0390	0.0204	0.5227	0.0330	0.0792	2.4025
	0.0390	0.0425	1.0897	0.0330	0.0979	2.9674
	0.0390	0.0623	1.5967	0.0330	0.0988	2.9959
	0.0390	0.0822	2.1077	0.0330	0.1064	3.2272
	0.0390	0.1025	2.6281	0.0330	0.1280	3.8812

Table A-10: Values of specific pressure drop and mass loading ratio at different air velocities (pressure drop measured between 0.9 m and 1.5 m)

Average air Velocity (m/s)	Air mass flow rate (kg/s)	Wheat mass flow rate (kg/s)	Mass loading ratio (μ)	Pressure drop Air Only (inch H2O)	Pressure drop of mixture (inch H2O)	Specific pressure drop (α)
30	0.0920	0.0000	0.0000	0.3255	0.3255	1.0000
	0.0920	0.0204	0.2216	0.3255	0.3943	1.2112
	0.0920	0.0425	0.4620	0.3255	0.4426	1.3596
	0.0920	0.0623	0.6769	0.3255	0.5386	1.6547
	0.0920	0.0822	0.8935	0.3255	0.5769	1.7721
	0.0920	0.1025	1.1141	0.3255	0.6600	2.0276
28	0.0850	0.0000	0.0000	0.2756	0.2756	1.0000
	0.0850	0.0204	0.2398	0.2756	0.3494	1.2677
	0.0850	0.0425	0.5000	0.2756	0.3962	1.4372
	0.0850	0.0623	0.7326	0.2756	0.4801	1.7417
	0.0850	0.0822	0.9671	0.2756	0.5245	1.9027
	0.0850	0.1025	1.2058	0.2756	0.5876	2.1319
26	0.0790	0.0000	0.0000	0.2475	0.2475	1.0000
	0.0790	0.0204	0.2581	0.2475	0.3092	1.2491
	0.0790	0.0425	0.5380	0.2475	0.3510	1.4181
	0.0790	0.0623	0.7882	0.2475	0.4230	1.7088
	0.0790	0.0822	1.0405	0.2475	0.4607	1.8611
	0.0790	0.1025	1.2974	0.2475	0.5122	2.0691
24	0.0730	0.0000	0.0000	0.2125	0.2125	1.0000
	0.0730	0.0204	0.2793	0.2125	0.2713	1.2770
	0.0730	0.0425	0.5822	0.2125	0.3063	1.4418
	0.0730	0.0623	0.8530	0.2125	0.3639	1.7128
	0.0730	0.0822	1.1260	0.2125	0.3995	1.8800
	0.0730	0.1025	1.4040	0.2125	0.4390	2.0659
22	0.0660	0.0000	0.0000	0.1802	0.1802	1.0000
	0.0660	0.0204	0.3089	0.1802	0.2311	1.2827
	0.0660	0.0425	0.6439	0.1802	0.2625	1.4569
	0.0660	0.0623	0.9435	0.1802	0.3095	1.7181
	0.0660	0.0822	1.2455	0.1802	0.3403	1.8890
	0.0660	0.1025	1.5530	0.1802	0.3790	2.1034
20	0.0600	0.0000	0.0000	0.1528	0.1528	1.0000
	0.0600	0.0204	0.3398	0.1528	0.1992	1.3043
	0.0600	0.0425	0.7083	0.1528	0.2232	1.4609
	0.0600	0.0623	1.0379	0.1528	0.2615	1.7121
	0.0600	0.0822	1.3700	0.1528	0.2873	1.8807
	0.0600	0.1025	1.7083	0.1528	0.3168	2.0740

Table A-10 (continues): Values of specific pressure drop and mass loading ratio at different air velocities (pressure drop measured between 0.9 m and 1.5 m)

Average air Velocity (m/s)	Air mass flow rate (kg/s)	Wheat mass flow rate (kg/s)	Mass loading ratio (μ)	Pressure drop Air Only (inch H2O)	Pressure drop of mixture (inch H2O)	Specific pressure drop (α)
18	0.0540	0.0000	0.0000	0.1290	0.1290	1.0000
	0.0540	0.0204	0.3775	0.1290	0.1663	1.2894
	0.0540	0.0425	0.7870	0.1290	0.1842	1.4283
	0.0540	0.0623	1.1532	0.1290	0.2175	1.6865
	0.0540	0.0822	1.5222	0.1290	0.2386	1.8499
	0.0540	0.1025	1.8981	0.1290	0.2684	2.0809
16	0.0480	0.0000	0.0000	0.1048	0.1048	1.0000
	0.0480	0.0204	0.4247	0.1048	0.1361	1.2988
	0.0480	0.0425	0.8854	0.1048	0.1472	1.4049
	0.0480	0.0623	1.2973	0.1048	0.1726	1.6472
	0.0480	0.0822	1.7125	0.1048	0.1907	1.8205
	0.0480	0.1025	2.1353	0.1048	0.2180	2.0812
14	0.0420	0.0000	0.0000	0.0813	0.0813	1.0000
	0.0420	0.0204	0.4854	0.0813	0.1081	1.3296
	0.0420	0.0425	1.0119	0.0813	0.1137	1.3995
	0.0420	0.0623	1.4826	0.0813	0.1341	1.6502
	0.0420	0.0822	1.9571	0.0813	0.1562	1.9213
	0.0420	0.1025	2.4404	0.0813	0.1972	2.4264
13	0.0390	0.0000	0.0000	0.0716	0.0716	1.0000
	0.0390	0.0204	0.5227	0.0716	0.0943	1.3170
	0.0390	0.0425	1.0897	0.0716	0.0976	1.3631
	0.0390	0.0623	1.5967	0.0716	0.1177	1.6440
	0.0390	0.0822	2.1077	0.0716	0.1545	2.1581
	0.0390	0.1025	2.6281	0.0716	0.4788	6.6896

\

Table A-11: Values of specific pressure drop and mass loading ratio at different air velocities (pressure drop measured between 1.5 m and 2.1 m)

Average air Velocity (m/s)	Air mass flow rate (kg/s)	Wheat mass flow rate (kg/s)	Mass loading ratio (μ)	Pressure drop Air Only (inch H2O)	Pressure drop of mixture (inch H2O)	Specific pressure drop (α)
30	0.0920	0.0000	0.0000	0.3261	0.3261	1.0000
	0.0920	0.0204	0.2216	0.3261	0.3678	1.1278
	0.0920	0.0425	0.4620	0.3261	0.3950	1.2111
	0.0920	0.0623	0.6769	0.3261	0.4480	1.3736
	0.0920	0.0822	0.8935	0.3261	0.5283	1.6199
	0.0920	0.1025	1.1141	0.3261	0.5465	1.6757
28	0.0850	0.0000	0.0000	0.2794	0.2794	1.0000
	0.0850	0.0204	0.2398	0.2794	0.3260	1.1668
	0.0850	0.0425	0.5000	0.2794	0.3548	1.2696
	0.0850	0.0623	0.7326	0.2794	0.4048	1.4486
	0.0850	0.0822	0.9671	0.2794	0.4721	1.6895
	0.0850	0.1025	1.2058	0.2794	0.4899	1.7531
26	0.0790	0.0000	0.0000	0.2489	0.2489	1.0000
	0.0790	0.0204	0.2581	0.2489	0.2905	1.1671
	0.0790	0.0425	0.5380	0.2489	0.3159	1.2692
	0.0790	0.0623	0.7882	0.2489	0.3572	1.4351
	0.0790	0.0822	1.0405	0.2489	0.4225	1.6976
	0.0790	0.1025	1.2974	0.2489	0.4424	1.7775
24	0.0730	0.0000	0.0000	0.2138	0.2138	1.0000
	0.0730	0.0204	0.2793	0.2138	0.2539	1.1874
	0.0730	0.0425	0.5822	0.2138	0.2784	1.3017
	0.0730	0.0623	0.8530	0.2138	0.3156	1.4760
	0.0730	0.0822	1.1260	0.2138	0.3707	1.7336
	0.0730	0.1025	1.4040	0.2138	0.3982	1.8624
22	0.0660	0.0000	0.0000	0.1821	0.1821	1.0000
	0.0660	0.0204	0.3089	0.1821	0.2151	1.1814
	0.0660	0.0425	0.6439	0.1821	0.2373	1.3035
	0.0660	0.0623	0.9435	0.1821	0.2726	1.4971
	0.0660	0.0822	1.2455	0.1821	0.3189	1.7516
	0.0660	0.1025	1.5530	0.1821	0.3523	1.9351
20	0.0600	0.0000	0.0000	0.1554	0.1554	1.0000
	0.0600	0.0204	0.3398	0.1554	0.1870	1.2039
	0.0600	0.0425	0.7083	0.1554	0.2068	1.3312
	0.0600	0.0623	1.0379	0.1554	0.2351	1.5130
	0.0600	0.0822	1.3700	0.1554	0.2760	1.7762
	0.0600	0.1025	1.7083	0.1554	0.2974	1.9141

Table A-11 (continues): Values of specific pressure drop and mass loading ratio at different air velocities (pressure drop measured between 1.5 m and 2.1 m)

Average air Velocity (m/s)	Air mass flow rate (kg/s)	Wheat mass flow rate (kg/s)	Mass loading ratio (μ)	Pressure drop Air Only (inch H2O)	Pressure drop of mixture (inch H2O)	Specific pressure drop (α)
18	0.0540	0.0000	0.0000	0.1312	0.1312	1.0000
	0.0540	0.0204	0.3775	0.1312	0.1561	1.1897
	0.0540	0.0425	0.7870	0.1312	0.1728	1.3172
	0.0540	0.0623	1.1532	0.1312	0.2001	1.5258
	0.0540	0.0822	1.5222	0.1312	0.2322	1.7701
	0.0540	0.1025	1.8981	0.1312	0.2621	1.9985
16	0.0480	0.0000	0.0000	0.1079	0.1079	1.0000
	0.0480	0.0204	0.4247	0.1079	0.1306	1.2097
	0.0480	0.0425	0.8854	0.1079	0.1440	1.3340
	0.0480	0.0623	1.2973	0.1079	0.1657	1.5350
	0.0480	0.0822	1.7125	0.1079	0.2030	1.8803
	0.0480	0.1025	2.1353	0.1079	0.2289	2.1209
14	0.0420	0.0000	0.0000	0.0860	0.0860	1.0000
	0.0420	0.0204	0.4854	0.0860	0.1055	1.2269
	0.0420	0.0425	1.0119	0.0860	0.1178	1.3694
	0.0420	0.0623	1.4826	0.0860	0.1386	1.6120
	0.0420	0.0822	1.9571	0.0860	0.1777	2.0655
	0.0420	0.1025	2.4404	0.0860	0.2343	2.7236
13	0.0390	0.0000	0.0000	0.0757	0.0757	1.0000
	0.0390	0.0204	0.5227	0.0757	0.0939	1.2394
	0.0390	0.0425	1.0897	0.0757	0.1063	1.4034
	0.0390	0.0623	1.5967	0.0757	0.1319	1.7417
	0.0390	0.0822	2.1077	0.0757	0.1886	2.4907
	0.0390	0.1025	2.6281	0.0757	0.4390	5.7967

APPENDIX B: MATLAB CODE FOR PARAMETER ESTIMATION

```
% Import mass loading ratio (mu) and specific pressure drop (alpha) data from file
function [estimates, model] = p_est(mu,alpha) %function accepts values
start_point = rand(1, 2);
model = @expfun;
estimates = fminsearch(model, start_point);
    function [sse, Fit_ab] = expfun(params)
      %A and B are defined as parameters
       A = params(1);
       B = params(2);
       Fit_ab = 1+ A*mu+ B*(mu).^(0.5) ;
       ErrorValue = Fit_ab - alpha;
       sse = sum(ErrorValue .^ 2);
    end
end
```